Optical Fiber Transmission Systems for In-door Next Generation Broadband Access Network.

Uchenna Okonkwo Igweani

A Thesis submitted within respect of the guidelines for the Degree of Doctor of Philosophy (PhD)

Electronic and Computer Engineering

Wireless Network and Communication Centre (WNCC)

School of Engineering and Design

Brunel University,

Uxbridge

United Kingdom

September 2014

Abstract

This thesis investigates the generation and radio-over-fibre (RoF) transport of unlicensed 60 GHz millimetre-wave (mm-wave) frequency band. The investigated benefits of transmission schemes applicable for the mm-wave generation include optical carrier suppression (OCS), optical frequency multiplication (OFM) and remote heterodyne detection (RHD). For the in-door cabling of the mm-wave transmission, a low-cost polymer optical fibre (POF) along with bend-insensitive single mode fibre (BI-SMF) has been investigated for short-range networks.

Transporting mm-wave generated signals over POF and BI-SMF cables based on OCS scheme showed results with the highest spectral efficiency and least inter-symbol interference over a 2.5 Gbit/s data delivery. Based on this thesis analysis, OCS simulation of POF showed the most reliable power penalty performance and receiver sensitivity at 30-m whilst the BI-SMF fiber produced equal observations at 150-m and more. In observing the free space links of delivering the RoF signal, the attenuation on the received signal power for both POF and BI-SMF was insignificant but expected, as the simulation assumed complete and total collimation of the light beams onto the aperture of the photodetector. OCS scheme for mm-wave generation and transport was explored based on the cost effectiveness of using one external modulator compared to other generation schemes that utilised more than one external modulator. OFM scheme was simulated to transport LTE and Wi-Fi signals along with 60 GHz RF band through both SMF and MMF-POF/BI-SMF cables. OFM transport scheme produced the highest attenuation on LTE, Wi-Fi and mm-wave signals carrying 100 Mbit/s data as simulated POF lengths increased. The best performance POF length was observed at 10-m. The application of offset launch technique at the coupling of SMF and POF showed insignificant improvement on signal bandwidth. The free space OFM transmission also demonstrated negligible change to the received signal power. This reinforces the attributes of deploying OWC system in an in-door environment. In other investigation, the simulated successful delivery of mm-wave signal using RHD scheme modulated and transported 10 Gbit/s data signal over POF and BI-SMF cables. Additional observed unrecorded result also showed BI-SMF cable maintained a 2% reduction of received power for 450-m fiber cable from 150-m. The attributes to RHD includes its low operating power system application and delivery of localised 60 GHz signal for uplink RoF transmission.

The conceptualised design of Gigabit data delivery for indoor customer applications either through POF or BI-SMF cable, transporting various wireless channels has been presented in this thesis for the design of a robust next generation Broadband access network to reinforce the fiber-inside-the-home (FiTH) deployment.

Acknowledgements

Firstly, I would like to thank my supervisor Professor Hamed S. Al-Raweshidy for his complete support, advice and assistance throughout the duration of my PhD academic study.

I would also like to thank especially all my research colleagues and staff in the electronics engineering department for their continued support.

Dedication

I dedicate this thesis to my Parents and entire Family

Contents

List of Figures

List of Tables

Abbreviations

ADC	Analog-to-Digital Converters
ADSL	Asymmetric Digital Subscriber Line
AM	Amplitude Modulation
AN	Access Node
APD	Avalanche Photodiode
AWG	Array Waveguide Grating
BPON	Broadband Passive Optical Network
BS	Base Station
CAPEX	Capital Expenditure
CATV	Community Access Television
CDM	Code-Division Multiplexed
CDMA	Code-Division Multiple Access
CMOS	Complementary Metal Oxide Semiconductor
CNR	Carrier-to-noise-ratio
CO	Central Office
CS	Central Station
CW	Continuous Wave
CYTOP	Cyclic Transparent Optical Polymer
DAC	Digital-to-Analog Converters
DAS	Distributed Antenna System
DBA	Dynamic Bandwidth Allocation
DCF	Dispersion Compensating Fiber
DD-MZM	Dual-Drive Mach-Zehnder Modulator
DFB	Distributed Feedback Laser
DMA	Differential Mode Attenuation
DMD	Differential Mode Delay
DMT	Discrete Multi-tone
DRoF	Digital Radio-over-Fiber
DSB	Double Sidebands
DSLAM	Digital subscriber line-access multiplexer
DSP	Digital Signal Processing
DWDM	Dense Wavelength Division Multiplexing
EA	Electrical Amplification
EMI	Electromagnetic Interference
EMI	Electromagnetic Interference
EPON	Ethernet Passive Optical Network

EU	European Union
F*i*TH	Fiber-inside-the-home
FM	Frequency Modulation
FPI	Fabry-Perot Interferometer
FSK	Frequency-Shift Keying
FSL	Free Space Loss
FSO	Free Space Optics
FTTC	Fiber-to-the-cabinet
FTTH	Fiber-to-the-home
FTTP	Fiber-to-the-premise
GDP	Gross Domestic Product
GE-PON	Gigabit Ethernet Passive Optical Network
GI-POF	Graded Index Plastic Optical Fiber
GPON	Gigabit Passive Optical Network
HFC	Hybrid Fiber Coaxial
HOE	Holographic Optical Element
IF	Intermediate Frequency
IM	Intensity Modulation
IM/DD	Intensity Modulation and Direct Detection
IoT	Internet of things
IPTV	Internet protocol television
IR	Infra-red
ISI	Intersymbol Interference
ISP	Internet Service Provider
LED	Light Emitting Diode
LO	Local Oscillator
LoS	Line of Sight
LTE	Long Term Evolution
MAN	Metropolitan Area Networks
MDU	Multiple Dwelling Unit
MMF	Multimode Fiber
MMPOF	Multimode POF
Mm-wave	Millimetre wave
MZI	Mach-Zehnder Interferometer
MZM	Mach-Zehnder Modulator
NA	Numerical Aperture
NGA	Next Generation Access
NGPON	Next Generation Passive Optical Network
NIR	Near Infra-red

OAP	Optical Access Point
OBI	Optical Beat Interference
OBPF	Optical Band-pass Filter
OCDMA	Optical Code-Division Multiple Access
OCS	Optical Carrier Suppression
OFDM	Orthogonal Frequency Division Multiplexed
OFDMA	Orthogonal Frequency Division Multiple Access
OFL	Over Filled Launch
OFM	Optical Frequency Multiplication
OLT	Optical Line Terminal
ONU	Optical Network Unit
OOFDM	Optical Orthogonal Frequency Division Multiplexed
OWC	Optical Wireless Communication
PC	Personal Computer
PD	Photo-Detector
PF (POF)	Perfluorinated (POF)
PLC	Power Line Communication
PM	Phase Modulation
PMMA	Polymethylmethacrylate
POF	Plastic/Polymer Optical Fiber
PON	Passive Optical Network
POP	Point of Presence
PRBS	Pseudo-Random Bit Sequence
QAM	Quadrature Amplitude Modulation
QoS	Quality of Service
QPSK	Quadrature Phase-Shift Keying
RAP	Radio Access Point
RF	Radio Frequency
RG	Residential Gateway
RHD	Remote Heterodyne Detection
RoF	Radio-over-Fiber
RoMMF	Radio over Multimode Fiber
RSOA	Reflective Semiconductor Optical Amplifier
SCM	Subcarrier Multiplexed
SCMA	Subscriber-Division Multiple Access
SFU	Single Family Unit
SI-POF	Step Index Plastic Optical Fiber
SMF	Single Mode Fiber
SMPOF	Single-mode POF

SNR	Signal-to-Noise-Ratio
SSB	Single Side Band
SSFBG	Super Structure Fiber Bragg Grating
SSMF	Standard Single Mode Fiber
TDM	Time Division Multiplexed
TDMA	Time-division Multiple Access
Teleco	Telecommunication Company
UTP	Unshielded Twisted Pair
VCSEL	Vertical Cavity Surface Emitting Lasers
VDSL	Very high bit-rate Digital Subscriber Line
VLC	Visible Light Communication
VoD	Video on Demand
VoIP	Voice over Internet Protocol
VSB	Vestigial Sideband
WDM	Wavelength Division Multiplexing
WDMA	Wavelength-Division Multiple Access
WiGig	Wireless Gigabit
WiMax	Worldwide Interoperability for Microwave Access
WLAN	Wireless Local Area Network
WLED	White Light Emitting Diode

Chapter 1

Introduction

1.1 Broadband Communication

Perhaps our addiction to the fast pace of communication has spurned the necessity to improve on the current technologies that offer increased broadband internet or the increase in internet human-population has warranted the recitation of past telecommunication infrastructure models.

The proliferation of optical fiber as a means of Gbit/s data delivery has been around for decades and has been at the forefront in the transmission of both fixed and wireless network connectivity. As such, the abbreviation FTTH which stands for Fiber-to-the-home is defined as the access network architecture where the final connection to the customer's premises is made using optical fibre. FTTH has seen much real advancement in broadband delivery at the access network in most developed countries. In the UK for example, the Tier 1 internet service provider in 2006 created an infrastructure deployment division taskforce to deal with the advancements in optical fiber next-generation access (NGA) network development which was approved by the UK telecommunication (telecom) regulator [1]. As part of the 'Digital

Agenda' initiative, the European Commission and the telecom regulator set a target for operators to deliver future superfast broadband (SFBB) connectivity (download speed > 30Mbit/s) to the UK households by 2020 [2].

In the perspective of the ever increasing high data rate and multimedia service consumers on mobile devices leads to severe strain on the cellular networks whether it is in an indoor public space such as airports, shopping malls and train stations or in private places such as business offices or residential environments. To solve this issue, a number of small cell network (SCN) concepts are deployed at locations as femtocells, picocells, microcells and metrocells [3]. These SCN concepts made up for an optical fiber based microcellular wireless access (Fi-Wi) systems have been investigated as early as the nineties [4] and have several advantages such as data offloading and improved radio coverage capacity through thick building walls. The Fi-Wi system deployment made it possible to deliver wireless services to target locations such as underground train stations, game events and mines. For example, the London 2012 Olympics deployed over 1500 wireless access points, interconnected by more than 100 kilometres of cable in order to handle the expected wireless traffic load [5]. The London Olympic event was recognised as the first ever social media driven event, making the official website achieve a remarkable 431 million visits, 15 million app downloads and 4.73 billion page views, totally 4 billion viewers globally [6].

1.2 Edge Network Optical Fiber Technology

In focusing on broadband services mainly at the edge access network technology, the prime reason to focus on fiber deployment is as a result of an economical one. In deploying these access networks the network providers look for a system that is cost

effective, delivers the required QoS and has ease of installation and maintenance. In this section, the different technologies that offer broadband services to the end-users premises are investigated.

1.2.1 Introduction to Optical Access Network Technology

The application of wireless communication is constantly evolving and as consumers move from the usual voice data to mostly multimedia data the underlying technology needs to evolve also. Mobile data increases exponentially globally and its forecast for 2012 and 2017 is set to increase by 13-fold. The annual data traffic will grow from 1 petabyte per month in 2012 to 83.8 exabytes per month in 2015 while in 2017 data traffic would increase to 120.6 exabytes per month or 1.4 zettabytes per year [7]. As shown in Fig 1.1, there will be a dramatic rise of wireless data demand over various regions by consumers.

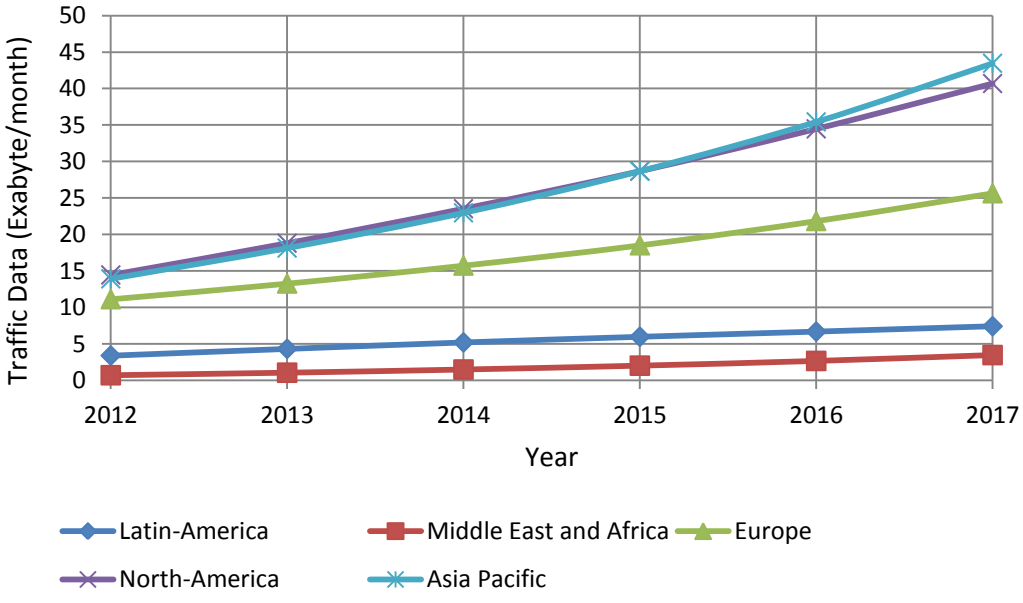

Figure 1.1: Forecasted Internet traffic data over wireless networks, Cisco [7]

Telemedicine has been viewed by many across the medical industry as an example in answering the dwindling access to health care and information on a rapid scale to many patients living across an urban or rural environment who may not have had such easy access. To most stakeholders of telemedicine, it is viewed as a cost effective advantage because it provides vast healthcare benefits [8], whilst it is also arguably that the practise isn't beneficial across all medical diagnosis [9].

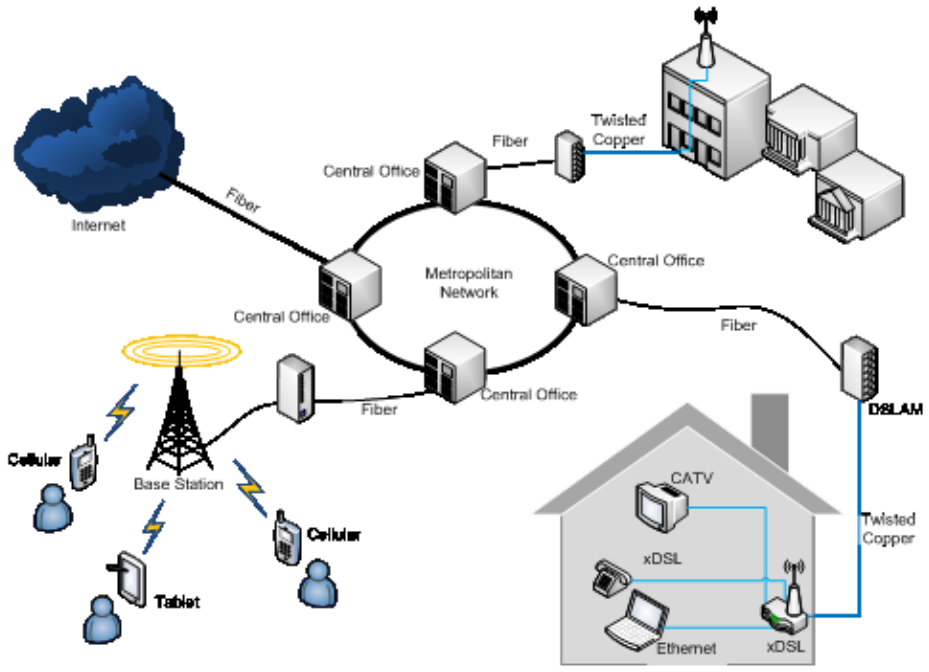

Figure 1.2: Traditional Access to the Internet

Optical fiber cabling is being used for the widespread network of data traffic at the metropolitan network [Fig 1.2]. The SMF is being deployed to connect the metropolitan network to the access nodes (AN) and base stations (BS). To an extent in the edge network (or access network) the optical fiber is deployed extensively to address the insufficient bandwidth capacity of the copper links with to some

scenarios have seen the extensive replacement of copper in the access network with fiber links all the way to the users home or wireless access point. Traditionally the fiber cable runs from the central office to a digital subscriber line-access multiplexer (DSLAM) or street cabinet before asymmetric digital subscriber line (ADSL) or very high bit-rate Digital Subscriber Line (VDSL) copper wires are connected to the user's home. These copper wires are then connected to an xDSL modem in the customer's premises to provide broadband services using various signal processing schemes like the discrete multitone (DMT) and quadrature amplitude modulation (QAM) to further increase the data throughput over the deficient bandwidth capacity of the copper links. As stated earlier, the further away in distance that the copper link is terminated from the building to the DSLAM significantly reduces the transported data rate. For most residential networks in the European Union (EU), ADSL can provide data rate of approximately 8 Mbits/s while the latest VDSL technology (where it is used as a hybrid of FTTC) can provide a download speed of 41 Mbits/s but average achieved speed is at 30 Mbits/s and copper cable deliver 33 Mbits/s [10], [11].

1.2.2 Traditional Television delivery network

The application of coaxial copper cable for cable television transmission for analog television channels is set at 8 MHz, this already makes the use of UTP incapable of transmitting television channels at adequate lengths. Coax cable has little attenuation over a 30 m span of about 1 dB which makes it advantageous for operators to transmit various television channels using a coaxial cable but at lengths in the region of 200 m the use of amplifiers becomes more prevalent. This makes the use of coaxial cable less cost effective for long haul trunk links. In the network design, the use of amplifiers to mitigate the signal loss is greatly dependent on the guidelines of

the received CNR that has to be met and in most deployments; several amplifiers are required to deliver a good CATV QoS. Since there is significant attenuation on the signal over coaxial cable as a result of the resistance of copper wire and the frequency dependent losses caused by radiation, operators have adopted the SMF to transmit several television channels to a destination point (or fiber node) in the network before optical-to-electrical conversion is done for distributed transmissions over several coaxial cables to their subscribers. This schematic known as *hybrid fiber coaxial* (HFC) networks is carried out in most parts of Western Europe and in some states in America. Fig 1.2 demonstrates how the HFC can be implemented to deliver CATV channels to a subscriber, from a distribution network to the CO using SMF cables, after which the edge network uses coaxial cable to connect to the customer's premises. Where there are multiple customer premises for CATV distribution there are two main HFC network distribution schemes that address several connectivity by multiplexing the signals after the CO using a tree-branch network [12] but this would be discussed at breadth in the subsequent section.

1.3 Optical Fiber Access Technology and Network

As illustrated in Fig 1.2, most national access network architecture consists of central offices, transmission devices, network equipments to aggregate links. Where the cabling is carried out by optical fiber right through to the access network which connects several subscribers to a particular point or node is referred to as fiber to the home (FTTH) network.

Fig 1.2 shows the access network where traditionally a metro access network will only have the copper feeder link from the telephone pole or street cabinet to the subscriber's home. In the conventional legacy infrastructure, the ADSL (or VDSL) line

running over a twisted copper pairs would have a connection that runs from the street cabinet to the subscriber's home. This network topology is referred to as fiber to the curb (FTTC) which was the widespread guideline for broadband delivery to the subscriber's home. To replace the same multiple access schematic of various subscribers onto the local exchange and subsequently the entire network, optical technology redefined the FTTH access network topology into three architectures which are described as follows:

a) ***Point-to-point topology***: this consists of having several dedicated optical fibers between the access node, point of presence (POP) or local exchange and the subscriber homes [Fig 1.3(a)]. A direct optical fiber link terminates at a subscriber home from the local exchange which means several optical fibers are needed to build the network. This approach has the advantage of providing the network operators with an ease of subscriber network upgrade along with significant capacity (as it is a direct connection from the local exchange) but the resultant factor becomes the high installation cost per single fiber to the subscriber's home.

b) ***Point-to-multipoint topology***: or Passive network, is where a single optical fiber carries all data traffic from the local exchange down to a passive optical splitter situated closer to a cluster of buildings with the purpose of connecting individual buildings with a dedicated optical fiber (like a tree branch) [Fig 1.3(b)]. This topology has the advantage of cost reduction by removing the need to power and maintain active/electrical equipments along the access network, making it a passive optical network

(PON). The complete isolation of active elements in the passive network means that lifespan of the field plant is ultimately increased. This passive network approach also has the benefit of being cost effective as the feeder connection from the local exchange to the passive optical splitter is reduced to a single optical fiber. This topology has almost become the standardized approach in deploying FTTH access network in mainland Europe, especially its gigabit passive optical network (GPON) variant.

c) ***Active Ethernet topology***: or Active optical network which is similar to PON but combines the application of an active element at a node point in the field. In this network design, a feeder fiber also connects the local exchange to an active node (rather than an optical splitter) which is also located at a point close to a cluster of buildings before each subscriber building is linked with their dedicated optical fiber [Fig 1.3(c)]. The practicality of this topology makes it a more expensive measure than its counterpart as it requires the powering and maintenance of field active equipments but also has the cost saving benefits of reducing the feeder fiber to a single optical fiber. The active equipment used in this scenario is mostly and Ethernet module (e.g. a switch) to control the shared access of connected subscribers. In Asia the Ethernet passive optical network (EPON) has been widely adopted due to its Ethernet capability to manage the traffic access of multiple subscribers from the several fiber branches to a single feeder fiber using a time division protocol.

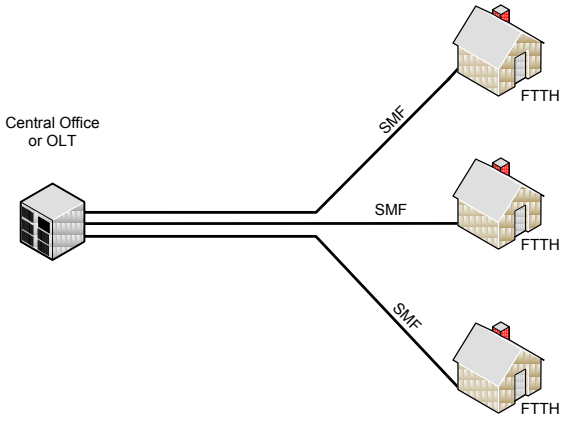

Figure 1.3(a): Point-to-Point FTTH access architecture

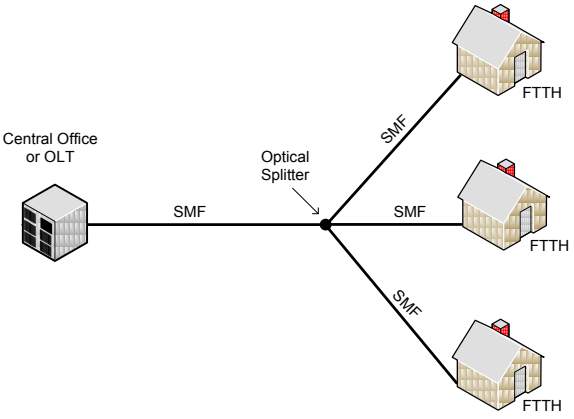

Figure 1.3(b): Passive (PON) FTTH access architecture

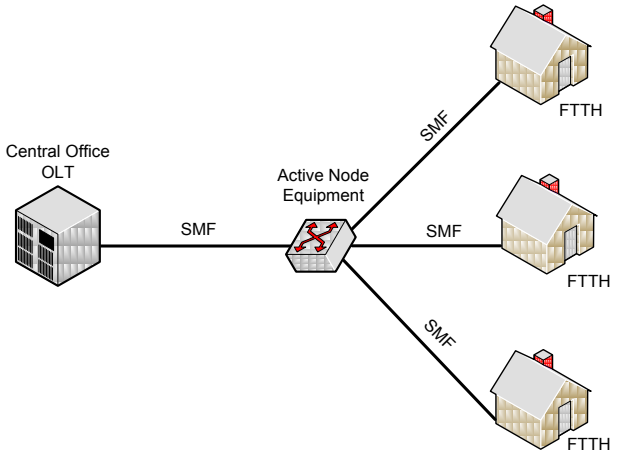

Figure 1.3(c): Active Ethernet FTTH access architecture

In a 2013 case study of FTTH access technology deployment [13] across Europe, several countries outlined their justification of which technology their ISP rolled out to achieve FTTH capability. There are several multiple access transmission schemes that can achieve this and are currently being used [14] but the four significant multiple access schemes are:

- Time-division multiple access (TDMA)
- Wavelength-division multiple access (WDMA)
- Code-division multiple access (CDMA)
- Subcarrier multiple access (SCMA)

These four unique schemes are for the transport of upstream data traffic from the ONU to the OLT. The method used for multiplexing data in the downstream from the OLT to the ONU shall be discussed subsequently. Overview on these four different multiple access transmission schemes shall be discussed but not profoundly.

A. Time-Division Multiple Access (TDMA)

This by enlarge is one of the widely adopted multiple access transmission scheme to deliver upstream data traffic from the ONU at the subscribers premises to the OLT. When designing PON architecture, the TDMA has its merits in delivering the ultimate Broadband services in an MDU. The topology of the TDMA technology system as illustrated in Fig 1.4(a) operates by allocating portioned time slots to each of the multiple ONU receivers connected to the OLT infrastructure. At the time slot allocated to a subscriber, the theoretical maximum bandwidth of the optical signal at the feeder fiber network is available for the subscriber's upstream data transmission. Each ONU and feeder fiber of a subscriber is combined into a single SMF using a passive optical splitter. The upstream data packets transported from the various ONUs are scheduled and separated in time domain and requires a complex method to synchronise the upstream data. This time scheduling and complex process is done at the OLT and requires a substantial amount of processing power.

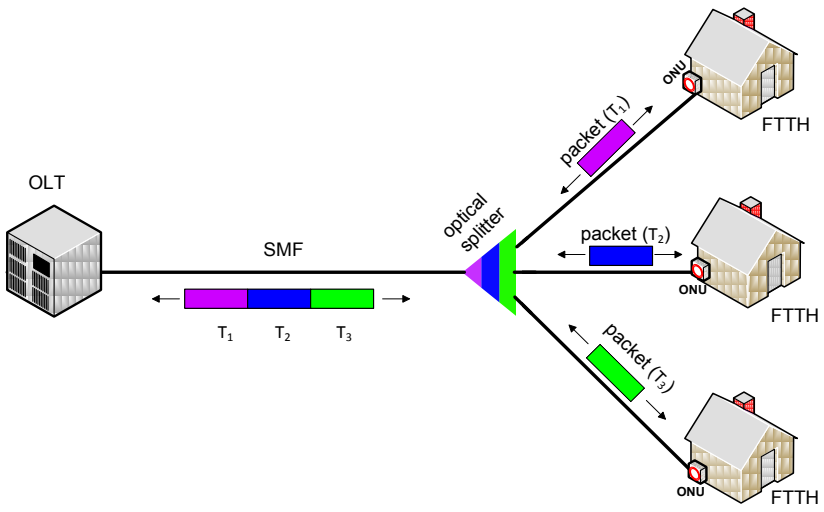

Figure 1.4(a): TDMA passive optical network

B. Wavelength-division multiple access (WDMA)

In a PON system where multiple optical light-waves are used to transport data is made possible by a wavelength division multiplexing (WDM) technology. The system can be referred to as WDM-PON or WDMA. This type of optical access network is widely adopted as almost the industry standard for the future proof PON systems and paves way for the latest brand of PON systems, the Gigabit passive optical network (GPON) and the Gigabit Ethernet passive optical network (GE-PON). The two systems are prevailing in PON deployments globally in places such as the Northern part of America, which adopts the GPON architecture as well as in Europe, whilst in Asia, the GE-PON has be documented as their preferred alternative. Further policy on the GPON system can be found under the ITU-T G.984 (GPON) guidelines [15] and the IEEE 802.3ah (GE-PON) guidelines [16]. Fig 1.4(b) illustrates the system of WDMA where each ONU transmits a single wavelength upstream to the OLT. For several users to adequately transmit different wavelengths to the OLT, a wavelength splitter such as an Array Waveguide Grating (AWG) is situated at the remote node and is used to multiplex the individual ONU wavelength signals from the feeder fiber onto the SMF fiber that connects to the OLT. In the downstream data transport, an additional AWG demultiplexing of the individual wavelengths is applied at the OLT. Each ONU would effectively utilize a different coloured wavelength to transmit data using a Laser Diode (which has additional cost) but this that means the system becomes more complex and prone to severe processing interruption. To mitigate this, innovative solutions have been demonstrated in the use of colourless light-wave at each ONU, meaning each ONU is not tuned to a specific wavelength by default. This significantly reduces the cost burden in network deployment and as such yielded four popular approaches to colourless transmission; the wavelength tuning

technique [17], the spectrum slicing technique [18], the injection locking technique and the wavelength seeding technique.

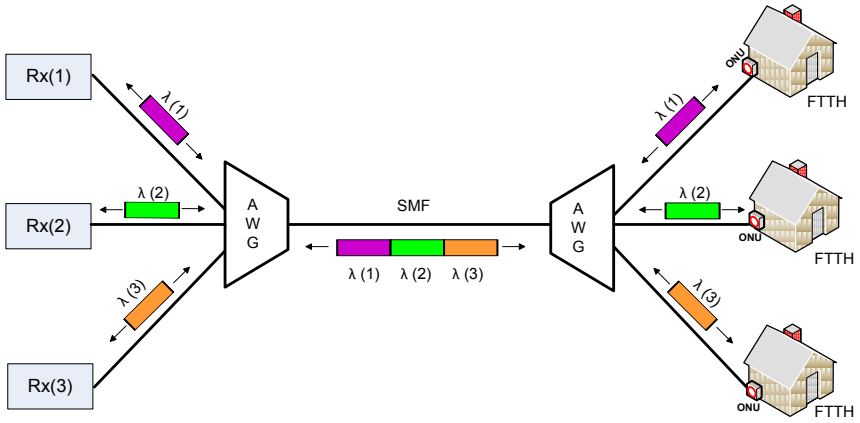

Figure 1.4(b): WDMA passive optical network

C. Code-division multiple access (CDMA)

Similar to the technology used in current satellite and cellular networks, CDMA when used in the optical domain (as in this case of OLT to ONU transmission) is referred to as optical-CDMA (OCDMA) and can exist in two variations, the spectrum-sliced OCDMA and the time-sliced OCDMA.

The spectrum-sliced OCDMA technology the individual ONU share a wavelength spectrum for data transmission to the OLT. The spectrum is encoded by splitting the wavelength into wavelength sequences and each spectral component has its amplitude modulated with the upstream data [Fig 1.4(c)]. In the time-sliced OCDMA technology the ONU data to be sent is encoded by splitting the data into time sequences. Each time sequence has its unique waveform envelope which is referred

to as the optical code sequence. The code sequence is a short pulse generated simply as a “zero” or “one” sequence then modulated with the upstream data. Each ONU is assigned a unique optical code sequence for upstream data transmission to the OLT. At reception in the OLT, in order to decode (or demultiplex) the data from the ONU, the overlapping codes of the upstream data are detected in sequence and decoded using the exact same optical code sequence. This pattern of transmission gives OCDMA the benefit in performing the ultimate data security and ascertains network integrity. The high coherency or incoherency of matched codes allows for simultaneous and asynchronous operation data transmission with low end-to-end delay [19]. There has been a report on a technological advancement that has proven to ease the burden on the optical encoders and decoders at the OLT [20], [21]. The ideology behind this experiment is the application of an individual multiport decoder and encoder at the OLT which can be utilised by all the other subscribers attached to the OLT network [22].

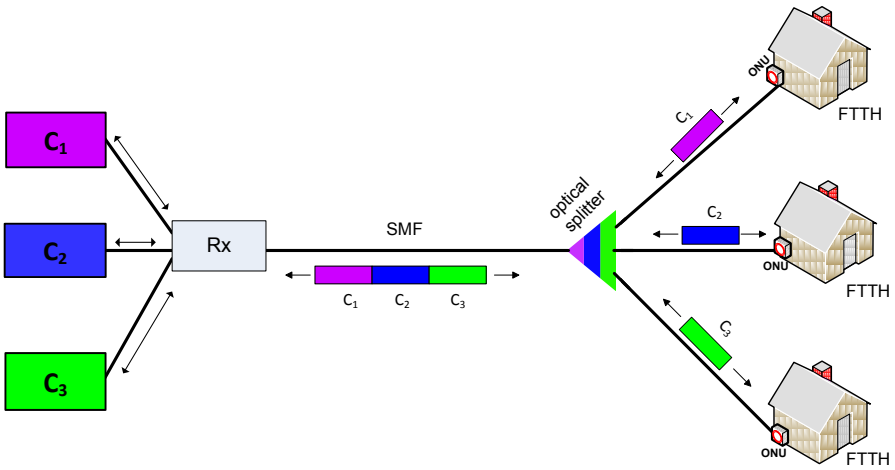

Figure 1.4(c): CDMA passive optical network

D. Subcarrier multiple access (SCMA)

As the name implies and as demonstrated in Fig 1.4(d), the upstream data from the subscribers ONU is a baseband signal that is modulated onto an electrical carrier with a frequency that is independent to each subscriber in the PON network. The electrical signal is then converted to an optical signal for fiber optic transmission to the OLT. Hence the electrical carrier is the *subcarrier* whilst the optical carrier is the principal carrier [23]. At the OLT, the received optical signal on a single photodetector (PD) receiver converts the optical signal back to an electrical signal whilst demultiplexing them into the frequency domain. The received optical signal comprises of a single wavelength but contains several RF frequency bands that each represents the different individual subscribers respectively.

Unlike the TDMA scheme, SCMA does not require any time synchronisation technology for syncing each transmission channel since each RF channel is unique to individual subscribers; there can be less probable collision occurrence of channels. In some cases where the optical wavelengths at each ONU for upstream data transmission are close together, there can be a very narrow spacing between the independent wavelengths which results to beat noise at the PD optical receiver. This is due to the mixing of the individual wavelengths at the PD. The beat noise is referred to as optical beat interference (OBI) [24] and constitutes a major drawback in adopting the SCMA scheme as an access technology.

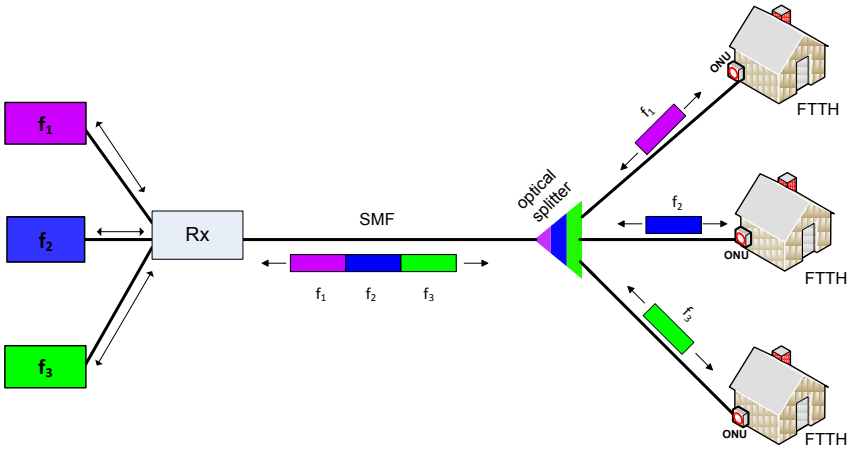

Figure 1.4(d): SCMA passive optical network

1.3.1 Comparison of Access Technologies

All the discussed four different technologies for upstream access technology have various benefits in a PON infrastructure either from the cost effective benefit or efficiency in scaling new subscribers but the one which has been widely adopted in industry is the TDMA access technology due to its capability to transport significantly high data rate than its counterpart with a less complex electronics inclusion and also it being the most cost effective as a standalone system. However some of the key advantages and disadvantages of all four access technology can be summarised in Table 1.1 as illustrated below [35].

	TDMA	WDMA	CDMA	SCMA
ONU bandwidth	Low	Very High	High	Intermediate
Splitting/MUX loss (dB)	High	Low	High	High
Technology Upgrade Capability	No: • Additional wavelengths required	Yes: • Increasing channel bitrate	No: • Complex signal processing	Yes: • additional subscribers • additional wavelengths
Costly System Electronics	• OLT optical receiver • ONU Laser	• Dense WDM demultiplexer • Wavelength stabilizer	• OLT optical receiver	• OLT optical receiver • Analog components • ONU Laser
ONU Simultaneous Transmission	Number of ONUs affects transmission	Number of ONUs does not affect transmission	Number of ONUs does not affect transmission	Number of ONUs does not affect transmission
Modulation format transparency	No	Yes	Yes	Yes
ONU Synchronisation Management	Yes	No	TS* : Yes SS** : No	No

***** : Time-Sliced OCDMA
****** : Spectrum-Sliced OCDMA

Table 1.1: Features of the Access Transmission Technology in a PON network, [35].

1.4 Optical Technology for Downstream Data Transmission

The previous section aimed to present the four significant uplink transmission schemes used in PON infrastructure. In the case of the downstream data transmission, the four technology schemes are Time Division Multiplexed (TDM), Wavelength Division Multiplexed (WDM), Code-Division Multiplexed (CDM) and Subcarrier Multiplexed (SCM) schemes.

WDM-PON has its benefits in being a cost effective scheme as it can utilize low cost optical laser sources for long haul transmission and still deliver high data rate traffic. In this scheme, the ONUs can make use of tunable lasers such as the distributed feedback (DFB) laser [25] and the vertical cavity surface emitting lasers (VCSEL) [26] to tune to the pre-allocated transmitted wavelength in a NGA PON network.

	TDM-PON	**WDM-PON**
Bandwidth	Good	Better
Cost	Low	Higher
Security	None	Guaranteed
Scalability	Complex	Simple
QoS	Good	Better
Bitrate	approx. 1 and 2.5 Gbit/s	1, 2.5, 4, 10 Gbit/s
Max. Splitting ratio	> 1 : 320	> 1 : 32

Table 1.2: Comparison of TDM-PON and WDM-PON for downstream access solution, [35].

Looking at the benefits in using WDM-PON against TDM-PON, a brief comparison can be made in Table 1.2. This table evidently demonstrates the advantages of the WDM-PON access technology over TDM-PON. The downstream transmission speed

requirement for Next-Generation PON (NG-PON) is set at a minimum 10 Gbit/s whilst the upstream speed requirement is set at 2.5 Gbit/s (*value is subject to increase with technology advancement*). NG-PON will meet the next generation access (NGA) requirement which was created by the task force ITU-T to support the standardization of a bidirectional Gigabit capacity for PON networks (XG-PON) [27][28]. As discussed above, WDM-PON will meet the requirements as well as a combination of WDM and TDMA technologies classified as WDM/TDMA-PON [29] [30] but WDM-PON remains the principal focus of this thesis.

E. Coherent Optical Communication in Access Network

As the use of WDM technology advanced in recent years and more capacity is required at the receiver station, coherent optical access network [31] became apparent to sustain the growth in data rate. The downlink transmission involves coherently combining two SMF fibers with continuous light-wave signals emitting wavelengths at different spectrums, with one light-wave upconverted with the modulated digital data [Fig 1.5]. The received signal at the ONU correspondently has a coherent optical detection scheme in place. There have been several variations of coherent optical detection since its first introduction by DeLange in 1970, [32] but did not gain traction until 1980's. In the coherent access network, some early experiments demonstrated the receiver station using four outputs to detect the amplitude and phase of the signal alongside the generated local oscillator (LO) and can include optical splitters, combiners or optical interleaver. These four outputs are then detected by a four PD. The primary detection scheme behind coherent optical detection can be distinguished into two variations, homodyne and heterodyne detection (*the latter being important to this thesis*). Both schemes differ in the

method of retrieving the LO at the receiver station which can then be used for the upconversion of the upstream data. The benefits of the coherent detection in the access network are numerous. One of which is the ability to tune to the desired LO. Also the WDM-PON network is extended and becomes a long reach optical access network largely due to the intrinsic nature of an entirely optical data transmission. The infrastructure becomes truly passive due to the disregard for amplification across the optical distribution network. Additional benefits to coherent optical communication shall be discusses at great depth in *Chapter 6*.

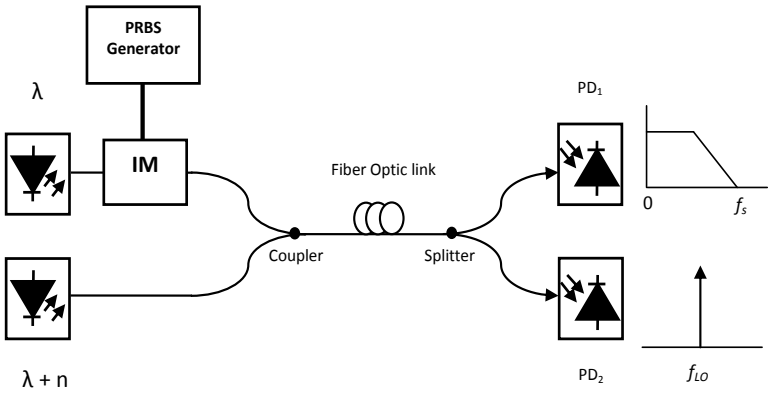

Figure 1.5: Conceptual configuration of a Coherent Optical Communication

F. Orthogonal Frequency Division Multiple Access (OFDMA)

Another multiple access solution that can provide the capacity requirements for NGPON-2 is the use of the orthogonal frequency division multiplexed (OFDM) modulation scheme in a PON infrastructure [33]. One of the reasons for utilizing (*the already widely adopted technology*) OFDM is due to its ability to offer high spectral efficiency by using low bit rate subcarriers to transport different QAM symbols simultaneously. The orthogonal nature of OFDM works by aggregating independent subcarriers closely across the spectrum with defined symbol duration. This makes the

subcarriers overlap without causing interference during transmission [Fig 1.6]. OFDM allows the possibility to allocate different users individual OFDM subcarriers making it a candidate for multiple access technology. It is also possible to manage and perform dynamic bandwidth allocation to different applications throughout the PON network. Another benefit in using OFDM in access network is due to its high resistance to linear dispersion such as chromatic dispersion. This characteristic makes OFDM a strong candidate in long reach network planning especially for in-door scenarios to deliver subscriber media content without the need for dispersion compensation.

The increase in capacity demand over optical communication channels has lead to the deployment of an all optical data transmission in the OLT making the disregard of electrical-to-optical processing less prevalent and adopting more of an all optical signal transmission scheme, in this case optical OFDM (OOFDM) [34].

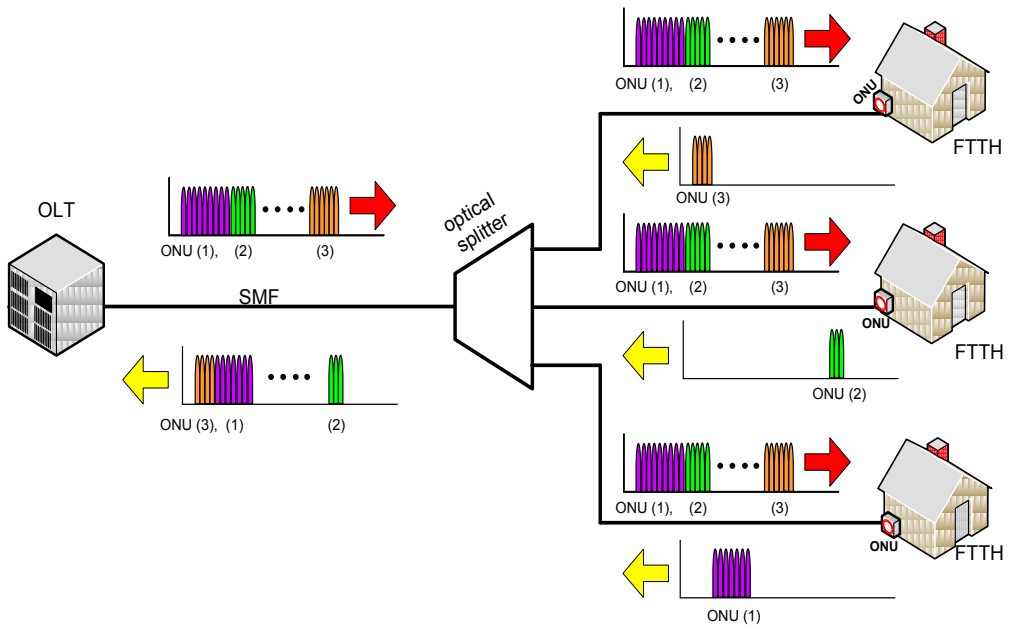

Figure 1.6: OFDMA architecture

1.5 Research Aim

The purpose of this thesis is described as follows:

- To demonstrate the application of both single mode fibre (SMF) and multimode fibre (MMF) POF (which is a cost effective alternative to copper cables) in an indoor environment using various optical transmission techniques to deliver high capacity optical modulated millimetre wave (mm-wave) signals.

- Comparing the applications of recently recommended in-door access optical fiber, BI-SMF as an alternative to MMF (POF) for millimetre-wave signal transmission.

- Review of the Offset Launch technique as a method of bandwidth enhancement between coupled SMF and GI POF fibre cables over mm-wave signal transmission schemes.

- Designing an optical mm-wave signal based on the optical carrier suppression (OCS) transmission scheme which creates a double sideband for effective throughput, less tolerance to chromatic dispersion and high receiver sensitivity for mm-wave signals e.g. 60 GHz band.

- To demonstrate RoF millimetre-wave (mm-wave) delivery based on Remote Heterodyne Detection (RHD) over GI-POF at the receiver station for indoor Gbit/s short reach baseband service. This transport scheme is further investigated over FSO system for the indoor application.

- Investigate the methodology of Free Space Optics (FSO) as an optical wireless communication between MMF optical fibre and photodetection in an indoor environment whilst considering the signal-to-noise ratio (SNR) and bit error rate (BER) performance of detected signals in both scenarios.

- Exploring the variables that affect the received optical signal in an optical wireless communication (OWC) system based on line-of-sight propagation with assumed absolute collinear lightwave beam transmission. Considered variables are the atmospheric impairments which comprises of beam spread loss and atmospheric attenuation in FSO link.

This thesis is compiled to report system modelling of the above aims by researching, modelling and simulating various methods of achieving Gbit/s data capability in an indoor environment by a means of utilising radio-over-fibre (Rof) technology.

1.6 Original Contributions

In relation to the research context of this report, the author has:

1. Demonstrated three key optical transmission techniques for the design of radio-over-fiber network for a fixed wireless access network operating in the microwave or millimetre-wave (mm-wave) frequency band by analysing three methods of transmitting mm-wave signals (i.e. 60 GHz) over optical fibre cables, namely OCS, OFM and RHD transport schemes.

2. A method transporting RF channels such as LTE, Wi-Fi and proposed IEEE 802.11ad (WiGig) as a 60 GHz channel band over SMF coupled with GI-POF or BI-SMF optical fibre cable lengths.

3. The Offset Launch technique to excite few propagation modes at the lightwave entry of the (MMF) GI-POF from the SMF optical fibre for bandwidth improvement on modulated optical mm-wave signal.

4. Addressed the effect on attenuation observed in the GI-POF optical fibre cable when using optical carrier-waves (CW) at 1550 nm and 850 nm wavelengths to transport mm-wave signal using OCS, OFM and RHD delivery scheme.

5. Demonstrated the network architecture of optical wireless communication system (OWC) for mm-wave signal over free-space optical (FSO) transmission performance whilst indicating atmospheric irregularities such as beam-spread loss and signal degradation.

1.7 Thesis Framework

This thesis is structured in 7 chapters.

Chapter 1: After presenting the objectives of this thesis, Chapter 1 sets out to highlight the principles of optical fibre technology for downstream data both in the traditional metropolitan network and in the fibre based access network. The comparison of different types of access transmission schemes are discussed along with a brief insight to the transmission schemes used in this thesis report.

Chapter 2: In this chapter, the introduction to polymer optical fibre (POF) as an access network optical fibre cable is explained along with its newly proposed counterpart, BI-SMF optical cable, as suitable candidates to meet the next generation access network and the cumbersome throughput data transmissions. The benefits to radio-over-fibre are discussed in addition to the conventional methods of mm-wave generation.

Chapter 3: Looks at the fundamentals of offset launch technique both the theory aspect and reported results describing its capabilities of bandwidth improvement between coupled SMF and MMF. This chapter also describes the concept of optical wireless communication (OWC) system for free-space optics transmission in an indoor environment. The atmospheric irregularities that create signal degradation are also discussed.

Chapter 4: Presents the mm-wave generation technology by optical carrier suppression (OCS). This chapter also highlights the simulation architecture of OCS transport over POF and BI-SMF fibers long with OWC whilst comparing the characteristics of the received signal.

Chapter 5: Examines the next method of mm-wave generation through optical frequency multiplication (OFM) creating RF harmonic components in the 60 GHz region. The theory of OFM using MZI filters is evaluated with the simulation of proposed design of a dual-drive modulator based OFM system for mm-wave generation. The effect of increasing spectral range to mm-wave region reduces bandwidth and increases signal error on OFDM modulated wireless signals such as the implemented LTE and Wi-Fi are explored. Whilst transmissions over POF, BI-SMF fibre cables along with OWC system are also analysed.

Chapter 6: Explores the final 60 GHz transport scheme based on remote heterodyne detection (RHD). This scheme demonstrates the ability of a low-power transport scheme of mm-wave signal using coherent optical communication. Concepts of implementing offset launch conditions are explored for bandwidth improvement along with utilising 850 nm wavelength band over MMF. The simulation of RF wireless channels representing IEEE 802.11 b/g/ad are also explored over POF, BI-SMF and OWC links.

Chapter 7: Finally, the conclusion to this thesis is presented with the premise of future work.

1.8 Summary

This chapter set out to highlight the research aim and thesis framework along with the original contribution to the application of broadband technology. Comparison of broadband data requirement trend were globally analysed along with already existing optical fiber technology that deliver the last-mile network. Further discussion was made to demonstrate existing network topology of various optical fibre access network and its relation to the research conducted in this thesis.

References

[1] Variation to and Exemption from BT's undertakings under the Enterprise Act 2002 related to Fibre-to-the-Premises and fibre Integrated Reception System, 23 March 2010, Ofcom.

[2] UK Communications Infrastructure Report, 6 October 2013, Ofcom.

[3] Winston I. Way, "Optical fiber based microcellular systems: An overview," *IEICE Transactions on Communications*, vol. E76-B, no. 9, pp. 1091-1102, September 1993.

[4] T. S. Chu and M. J. Fans, "Fiber optic microcellular radio," IEEE Trans. Vehicular Technology, vol. 40, no. 3, pp. 599-607, August 1991.

[5] Case study Wi-fi access at London 2012 – BT Wi-fi

[6] The Institution of Engineering and Technology 2013, *"Delivering London 2012: ICT implementation and Operations"*.

[7] Cisco Visual Networking Index: Forecast and Methodology 2013.

[8] Roine R, Ohinmaa A, Hailey D. "Assessing Telemedicine: A systematic review of the literature" *Canadian Medical Association Journal* 2001; 165(6): 765-771.

[9] Whitten P, Holtz B. "A series of papers for those yearning to propel telehealth to new heights". *Telemedicine and e-Health* 2008; 14(9): 952-956.

[10] "*FTTH Business Guide*", Fiber to the home Council Europe, 2013.

[11] European Commission, Quality of Broadband Services in the EU, March 2012.

[12] X. Lin and O. Sneizko, "The evolution of cable TV networks", in *Optical Fiber Communications IVB*, I. Kaminow and T. Li, Eds. New York: Academic, 2002.

[13] Case Studies Collection, FTTH Council Europe, January 2013.

[14] E. Harstead and P. H. Van Heyningen, "Optical access network," in *Optical Fiber Communications IVB*, I. Kaminow and T. Li, Eds. New York: Academic, 2002.

[15] "Gigabit-capable Passive Optical Networks (G-PON)," ITU-T Recommendation G.984 series.

[16] IEEE Standard for Local and Metropolitan Area Networks-Specific Requirements–Part 3: Carrier Sense Multiple Access With Collision Detection (CSMA/CD) Access Method and Physical Layer Specifications Amendment: Media Access Control Parameters, Physical Layers and Management Parameters for Subscriber Access Networks, IEEE Standard 802.3ah – 2040.

[17] H. Suzuki, M. Fujiwara, T. Suzuki, N. Yoshimoto, H. Kimura, and M. Tsubokawa, "Wavelength-tunable DWDM-SFP transceiver with a signal monitoring interface and its application to coexistence-type colorless WDM-PON," in Proc. 33rd European Conference and Exhibition of Optical Communication (ECOC2007), Post-deadline paper PD3.4.

[18] N. J. Frigo, P. P. Iannone, and K. C. Reichmann, "Spectral slicing in WDM passive optical networks for local access," in *Proc ECOC 1998,* pp. 119-120.

[19] K. Kitayama, X. Wang, and N. Wada, "OCDMA over WDM PON-Solution path to gigabit-symmetric FTTH," *J. Lightw. Technol.*, vol 24, no. 4, pp. 1654-1662, Apr. 2006.

[20] G. Cincotti, N. Wada, and K. Kitayama, "Characteritics of a full encoder/decoder in the AWH configuration for code-based photonic routes – Part 1: Modeling and design," *J. Lightw. Tehcnol.,* vol. 24, no. 1, pp. 103 – 112, Jan. 2006.

[21] N. Kataoka, G. Cincotti, N. Wada, and K. Kitayama, "Demonstration of asynchronous, 40 Gbps x 4-user DPSK-OCDMA transmission using a multi-port encoder/decoder," in *Proc. Eur. Conf. Opt. Commmun.,* 2011, paper Tu.C.4.

[22] Y. Tanaka, S. Yoshima, N. Kataoka, J. Nakagawa, N. Wada, and K. Kitayama, "100-km uplink transmission of 10G and 1G ONU co-existing TDM-OCDMA-PON system using dual-rate burst-mode receiver," in *Proc. Opt. Fiber Commun. Conf.* Mar. 2011, paper OThT5.

[23] T. E. Darcie, "Subcarrier multiplexing for multiple-access lightwave networks," *J. Lightwave Technol.,* vol. LT-5, pp. 1103-1110, Aug. 1987.

[24] C. Desem, "Optical interference in subcarrier multiplexed systems with multiple optical carriers," *IEEE J. Select. Areas Commun.,* vol. 8, pp. 1290 – 1295, Sept. 1990.

[25] H. Suzuki, M. Fujiwara, T. Suzuki, N. Yoshimoto, H. Kimura, and M. Tsubokawa, "Wavelength-tunable DWDM-SFP transceiver with a signal monitoring interface and its application to coexistence-type colorless WDM-PON," in *Proc. Eur. Conf. Opt. Commun.,* Sep. 2007, paper PD3.4.

[26] C. Chang-Hasnain, "Optically-injection locked tunable multimode VCSEL for WDM passive optical networks," in *Proc. Int. Nano-Optoelectron. Workshop (i-NOW),* 2008, pp. 98-99.

[27] 10–Gigabit–Capable Passive Optical Networks (XGPON): Physical Media Dependent (PMD) Layer Specification, ITU-T G.987.2, 2009.

[28] 10–Gigabit–Capable Passive Optical Networks (XGPON): General Requirements, ITU-T G.987.1, 2009.

[29] G. Talli and P. D. Townsend, "Hybrid DWDM-TDM long-reach PON for next generation optical access," *J. Lightw. Technol*, vol. 24, no. 7, 00. 2827-2834, Jul. 2006.

[30] J. –I. Kani, "Enabling technologies for future scalable and flexible WDM-PON and WDM/TDM-PON systems," *IEEE J. Sel. Topics Quantum Electron.,* vol. 16, no. 5, pp. 1290-1297, Sep.-Oct. 2010.

[31] S. Smolorz, E. Gottwald, H. Rohde, D. Smith, and A. Poustie, "Demonstration of a coherent UDWDM-PON with real-time processing," in *Proc. Opt. Fiber Commun. Conf. Nat. Fiber Optic Eng. Conf.,* Mar. 2011, paper PDPD4.

[32] O. E. DeLange, Proc. IEEE 58, 1683 (1970)

[33] N. Cvijetic, "OFDM for next-generation optical access networks," *J. Lightw. Technol.,* vol. 30, no. 4, pp. 384-398, Feb. 2012.

[34] J. Armstrong, "OFDM for Optical Communications," *J. Lightw. Technol.,* vol. 27, no. 3, pp. 189-204, Feb. 2009.

[35] Chang-Hee Lee, W. V. Sorin and B. Y. Kim, "Fiber to the Home Using a PON Infrastructure," *J. Lightw. Technol.,* vol. 24, no. 12, pp. 4568-4583, Dec. 2006.

Chapter 2

History of Polymer Optical Fiber

2.1 Overview of POF

The development of POF has been in existence as far back as the early seventies. A non-exhaustive compilation of the History of POF development [8] has been illustrated in Table 2.1. The list is thoroughly open to debate on the accuracy of the timeline and may have other unaccounted evolution of POF both acknowledgements have been reiterated by the publisher [8].

POF optical cables have been in existence for many years but it has been overshadowed by the much more publicly acclaimed industry game changer, the silica optical fibers. Nevertheless the rise in need for a low cost, short-reached and high speed optical data communication has sprung an unprecedented interest in POF cables. Countries such as China, Korea and Taiwan are at the forefront of POF manufacturing due to their earlier interest in the polymer fabrication. However other developed countries with existing optical fiber infrastructure such as America, Japan and European countries have taking up the initiative to further their industrial practises with the polymer technology because by not doing so puts them at an

economical and competitive disadvantage when POF industrialisation and globalisation manifests.

The earliest reported manufactures of POF was by Pilot chemical of Boston soon after came the widely accepted advancement by DuPont in the late sixties [1]. At this point in the lifecycle production of the type of monomer material used, the attenuation was approximately in the range of 1000 dB/km. Further Research and Development (R&D) by Mitsubishi Rayon of Japan led to better quality product with a much more reduced attenuation loss down to 125 dB/km at 650nm wavelength which was a step-index (SI) POF fiber with a bandwidth of 50 Mbit/s over 100 meters. The SI-POF can be addressed as the earliest type of polymer optical fiber from all variations and today it is seen as the most appreciated POF cable [2]. Its counterpart, the optical fiber made out of silica-glass was already in existence and accessible in voluminous quantities from the manufacturers at a lower price even though at now the loss of 1 dB/km at 1550nm wavelength was attainable.

In the quest to further develop better products, Yasuhiro Koike and his team at Keio University in Japan developed high-bandwidth graded-index polymer optical fiber (GI-POF) in 1992. This variant of GI-POF was made using polymethylmethacrylate (PMMA) and could boast of 1 GHz-km high bandwidth with an attenuation of 113 dB/km at 650 nm [3]. Then came the scientific discovery of doping GI-POF with fluorine (by Koike et al) since its absorption bands are further into the infrared zone. The perfluorinated polymer was adapted to GI-POF structure and became PF-GI-POF which had attenuation of <50 dB/km at 1300 nm wavelength [4]. It then became feasible to further reduce the attenuation of PF-GI-POF to 30 dB/km [5], 15 dB/km [6] and then 8 dB/km at 1070 nm wavelength which is classified as one of the lowest POF attenuation till date [7]. This was achieved by using the material cyclic transparent optical polymer (CYTOP) to create the significant reduction in low

attenuation (less than 10dB/km) in a POF cable produced by Asahi Glass in Japan. With POF attenuation produced at 20 dB/km means data communication of 1 kilometre (km) can be achieved. This evidentially places POF as an alternative to provide data commutation as a transmission medium where traditional copper data cables and glass multimode fibres have been deployed such as in access networks and indoor applications.

Year	History of Polymer Optical Fiber (POF) Evolution.
1968	DuPont first develop PMMA
1977	PMMA – d8 developed by DuPont
1978	DuPont sold all products and patents to Mitsubishi Rayon (MR)
1990	Step Index Plastic limited to 5 MHz/km
1990	Koike announced development of GI-POF with bandwidth of 3 GHz/km
1991	Koike develops single-mode POF (SI-POF)
1992	Bates of IBM demonstrates 500 Mbps over 100-m of SI-POF
1992	Koike et al show 2.5 Gbit/s over 100-m POF using red laser
1993	Sasaki et al., of Keio University report POF optical amplifier
1994	2.5 Gbit/s over 100-m transmission with GI-POF is demonstrated using 650nm laser diode.
1995	Keio University & KAST develop fluoropolymer
1996	Yamazaki of NEC demonstrates 155 Mbit/s ATM LAN
1997	Yamazaki of NEC reports 400 Mbit/s POF link for 1394 over 70-m
1997	Asahi Glass reports on perfluorinated POF GI-POF
1997	Imai of Fujitsu reports 2.5 Gbit/s over 200-m using 1.3nm FP-LD, InGaAs APD and GI-POF
1998	Asahi Glass reports at OFC-98 new PF fiber CYTOP with attenuation of 50 dB/km from 650-1300nm with further improvements in bus possible. Bandwidth of 300-500 MHz-km.
1998	XaQti demonstrates at Interop 1 Gbit/s over 200-m using PF GI-POF
1999	Lucent reports 11 Gbit/s over 100-m of Lucina fiber (PF GI-POF)
2000	Asahi Glass claims Lucina PF GI-POF will be available in June 2000
2000	European Commission starts three POF programs under Optomist name: Agetha, I/O and Home Planet

2001	Redfem Optics and KAIST of Korea announce developments of photonic crystal POF
2002	IEEE 1394B Standard ratified; IDB-1394 for Automobiles completed
2002	Fuji film announces availability of GI-POF
2003	Digital Optronics plans to offer graded index POF for commercial sale
2004	Optimedia of Korea offers OMMA GI-POF for sale in the US
2005	Chromis fiber optics announces the availability of PF GI-POF commercially as fiber only
2006	Fuji Photo Film announces GI-POF with a bandwidth of 10 Gbit/s over 50-m
2007	Georgia Tech researchers show 30 meters at 40 Gbit/s over PF GI-POF
2008	Georgia Tech researchers show 100 meters at 40 Gbit/s over PF GI-POF

Table 2.1: Published developments of Polymer Optical Fiber, [8]

2.2 What is POF's structure?

As discussed earlier, POF is a polymer optical fiber used for optical communication. It is made from the PMMA material known for its characteristics to create a transparent polymer. The POF fiber structure is circular in shape at its cross section and has three key layers that describe the overall cable. The simplistic three layers of the polymer optical fiber is; the Core, Cladding and Buffer coating or Jacket used as a protective coat [Fig 2.1]. The core material can be made to have a varying refractive-index profile to produce different types of POF cables.

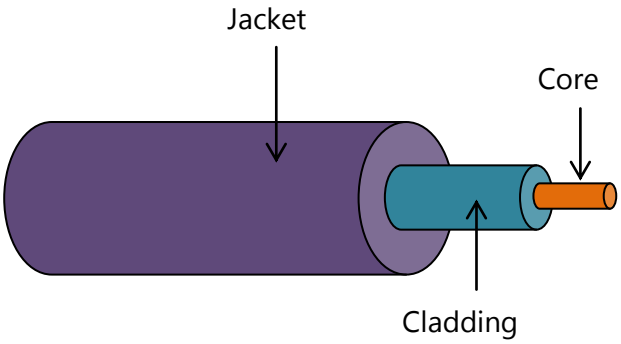

Figure 2.1: Polymer Optical Fiber Structure

The two types of optical fibers used widely in optical communication are the Step index (SI) profile fibers and Graded Index (GI) profile fibers. This relationship also reflects on the type of mode the optical fibers have in which there are two categories, the single mode and multimode fiber.

Moreover in the development of POF there are also single-mode POF and multimode POF fibers. Single-mode POF (SMPOF) developed in the early nineties [9] is very lossy by having a larger attenuation compared to single-mode (silica) glass fibers and also conventionally brittle making it not suitable for rigorous handling. The other type of POF is the PMMA POF which also has its two variants, the SI and GI models. The PMMA GI-POF has a greater bandwidth than the SI-POF because of the continued reduction in refractive index (as a gradient) from the fiber axis and moving outwards to the cladding. This also is interpreted as quoting the SI-POF as having more modal dispersion than the GI-POF [2]. The PMMA POF has a cored diameter between 250 and 1000 µm inclusive and the PF GI-POF has a core diameter between 50 and 120 µm inclusive (but mostly at 65 µm) whilst SMF has a core diameter between 5 and 20 µm inclusive making fibers with a larger core diameter and numerical aperture (NA)

less difficult in coupling the planar waveguides with other connectors or fibers, making them cost effective in wise spread installation deployment with no need for expensive alignment machinery. Additionally there are several other types of fibers worth mentioning with different profile indices such as the double-step index fiber, the multi-core step index fiber, the double step index multi-core fiber, the multi-step index fiber and the semi-graded index fiber. All these mentioned optical fibers have attributes which are not pertaining to the requirement for modern broadband delivery and as such their adaptation has been negligent. Throughout the report of this thesis, the focused applications of the GI fiber in system simulation are almost constantly implied.

2.2.1 Attenuation

In every optical fiber cable the laser light that travels along a straight optical fiber cable experiences a power loss. This power loss is known as *attenuation* and as a rule of thumb, the power decreases as the distance of the optical fiber increases. The decrease in optical signal power is exponential to the distance of the optical fiber and has the formula expressed as:

$$P(l) = P(0)10^{-\alpha \cdot l\,/\,10} \tag{2.1}$$

Where l is the symbol that represents the length of the optical fiber and α is the *attenuation coefficient* of the optical fiber. In most documented description of attenuation, it is expressed as a function of the fiber length with the attenuation expressed in decibels. This transforms equation (2.1) to:

$$\alpha = -\frac{1}{l}10 \cdot \log\frac{P(l)}{P(0)}\,\mathrm{dB/km} \tag{2.2}$$

Fig 2.2 shows the different wavelength dependence of attenuation in POF fabricated using the material PMMA. As indicated by the figure, the loss curve for a PMMA POF fiber shows a transmission window with least attenuation at 530 nm, 570 nm and 650 nm. Theses wavelength values correspond to the colour of electromagnetic waves which are blue (530 nm), green (570 nm) and red (650 nm). All these colours (or wavelengths) are located in the visible wavelength region and hence making this POF optical fiber cable applicable eye-safe for in-building cabling distribution for broadband connectivity as it can easily be tested for defaulting by simply observing if there is illumination at the end of the POF cable. This is a major advantage as it simplifies troubleshooting for the POF installer. The minimal attenuation at 650 nm is also a transmission window that makes PMMA POF applicable for red light emitting diode (LED) transmission. It is also important to observe that in Fig 2.2, the 125 dB/km attenuation at 650 nm restricts the use of PMMA optical fibers for data communication to less than 100m. This is also true for the 530 nm and 570 nm transmission windows which have attenuation at 90 dB/km.

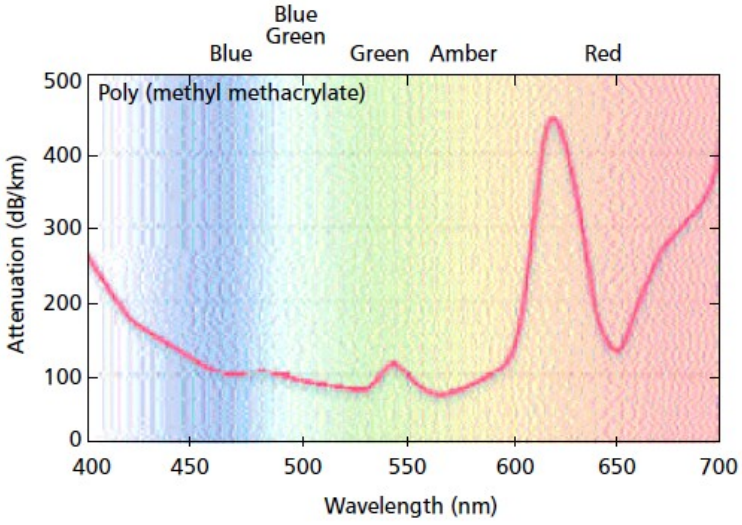

Figure 2.2: Transmission loss spectrum for PMMA POF [10]

The more modern variant of POF optical fiber, the PF-GI-POF, has a wider acceptance for shorter distance data connection due to its larger core diameter as discussed earlier but the most distinguished feature of importance is the transmission window. The PF-GI-POF has a longer acceptable wavelength loss curve that ranges from 650 nm to 1300 nm. This transmission window has the advantage of using longer wavelengths on this particular POF material. It is beneficial in wavelength division multiplexing (WDM) where several wavelengths may be required with low attenuation values. It also implies that PF-GI-POF fiber or fibers made using the fluorinated material, can operate with the less expensive emitters and receiver connectors designed for the silica mode optical fibers at 850 nm to 1300 nm. By observing Fig 2.3 it can be concluded that the attenuation from 650 nm to 1300 nm is below 40 dB/km throughout the wavelength range. This low attenuation attribute allows for the PF-GI-POF fiber to be used for longer lengths spanning several hundreds of meters. It has been demonstrated that attenuation values of 8 dB/km which allows transmissions of up to 1000-m and more has been demonstrated by Chromis Fiberoptics Company and others [11] and [12] respectively.

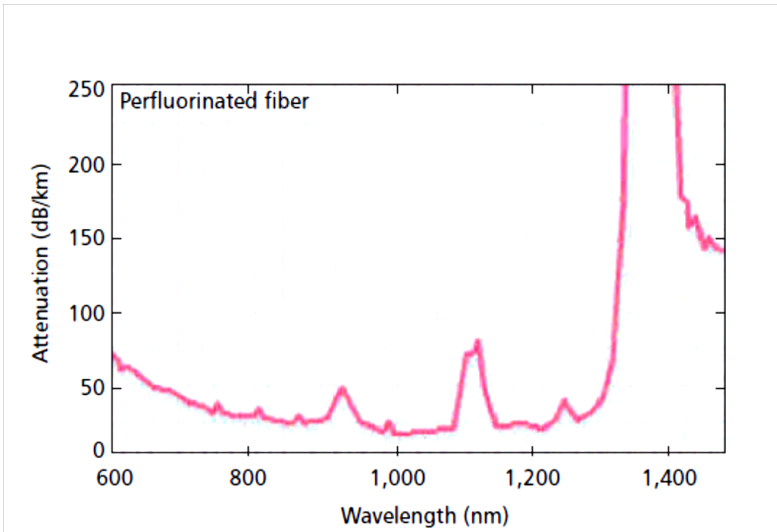

Figure 2.3: Transmission loss spectrum for PF POF [10]

2.2.2 Benefits of POF over Silica Fiber and Copper

As discussed earlier, there are potential advantages to using POF and its variants over silica (glass) fiber or copper wire in an in-home LAN network, some of which are described in section 2.4. However here are the outlines of the key benefits:

- **Larger core diameter:** This characteristic of POF plays a pivotal role because with a large core diameter (compared to silica fibers) of up to one millimetre (1 mm), it makes the polymer a lot easier to handle than silica fibers. This also makes it less expensive (not needing costly tools to make connection) than silica fibers when acquiring tools for splicing and alignment of fibers which may be needed at home for frequent cabling installation and maintenance.
- **Connection simplicity**: As outlined above. POF can be cut with a razor blade at home and does not need a trained expensive engineer or equipment.
- **Low-priced**: The price of POF has become relatively cheap. Its market price has reduced year-on-year and it with as little as $1 a one meter GI-POF can be purchased. This also reflects on the price of components used with POF which also are relatively cheap.
- **Bandwidth**: This factor depends on fabricated manufacturer's specification. Theoretical bandwidth can range from 160 MHz to 1200 MHz for 850-nm and 1300-nm respectively.
- **Interference:** Copper which is a metal conductor suffers from electromagnetic interference (EMI) especially when bundling of copper cables is installed. POF doesn't suffer from this effect irrespective of bundling.

2.3 Bending-loss insensitive single mode fiber (BI-SMF): An alternative to POF

2.3.1 Introduction to BI-SMF optical fiber

As discussed previously, the application of POF cables for in-house broadband access networks has been witnessing almost an exponential growth [13]. The article [13], demonstrates a sustainable percentage increase in market revenue for POF application for wiring buildings. In year 2008, 2009, 2010 and 2011 yielding a 20%, 20% and 26% increase, respectively. In these four years alone, the total revenue for the building wiring market was a substantial $ 637 million. When considering all other industry application of POF from industrial, medical, automobile, consumer and miscellaneous the total US market in the four years to 2011, generates $ 8581 million.

However there is also another alternative to POF cables that have recently gained notification. POF cables has several disadvantages one of which is due to its bandwidth limitations as a result of its huge modal dispersion, also it can be limited to data rate/length compared to single mode fibers. There are also disadvantages such as coupling loss alignment between the SMF and POF.

The single mode fiber technology has been well advanced and can support the back haul network in transporting terabit per second data over a single mode fiber (SSMF) [14], [15], [16] and [17]. In the access network where there are a lot of manipulations of the fiber, drop-cable networking in a limited space, a standard SMF (SSMF) has to be carefully manoeuvred for connection around bends and may not be durable for such environments. To mitigate this issue, there have been several recommendations by the International Telecommunication Union - Telecommunication Standard (ITU-T) to regulate the manufacturing of single-mode fiber cables which will be suitable

for in-building access network applications. These BI-SMF cables have a reduced attenuation effect on the optical light power when the optical fibers are bent to an acceptable radius. The ITU-T standardization lists the Category B fibers (ITU-T G.657.B3) specification that is required to accept bending loss of 5mm minimum radius for distances less than 1000-m over the 1260 to 1625 nm wavelength range [18]. The recommended ITU-T attenuation of the BI-SMF optical cable is 0.4 dB/km whilst its dispersion is set at 18 ps/nm/km. There are several reported experiments with these BI-SMF optical fibers deployed for in-building optical networks [19], [20], [21], [22] and also reported fabrication of BI-SMF with a progressive reduced attenuation [23], [24], [25], [26] and in some reported experiments BI-SMF optical fibers are used to deliver terabits/s data for long haul links [27]. An additional benefit in using BI-SMF cable is the case of mode alignment and compatibility. The multimode fiber has several active modes (e.g. 10 – 20 modes) during signal propagation and the long-haul SMF has only a few, one or two modes. At the residentially gateway where cross-connectors are used such as wavelength-convertors which requires single mode operation can cause impairments and mode filtering. To solve this impairment an all-SMF-fiber coupling or all-MMF-fiber connections should be deployed [28].

In this thesis the application of BI-SMF optical fiber is simulated with different transmission schemes to compare its performance alongside POF so as to determine its suitability for an optical access network cable for in-building installation. The various attenuation effect of different *realistic* bending radius witnessed in an in-house wiring installation of the BI-SMF optical cables would also be considered for simulation investigation.

2.4 Application of Access Network Links

In the late eighties, shorter-distance data communication from LANs, data centres or any machine to machine communication were still predominantly in their analogue operated prominence where twisted pair cables (UTP) were deployed to provide the then sufficient baseband transmission schemes of 10 Base-T Ethernet. A report outlines the (approximate) increase in connected private customers globally by number and bandwidth [Fig 2.4]. The report goes on to explain that there will be 500 million broadband connections globally as early as 2010. This makes the argument that in the anticipated future, the average household or building connections will have data rates from 100 Mbit/s to 1 Gbit/s as an average broadband connection.

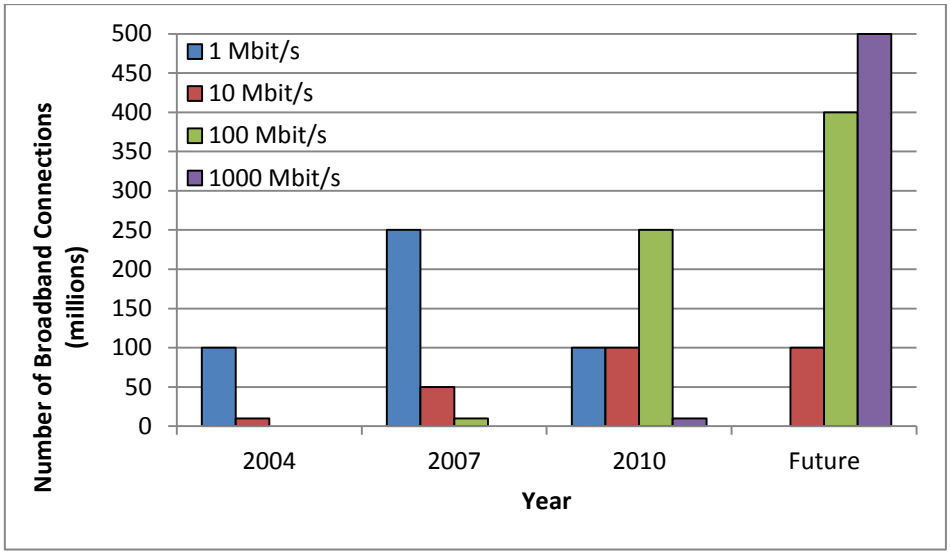

Figure 2.4: Demand for Broadband access connections worldwide (estimation from Teleconnect Dresden)

The in-home broadband network is mostly connected using wireless network to transmit radio based signals like wireless local area network (WLAN) and wired network which uses unshielded twisted pair (UTP) cable throughout the building. UTP

lags behind in terms of delivering the required broadband QoS as explained previously and is susceptible to electromagnetic interference (EMI) with increasing frequency.

	Copper	Silica (SMF)	POF
Bandwidth	100 Mbit/s over 100-m	approximately unlimited	40 Gbit/s over 100-m
Deploy	Cumbersome Installation	Difficult Installation	Very Simple Installation
Loss	High attenuation/distance	Very Low attenuation/distance	Low attenuation/distance
Flexibility	Flexible	Brittle	Flexible

Table 2.2: Comparison of Copper, Silica Optical Fiber and POF, [8].

The first real multimedia transmission based on POF installation in the home network to provide triple play services (Data, IPTV and VoIP) has been reported [29]. Several other reports have demonstrated the improvement of using POF for access network in the customer's premises [30], [31]. For the future home network that will deliver wireless gigabit data capacity using microwave signals at 60 GHz region has also been explored [32],[33] and using the 60 GHz band in the indoor environment over standard MMF [34],[35] and POF [36] has been reported.

2.5 Benefits of Radio-over-Fiber (RoF)

As discussed earlier in Chapter 1, the legacy telephony network has become incapable of handling the high bandwidth data services. Morden deployed wireless services and standards such as the Wi-Fi (or IEEE 802.11 standards) WiMax, UMTS

and LTE are all situated and operate in the lower spectrum of microwave RF band between 2 to 4 GHz. These bands are already congested and cause a heavy burden on the network when trying to introduce more data throughput down the channels. Higher radio frequency channels between the 40 – 64 GHz bands have been experimented on especially the 60 GHz band [37], [38], [39] but undoubtedly the higher the radio frequency the more attenuation due to propagation loss is experienced hence meaning more remote antennas (picocells) would be deployed to inter-connect radio access points (RAP) so as to cover a vast space of consumer presence to create a Distributed Antenna System (DAS). Overlaying the high frequency bands or microwave signals over optical fiber links (meaning Radio-over-Fiber) at every RAP overburdens the antennas processing capability in switching and routing the extremely high throughput data of microwave signals. The adapted solution is to consolidate all the signal processing, routing and switching functions of the RAP to the central office (CO) or OLT site. This becomes another strategic solution to reduce the cost value of the RAP by making it a simpler technology unit. This approach has the advantage of reducing network upgrade time, maintenance and new wireless technology when all management and signal processing are situated in one location. This also reduces the need for subscriber door-to-door maintenance. Delivery of microwave or millimetre-wave (mm-wave) signals over the traditional SMF, MMF or the recent BI-SMF optical fibers for access network functions shall be discussed in the subsequent chapters.

2.6 Why mm-wave technology?

The major interest in mm-wave spectrum (i.e. from 30 – 300 GHz) has tremendously increased but the main incentive for further research in these bands has come from the development of complementary-metal-oxide-semiconductor (CMOS) circuits. These compact CMOS transceiver circuits allows the development of mm-wave frequencies at similar manufacturing cost of equal circuitry that traditionally generate gigahertz (or less) radio signals. There is also the benefit of low loss and cost effective aspect that makes mass production a desirable consideration for developers. One of the first ever CMOS transceiver has been developed over the 60 GHz mm-wave radio [37], as a result making 60 GHz the most desirable frequency band for transceiver devices.

The main reason why 60 GHz has been selected as the RF band for WLAN device communication is based on it being an unlicensed frequency band in most developed and developing countries. This gives operators leverage in rapidly deploying a WLAN infrastructure at a reduced cost from spectrum licensing. Therefore due to the widely available electronics and research in 60 GHz radio frequency [38], [39], [40], the Wireless Gigabit (WiGig) Alliance was created with a mandate to create an interoperability specification for RF device communication at gigabit speed rate [41]. The MAC and PHY specification would allow data rates of at least 7 Gbit/s over the 60 GHz frequency band, faster than the current traditional Wi-Fi by a factor of 10. These specifications are drafted under the IEEE 802.11ad standard and are based on the IEEE 802.11n standard, meaning seamless integration between the existing 2.4 GHz and 5 GHz bands. Devices with capability of the tri-bands switching would be manufactured.

The 60 GHz mm-wave isn't without its impediments. The HF is vulnerable at high humidity because at this atmospheric condition the free-space loss is at 21 dB, lower than at 5 GHz RF band transmission in the same environmental condition. This limiting attenuation penalty is about 15 dB/km over an 8 GHz bandwidth. The 60 GHz has further attributes based on its free-space attenuation property such as creating spatial loss areas that can be of benefit when structuring frequency reuse in an indoor DAS network. This also makes it possible to have a secure network over short-range point-to-point links. With the capability of multi gigabit data transmission speed, the 60 GHz band becomes a great contender for indoor high speed wireless connectivity.

2.7 Millimetre-wave (mm-wave) generation techniques

In general, the concept of RoF can be based on three techniques which are distinguishable by the method of generating the local oscillator needed for signal up-conversion and the method of data distribution over the optical fiber. The three most widely adopted schemes for carrier generation are based on: (i) RF band transport, (ii) Intermediate Frequency (IF) band transport and (iii) Baseband transport, all over optical fiber. In the transport of mm-waves over fiber, the carrier and data signal can be generated and transmitted by these methods namely: (i) Radio Frequency Intensity Modulation, (ii) Optical Frequency Multiplication (OFM) and (iii) Optical Heterodyning.

2.7.1 Radio Frequency Intensity Modulation

This is one of the non complex forms of RF transport over optical fiber that has two schemes of achieving baseband data modulation, either by *direct* or *external* methods. The baseband RF signal *directly* modulates the laser Lightwave for transmission and then injected into the optical fiber from the transmission point to the receiver station, [Fig 2.5]. Regardless of the simplicity of this method direct intensity modulation isn't recommended for mm-wave frequency transport as the baseband spectral range decreases as the mm-wave carrier frequency increases [42]. There is the burden of complexity and cost at the CO and BS where up-conversion and down-conversion respectively would be needed for frequency translation. This requires electronics and local oscillators at the CO and BS to operate at mm-wave frequencies putting majority of the burden on photodetectors required to directly translate the optical signals back to RF mm-wave signals.

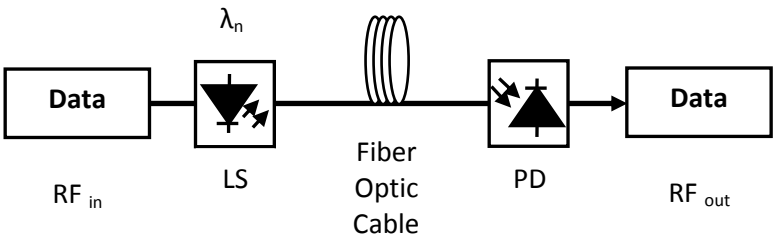

Figure 2.5: RF Direct Intensity Modulation

This makes *external* modulation, [Fig 2.6] an alternative transport scheme as it utilizes high speed MZM to modulate the mm-wave signal onto the laser optical carrier wave generating double sidebands (DSB). The two optical sidebands are situated at either side of the optical carrier frequency displaced by the RF carrier frequency. Nevertheless, the mm-wave signal undergoes optical fiber dispersion which results in

DSB fading of the mm-wave the photodetector. Although compensation for the DSB fading effects can be achieved for mm-wave signals at 60 GHz [43], [44] using dispersion compensating fibers, this effect of chromatic dispersion is not negligible and rather incremental when operating at mm-waves using external modulation [45].

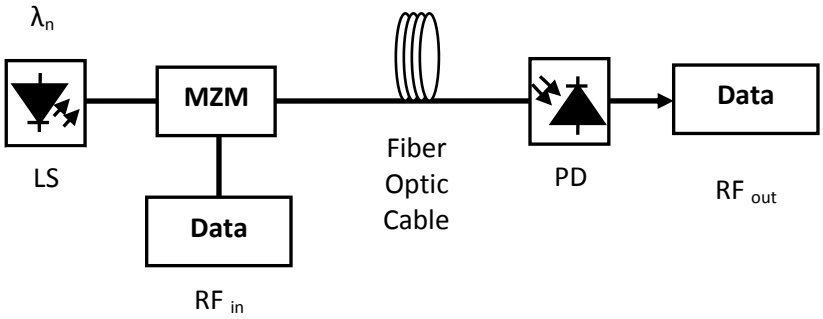

Figure 2.6: RF External Intensity Modulation

As part of significantly reducing the effects of fading, optical carrier suppression (OCS) which is an alternative approach that uses DSB to generate mm-wave signals using a much lower local oscillator frequency has been proposed [46], [47]. OCS doubles the RF carrier frequency by heterodyning both optical sidebands. This produces a doubling effect of the RF carrier frequency hence generating a significantly higher mm-wave. As a result OCS scheme allows the use of modulators with considerably lower bandwidth to be operable in generating mm-wave signals. This reduces the component cost burden at transmission and makes OCS a promising scheme for mm-wave generation. However there are major drawbacks that make OCS technique inapplicable in commercial application deployment. One of which is the issue concerning modulating mm-wave for upstream transmission, OCS would require RAUs to generate local oscillators at mm-wave frequency. This isn't practical as mobile devices are incapable of generating mm-wave frequency (as of

yet). Hence other proposed upstream techniques use baseband modulation for upstream transmission because OCS would require mobile devices to deploy several bulky electro-optical devices and modulators. This makes the OCS arguably less practical for indoor RoF transmission.

2.7.2 Optical Frequency Multiplication

Another approach to mm-wave generation based on self-heterodyning of the optical side modes is optical frequency multiplication (OFM). The principle of OFM is based on the up-conversion of low frequency signal to a desired mm-wave frequency signal [48]. This is done by initially phase modulating the continuous light wave source with a low-frequency RF sweep signal, creating optical side modes spatially separated by the sweep signal. The phase modulated signal then undergoes intensity modulation (IM) by a periodic optical filter such as a Mach-Zehnder interferometer (MZI) to convert the signal to an intensity spectrum. The intensity of the wavelength signal is injected into the fiber and feeder network to the receiver. At the RAU, the PD is met with the intensity of the side modes that beat against each other to create a sequence of harmonics of electrical RF signals and both a microwave signal with carrier frequency. The spectrum characteristic of the intensity modulated signal is unchanged and is replicated at each harmonics including at the microwave signal. The required mm-wave frequency can then be selected by an electrical bandpass filter (BPF) for wireless radiation by an antenna.

The benefit of using this scheme of frequency multiplication can be numerous in comparison to the optical techniques of mm-wave generation. Firstly, at the phase modulation of the continuous laser lightwave by a sweep RF signal only requires a low RF sweep source to generate signals at mm-wavelengths (hence Giga Hertz

frequencies) at the RAU. This also means that the upstream transmission requires simple inexpensive electronics such as low frequency local oscillator to up-convert baseband data for mm-wave up-streaming. Also OFM process makes availability of generated microwave signal at the RAU to be utilized for upstream transmission by modulating the data from the mobile unit onto the carrier generated microwave signal and then down-converting the signal to an IF signal for upstream transmission [49]. More importantly OFM can be used in MMF operation making indoor optical fiber cabling essentially conducive for mm-wave communication [50]. Additional reduction in the complexity of OFM process can be achieved with the use of a Dual-Drive Mach-Zehnder Modulator (DD-MZM) which imitates the functions of a parallel phase modulation. This concept will be the bases of this thesis simulation and its approach to mm-wave transport shall be discussed further in this thesis.

2.7.3 Optical Heterodyning

Looking at both the OFM and Intensity modulation RoF transmission schemes which are based on external modulation as a result of mitigating signal distortion along the fiber due to chromatic dispersion at high intensity frequency [44]. This has focused research interest to adopt alternative approach to satisfactory mm-wave generation and transportation through the means of optical heterodyning. At the CO, this heterodyning process involves optically combining optical lightwave from two laser diodes with wavelength deviation that corresponds to the desired mm-wave signal and then injecting the output into an optical fiber [51]. Firstly, one of the optical lightwave is modulated with the desired baseband data for downstream transmission whilst the other is not modulated. After fiber transmission, at the receiver station the process of coherent mixing the optical signals at the photo-detector generates the

desired RF mm-wave signal. This coherent mixing process method is mostly referred to as Remote Heterodyne Detection (RHD) scheme [52]. This optical heterodyning technique creates a huge benefit in RoF transport as the complex signal processing is carried out at the OC making the RAU needing only inexpensive electronics such as an amplifier and antenna to transmit the modulated mm-wave data signal wirelessly. A combination of WDM filters can also be used to select wavelengths of the desired channels including RF carrier frequency which can be carefully selected to achieve mm-wave RF carrier for uplink transmission at the receiver station. Another advantage of this scheme is that it is highly less susceptible to fiber dispersion than OFM and RF Intensity Modulation.

2.8 Radio over Multimode fiber (RoMMF)

The interest in using MMF for in-door cabling of antennas has been at the forefront front of research for decades, especially in RoF distributed antenna system. This approach can provide the necessary option to deliver gigabit data to the consumer in their home building for WLAN access. MMF (including POF) is deemed unsuitable for heterodyning techniques as a result of the phase delay of each optical mode. The modal group delay and coupling play a pivotal role in characterising the frequency response of the output signal spectrum and can be highly affected by the launching conditions preselected at the CO station or at the junction of coupling between a SMF and MMF. This creates a cumbersome level of problems in the signal dynamic range when factors such as the length of the MMF cable, bending radius and offset launch at coupling affects the signal strength in a RoMMF system. The modal bandwidth limitation in MMF reduces the mm-wave bands that can be transmitted, to only a few meters of MMF cable compared to kilometres of SMF fiber cable. As a

result, most focus has been to transmit passband signals over MMF to remain within the frequency response window, making mm-wave distribution over MMF a reality [53]. OFM as a choice of mm-wave RoF transmission technique has been reported to produce less dependency on the limiting frequency response of the MMF fiber cable [54] and the resistance to the effect of modal dispersion [55]. Details of SMF and MMF coupling at various modal offset launch conditions are explained in Chapter 3.

2.9 Summary

This chapter reviewed the history and transmission capabilities of POF until recent reported developments along with its application and benefits in comparison to SMF and Copper. The state-of-the-art access network cable, BI-SMF was also discussed as an alternative to POF deployment for a radio-over-fibre network. An introduction to mm-wave technology and the three generation techniques namely, RF-Intensity Modulation, OFM and Optical Heterodyning were also presented to highlight the basis of the subsequent simulation chapters.

References

[1] S. Minami: “The Development and Applications of POF: Review and Forecast”, POF’ 1994, Yokohama, 26.-28.10.1994, pp. 27-31

[2] O. Ziemann, J. Krauser, P. E. Zamzow, W. Daum. “*POF Handbook: Optical Short Range Transmission Systems.*” second edition. Springer, 2008.

[3] Y. Koike: “High bandwidth and low-loss polymer optical fibre”, POF’ 1992, Paris, 22.-23.07.1992, pp. 15-19

[4] Y. Koike: “Status of POF in Japan”, POF’ 1996, Paris 22.-24.10.1996, pp. 1-8

[5] G. D. Khoe: “Exploring the Use of GIPOF Systems in the 640nm to 1300nm Wavelength Area Design”, POF’ 1999, Chiba, 14.-16.07.1999, pp. 36-43

[6] Y. Koike: “Progress in GI-POF – Status of High Speed Plastic Optical Fiber and its Future Prospect”, POF’ 2000, Boston, 05.-08.09.2000, pp. 1-5

[7] J. Warrelmann, R. Schnell: “GF-Bündel für Datenkommunikation”, 15 Meeting of the ITG-SC 5.4.1, Offenburg, 25.-26.03.2003

[8] P. Polishuk, “POF Market and Technology Assessment Study,” IGI consulting, 2008, pp. 11

[9] Y. Kike, “High bandwidth and low loss polymer optical fiber”, in *Proc. First International Conference on Plastic Optical Fibres and Applications-POF’92*, Paris (France), pp. 15-19, 1992.

[10] P. Polishuk, “Plastic optical Fibers Branch Out,” *IEEE Commun. Mag.*, vol. 44, no. 9, Sept. 2006.

[11] Y. Watanabe, Y. Matsuyama, Y. Takano: “FTTH Utilizing PF-GIPOF in Apartment Complexes”, POF’2003, Seattle, 14.-17.09.2003, pp. 256-258

[12] W. White, R. Ratnagiri, M. Park, L. L. Blyler: “Engineering commercial Perfluorinated GI-POF Systems”, POF-world San Jose, 04.12.2002

[13] P. Polishuk, "Plastic Optical Fibers (POF) Market Trends," in (ECOC), Berlin, Germany, vol. 27, pp. 1 – 6, Sep. 2007.

[14] G. Gavioli, E. Torrengo, G. Bosco, A. Carena, S. Savory, F. Forghieri, and P. Poggiolin, "Ultra-narrow-spacing 10-channel 1.12 Tb/s D-WDM long-haul transmission over uncompensated SMF and NZDSF," *in IEEE Photon. Technol. Lett.*, vol. 22, no. 19 pp. 1419-1421, Oct. 2010.

[15] Y. Ma, Q. Yang, Y. Tang, S. Chen and W. Shieh, "1-Tb/s single-channel coherent optical OFDM transmission over 600-km SSMF fiber with subwavelength bandwidth access", *Opt. Exp.*, vol. 17, no.11, pp. 9421-9427, 2009.

[16] J. Yu, Z. Dong, J. Zhang, X. Xiao, H. Chien, and N. Chi, "Generation of coherent and frequency–locked multi-carriers using cascaded phase modulators for 10Tb/s optical transmission systems," *J. Lightw. Technol.*, vol 30, no. 4, pp. 458-465, Feb. 2012.

[17] Y. Tang and W. Shieh, "Coherent optical OFDM transmission up to 1 Tb/s per channel", *J. Lightw. Technol.*, vol. 27, no. 16, pp. 3511-3517, Aug. 2009.

[18] ITU, ITU-T Recommendation G.657, October. 2012

[19] R. Llorente, M. Beltrán, M. Morant, E. Pellicer, "Cost and energy efficient multi-standard OFDM integrated optical access and in-building network architecture", *in Proc. ICTON 2012,* Coventry, UK, Jul. 2012, paper Mo.C3.1.

[20] R. Llorente, M. Morant, M. Beltrán, E. Pellicer, "Fully converged optical, millimetre-wave wireless and cable provision in OFDM-PON FTTH networks", *in ICTON 2013*, pp. 1-4.

[21] R. Llorente, M. Morant, E. Pellicer, M. Herman, Z. Nagy, J. Herrera, J. Correcher, T. Alves *et al.* : "Radio-over-fiber quintuple-play service provision for deep fiber-to-the-home passive networks", *in Proc. Optical-Wireless*

Integrated Technology for Systems and Networks Workshop at IEEE International conference on Communications ICC2013, Budapest, Hungary, Jun. 2013.

[22] K. Himeno, S. Matsuo, N. Guan, and A. Wada, "Low-bending-loss single-mode fibers for fiber-to-the-home," *J. Lightw. Technol.*, vol. 23, no. 11, pp. 3494-3499, Nov. 2005.

[23] T. Matsui, K. Nakajima, Y. Goto, T. Shimizu, and T. Kurashima, "Design of single-mode and low-bending-loss hole-assisted fiber and its MPI characteristics," *J. Lightw. Technol.*, vol 29, no. 17, pp. 2499-2505, Sep. 2011.

[24] M.-J. Li, P. Tandon, D. C. Bookbinder, S. R. Bickham, M. A. McDermott, R. B. Desorcie, D. A. Nolan, J. J. Johnson, K. A. Lewis, J. J. Englebert, "Ultra-Low Bending Loss single-mode fiber for FTTH", *J. Lightw. Technol.*, vol 27, no. 3, pp. 376-382, Feb. 2009.

[25] K. Nakajima, T. Shimizu, T. Matsui, C. Fukai and T. Kurashima, "Single-mode hole-assisted fiber as a bending-loss insensitive fiber," Opt. Fiber Technol., vol.16, no. 6, pp. 392-398, Dec. 2010.

[26] L.-A. de Montmorillon, F. Gooijer, N. Montaigne, S. Geerings, D. Boivin, L. Provost, and P. Sillard, "All-solid G.652.D fiber with ultra low bend losses down to 5 mm bend radius," *in Proc. OFC 2009*, OTuL3, 2009.

[27] Z. Dong, J. Yu, X. Xiao, H.-C. Chien, S. Shi, Y. Xia, C. Ge, "24Tb/s (24x1.3Tb/s) WDM transmission of terabit PDM-CO-OFDM superchannels over 2400km SMF-28", *in Proc OECC 2011*, Kaohsiung, Taiwan, Jul. 2011, pp. 756-757.

[28] M.G. Larrode and A.M.J. Koonen, "All-fiber full-duplex multimode wavelength-division-multiplexing network for radio-over-multimode-fiber distribution of broadband wireless services", *IEEE Trans. Microw. Theory Tech.*, vol. 56, no. 1, pp. 248-255, Jan. 2008.

[29] H. Hirscher, "Triple Play Realization of Swisscom with POF," *16th Int'l. Conf. Polymer Optical Fiber*, Turin, Italy 2007.

[30] Yan Shi, Maria Morant, et al., "Multistandard Wireless Transmission over SSMF and Large-Core POF for Access and In-Home Networks" *IEEE Photonics Technology Letters*, vol. 24, pp. 736-738, May 2012.

[31] M. Morant, T. Quinlan, R. Llorente, and S. Walker, "Full Standard triple-play bi-directional and full duplex CDWM transmission in passive optical networks," in *Proc. OFC 2011*, Los Angeles, CA, Mar., pp. 1-3, paper OWB3.

[32] Pham T.T, Lebedev A, Beltran M, Yu X, er al., "SMF/MMF Based In-Building Gigabit Wireless Access Systems Using Simplified 60-GHz Transceivers" in *ECOC*, Geneva, September 2011.

[33] B. L. Dang, M. Garcia Larrode, R. Venkatesha Prasad, I. Niemegeers, and A. M. J. Koonen, "Radio-over-Fiber based architecture for seamless wireless indoor communication in the 60 GHz band," *Comput. Commun.,* vol. 30, pp. 3598-3613, 2007.

[34] A. Ng'oma, D. Fortusini, D. Parekh, W. Yang, M. Sauer, S. Benjamin, W. Hofman, M. C. Amann, and C. Chang-Hasnain, "Performance of a multi-Gb/s 60 GHz radio over fiber system employing a directly modulated optically injection-locked VCSEL." *J. Lightw. Technol.*, vol. 28, no. 6, pp. 2436-2444, Aug. 2010.

[35] F. Lecoche, E. Tanguy, B. Charbonnier, H. W. Li, F. Van Dijk, A. Enard, F. Blache, M. Groix, and F. Mallecot, "Transmission quality measurement of two types of 60 GHz millimetre-wave generation and distribution system," *J. Lightw. Technol.,* vol. 27, no. 23, pp. 5469-5474, Dec. 2009.

[36] A.M.J. Koonen, A. Ng'oma, H. van den Boom, I. Monroy, P. Smulders, and G. Khoe, "Carrying microwaves signals in a GIPOF-based wireless LAN." *in POF 2001,* 2001.

[37] C. Doan, et al., "Design Considerations for 60 GHz CMOS Radios," *IEEE Commun. Magazine,* December 2004, pp. 132-140.

[38] J. J. Vegas Olmos, T. Kuri, and K.-I. Kitayama, "Dynamic reconfigurable WDM 60 GHz millimetre-wave band radio-over-fiber access network: Architectural considerations and experiment," *J. Lightw. Technol.,* vol. 25, no. 11, pp. 3374-3380, Nov. 2007.

[39] J. Kim, Y.-D. Chung, K.-S. Choi, D.-S. Shin, J.-S. Sim, and H.-K. Yu, "60-GHz system-on-packaging transmitter for radio-over-fiber applications." *J. Lightw. Technol.,* vol. 26, no. 15, pp. 2379-2387, Aug. 1, 2008.

[40] Y. Hsueh, Z. Jia, H. Chien, J. Yu, and G. K. Chang, "A novel bidirectional 60-GHz radio-over-fiber scheme with multiband signal generation using a single intensity modulator," *IEEE Photon. Technol. Lett.,* vol. 21, no. 18, pp. 1338-1340, Sep. 2009.

[41] Wireless Gigabit Alliance, http://www.wigig.org

[42] A. P. S. Khanna, "Microwave oscillators: the state of the technology," Microwave journal, vol. 49, no. 4, pp. 22-44, April 2006.

[43] K. Kitayama and H. Sotabayashi, "Cancellation of the signal fading for 60 GHz sub-carrier multiplexed optical DSB signal transmission in nondispersion shifted fiber using midway optical phase conjugation," *J. Lightw. Technol.,* vol. 17, no. 12, pp. 2488-2497, Dec. 1999.

[44] G. H. Smith, D. Novak, and Z. Ahmed, "Overcoming chromatic-dispersion effects in fiber-wireless systems incorporating external modulators," *IEEE Trans. Microw. Theory Tech.,* vol. 45, no. 8, pp. 1410-1415, August 1997.

[45] U. Gliese, S. Norskov, and T. N. Nielsen, "Chromatic dispersion in fiber-optic microwave and millimetre-wave links," *IEEE Trans. Microw. Theory Tech.,* vol. 44, no. 10, pp. 1716-1724, 1996.

[46] J. Yu, M. F. Huang, Z. Jia, T. Wang, and G. K. Chang, "A novel scheme to generate single-sideband millimetre-wave signals by using low-frequency local oscillator signal," *IEEE Photon. Technol. Lett.,* vol. 20, no. 7, pp. 478-480, Apr. 2008.

[47] J. Ma, J. Yu, C. Yu, X. Xin, J. Zeng, and L. Chen, "Fiber dispersion influence on transmission of the optical millimetre-wave generated using LN-MZM intensity modulation," *J. Lightw. Technol.,* vol. 25, no. 11, pp. 3244-3256, Nov. 2007.

[48] N. G. Walker, D. Wake and I. C. Smith, "Efficient millimetre-wave signal generation through FM-IM conversion in dispersive optical fibre links", *Electron. Letters,* vol. 28, no. 21, pp. 2027-2028, Oct. 1992.

[49] T. Koonen, A. Ng'oma, M. G. Larrode, F. Huijskens, I. Tafur Monroy, and G. –D. Khoe, "Novel cost-efficient techniques for microwave signal delivery in fiber-wireless networks," *ECOC 2004,* Stockholm, Sweden, pp Th1.1.1.

[50] A. Koonen, and L. Garcia, "Radio-over-MMF techniques-Part II: Microwave to millimetre-wave systems," *J. Lightw. Technol.,* vol. 26, no. 15, pp. 2396-3408, Aug. 2008.

[51] L. Goldberg, R. D. Esman, and K. J. Williams, "Generation and control of microwave signals by optical techniques," IEE Proceedings, Part J – Optoelectronics, vol. 139, no. 4, pp. 288-295, August 1992.

[52] U. Gliese, T. N. Nielsen, S. Norskov, and K. E. Stubkjaer, "Multifunctional fiber-optic microwave links based on remote heterodyne detection," *IEEE Trans. Microw. Theory Tech.,* vol. 46, no. 5, pp. 458-468, May 1998.

[53] P. Hartmann, X. Qian, A. Wonfor, R. V. Penty, and I. H. White, "1-20 GHz directly modulated radio over MMF link," in *Proc. Int. Topical Meeting of Microwave Photonics (MWP'05),* Oct. 2005.

[54] M. Garcia Larrode, and A. M. J. Koonen, "Theoretical and experimental demonstration of OFM robustness against modal dispersion impairments in radio over multimode fiber links," *J. Lightw. Technol.,* vol. 26, no. 12, pp. 1722-1728, Jun. 2008.

[55] M. Garcia Larrode, A. M. J. Koonen, and J. J. Vegas Olmos, "Overcoming modal bandwidth limitation in radio over multimode fiber links" *IEEE Photon. Technol. Lett.,* vol. 18, no. 22, pp. 2428-2430, 2006.

Chapter 3

Offset Launch Theory and Optical Wireless Communication

3.1 Offset Launch Technique

3.1.1 Introduction

As discussed in *Chapter 2*, the deployment of high bandwidth in the Gigahertz range or Ethernet data at Gbit/s are in much need at the picocell level (i.e. residential home or offices) for NGA. The main difficulty network operators are challenged with is the bottleneck at the access level of deployment. Discussions of MMF application in subscriber's home premises for further bandwidth enhancements have been widely discussed in *Chapter 2*. However the prevailing disadvantages of utilizing MMF for mm-wave or long reach feeder fiber links have also been explored. The modal bandwidth limitation of MMF directly affects the transmission speed and connectivity distance in the access network. Furthermore the effects of modal group delays and modal coupling efficiency both affect the frequency response of a MMF link of which the preconditioning of the laser lightwave's radiation onto the MMF can significantly

impact the transmission performance. Further experiments on exciting modes at over-filled-launch (OFL) conditions [1] and varying launch conditions [2], have been demonstrated. In these reports attempts to reduce the impact modal dispersion has on the transitional signal has been established simply by radiating the lightwave on a proportion of available modes. It has also been experimented and reported that the selective excitation of a limited number of low modes using optical lightwave radiation from a SMF can increase the modal bandwidth of the MMF by a factor of two [3]. The next reported step proposed the launching of the lightwave into the MMF by a SMF at an angular ingress on the MMF [4]. This created a considerable bandwidth increase at the receiver but at the expense of using a stability axial laboratory setup to couple and adjust launch conditions between the fibers. Offset Launch technique is a passive operation that requires no inclusion of electrical power or electronics making it a cost effective step in mitigating the strong dispersion of mm-wave signal over MMF. This makes investigation of Offset Launch technique in RoF technology a necessity and the reason for its adaptation in this thesis.

The aim of this section is to address and highlight the advantages of preselecting the launching conditions of the laser lightwave signal already in SMF transmission onto a MMF at the junctions of SMF and MMF fiber coupling. The impact of modal noise at various offset launch positions with respect to different fiber lengths shall also be examined at various simulation analyses in this Thesis.

3.2 Theory of Offset Launch Technique

As lightwave from a laser source or from an optical SMF is injected onto a MMF, the lightwave is transported by the guidance of the propagation modes in the MMF. Each of the modes in the fiber travels at different velocity due to the different paths the modes traverse, this irregularity is referred to as differential mode delay (DMD). This creates pulse broadening and distorts the transmission bandwidth. GI-POF (*Chapter 2*) which has been described as the better candidate for indoor access links at high data transmissions already displays properties of having differential mode attenuation (DMA). This means that because the GI-POF refractive index gradually changes from the centre of the fiber core to its edge, a different group velocity is pre-established at each mode. This means by preconditioning the radiation beam launch of the lightwave onto a focal point closer to the edge of the GI-POF fiber core *further enhances* a substantial bandwidth improvement.

The procedure of offset launch involves the excitation of a fraction of propagation modes of the MMF when lightwave is injected onto the core surface. This places the circular spot of the lightwave from a SMF onto the MMF cores surface area about the radius of the core but its position displaces from the immediate centre axis, [Fig 3.1]. In doing so, only subsets of higher order mode groups are excited. The simulation parameters used in this thesis for offset launch technique are explained in Appendix A.

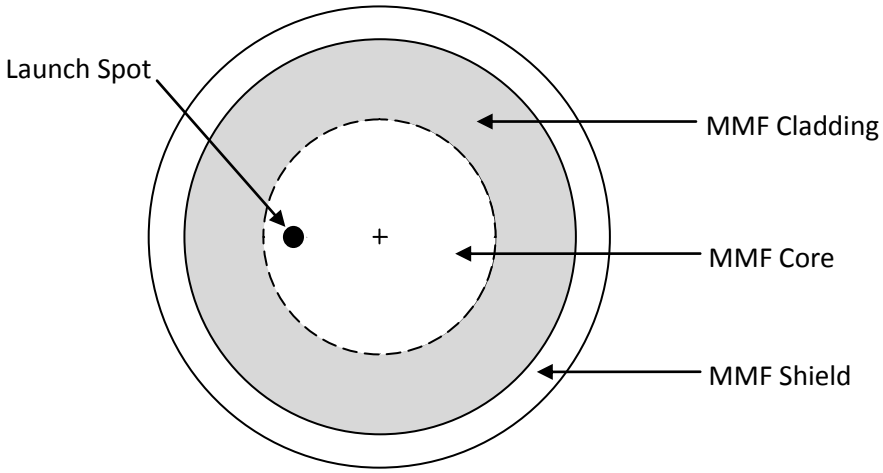

Figure 3.1: Offset Launch Technique

3.3 Analysis of reported result

In this reported experiment [5], laser lightwave was directly injected into a SMF before launching onto the MMF. The experimental procedure includes three methods of collimating the launch spot onto the core surface area of the MMF. Two of the methods included a mixture of lens focusing schemes to select the best focused laser beam spot on the MMF core surface area. The third method involved a direct launch from SMF to MMF (without lens). The experiment is conducted under various wavelengths with focus on utilizing the low attenuation windows in the wavelength spectrum of a MMF (*see Fig 2.4*). At the transmission section, a selected wavelength at 1300 nm was injected into a 9 μm core size SMF. Also at transmission, 850 nm wavelength beam is used but over a MMF. This to my assumption is done to maintain the signal envelope because wavelengths at 850 nm over SMF experience extreme chromatic dispersion than in MMF. The optical signal is modulated with a 2.5 Gbit/s pseudo-random bit sequence (PRBS) pulse stream before injected onto various MMF lengths and core sizes for detection. The eye-diagrams are clearly

visible at 1-km, 2-km and 3-km MMF transmission. Whereas when OFL is employed (direct coupling), a clear visible eye-diagram can be obtained for only up to 600 Mbit/s data rates. This is clearly a bandwidth gain of fourfold i.e. 400%. The experiment concludes that as low as a ±5 μm offset launch condition can achieve a significant bandwidth improvement. The offset launch technique shall be implemented in conjunction with most of the RoF methods described in this thesis as a means to improve the received bandwidth.

3.4 Summary

This section describes the application of Offset Launch Technique in coupled SMF and MMF fibers. The aim is to outline the principles of mode selection for optimal bandwidth gain. This is a passive optical operation that requires no amplification step or electrical powered system to improve signal gain thus making it a suitable cost effective measure in improving optical signal quality at the access point. The simulated adaptation of Offset Launch technique in RoF links for indoor applications is discussed further in Chapters 6 and 7 of this thesis.

3.5 Optical Wireless Communication System

The proliferation of wireless technology devices in the consumer's home has drastically broadened the bitrate requirement per household. This has created new wireless architecture standards such as small cells (incl. femtocells). As discussed earlier, the mm-wave wireless channels have a limited propagation range due to the huge path loss at such high (unlicensed) frequencies (57 – 64 GHz). This means that when the IEEE 802.11 ad standard gets adopted commercially, small cells that have wireless transceivers with 60 GHz throughput will become commonplace in most households with application service delivery such as bandwidth intensive HD video streaming (> 1.8 Gbit/s). Inside the building, the simplest form to deliver Gbit/s RF data transfer over the air is currently based on cost-effective RoF schemes but this scheme still requires expensive high speed opto-electronic device at the access point which to an extent hasn't been developed. The digital-RoF (DRoF) has also been reported to have a considerable bandwidth improvement over conventional RoF schemes but the application of analog-to-digital converters (ADC) and digital-to-analog converters (DAC) is said to be insufficient in its bandwidth capabilities.

An alternative sustainable approach to electronic wireless transmission (over-the-air) of extremely high data signals is to use free-space optics (FSO) as an optical wireless communication (OWC) system [6].

3.6 Outline of Optical Wireless Communication

Optical wireless communication (OWC) is simply the definition of optical beam radiation between an egress and ingress optical fiber [Fig 3.2]. The radiated optical beam modulated with data is collimated into another optical fiber either by the means direct line-of-sight (LoS) or diffuse. When the optical beam delivery is specifically LoS radiated, the system is commonly referred to as FSO [7].

OWC systems perform is two distinctive pattern of beam radiation either through beam diffuse or line-of-sight. OWC operates at the infrared (IR) to ultraviolet (UV) wavelength range and also in the visible light spectrum for some applications. The beam radiation system in OWC involves the complete beam spread of the optical signal as it emits the optical fiber as a means of spatial propagation to cover a larger reception area. This approach becomes unattainable due to increase in atmospheric attenuation or free space loss (FSL) but mainly because of multipath dispersion which affects the intersymbol interference (ISI) and yields lower transmission power. However it can serve as a major practicality in providing a wide coverage area of optical signalling and gives the added function of seamless mobility to the subscriber. In the LOS approach, a much narrower beam radiation is used to create a point-to-point transmission link between transmitter and receiver. This approach restricts the transceiver configuration to a static location in order to maintain connectivity. Additional requirement for seamless mobility would include constant repositioning of transceivers by the subscriber or adopting of the four main link configurations explained in, [8]. Nonetheless, this LOS system offers a much more improved ISI performance in OWC transmission.

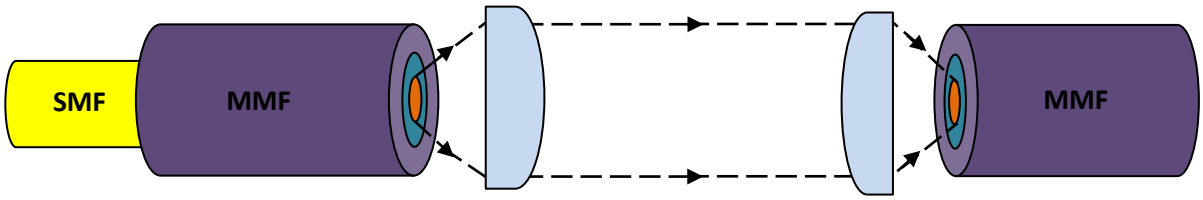

Figure 3.2: Optical Wireless link configuration

3.7 OWC for indoor application

The application of OWC in the indoor environment most certainly has a huge potential in delivery very high bit rate to the end user. With the already composed framework of 5G Wireless communication system that is anticipated to surpass its predecessor in delivering more than 1 Gbit/s downstream bit rate, existing access point systems alone isn't sufficient in advocating the required transmission speed. OWC is anticipated to assist as part of a wider heterogeneous network topology for close-range communication especially for indoor applications. There are several reasons as to why OWC can play a major role in the subscriber's home as an access system:

- **High bandwidth** – OWC systems operates in the Terahertz (approx. 193 THz @ 1550 nm) spectrum range meaning that a huge bandwidth in the terahertz band is available for modulating data. In comparison to wireless RF spectrum, the difference in useable bandwidth with current technology is merely in the Gigahertz range (at most).
- **License free spectrum** – optical signals operate at electromagnetic frequencies outside the required fee paying bands of RF spectrums. This

means that teleco operators are favouring an all optical technology scheme as it reduces both capital and operational expenditure [8] and [9].

- **Low Cost, Low Power** – at indoor application of OWC, eye safe wavelength range are expected to be utilised. This means that wavelengths in the range of 750 nm – 950 nm are seen as the optimal selection for operability. In this range, cheap (and low powered) optical devices such as LED and white-LED (WLED) based on visible light communication (VLC) technology are readily available for transmitter devices.
- **EMI immunity** – since the OWC operating wavelength carrier are in the optical domain hence the electromagnetic radiation of nearby wireless devices do not directly degrade the quality of the signal by interference. Therefore the well known effects of electromagnetic interference (EMI) are eliminated [9].
- **Security** – the optical radiated beam is generally confined within a room and as a result an additional layer of security is provided (at the physical layer) due to the impenetrable properties of the operated wavelength through walls or obscure objects [9].
- **Frequency reuse** – this limitation of optical carriers per room can indirectly open up the utilization of frequency reuse as applied to current mobile cellular base stations but in this case for indoor application [9].

3.8 Indoor OWC Block Diagram

The schematic of an OWC system in an indoor environment is illustrated in Fig 3.3. The block diagram describes the conventional configuration of a communication link

which is made up of a transmitter (optical source), the medium (atmospheric free space) and the receiver (optical detector).

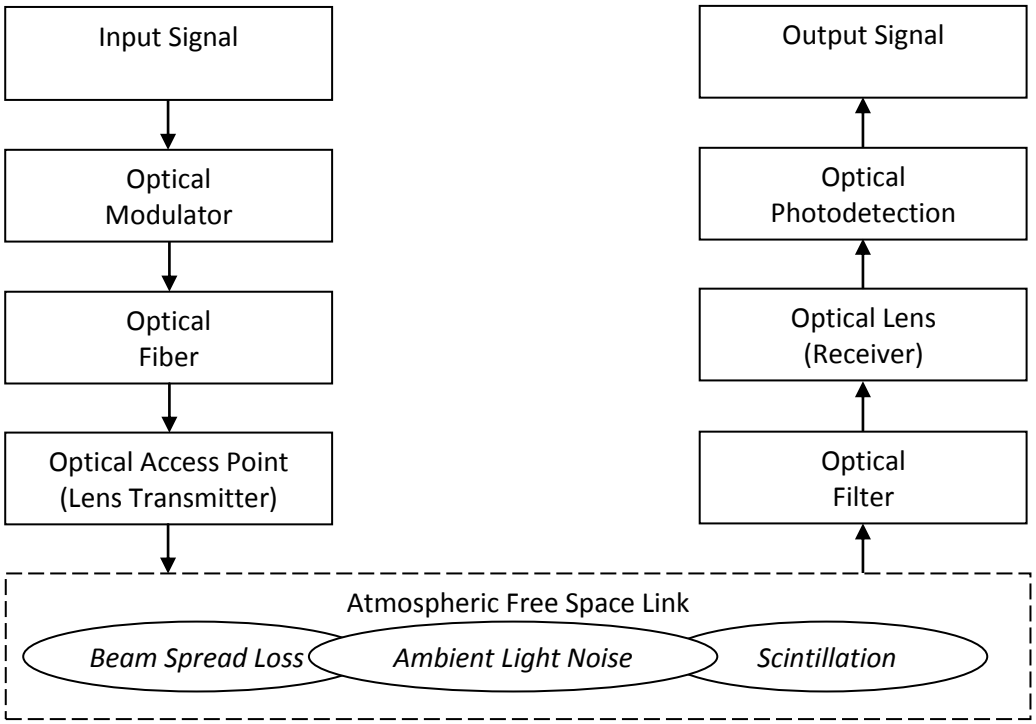

Figure 3.3: Block diagram of OWC transmission and receiver system

The above block diagram [Fig 3.3] represents the fundamental OWC system configuration. In the transmitter section, the pre-established FTTH network generates the optical modulated signal at the CO and is received at the optical control station (OCS) in the subscriber's home. The OCS unit serves as a port switch to connect multiple optical access points (OAP) distributed in individual rooms in the entire house building. The OCS module can also be fitted with pre/post amplification for downstream and upstream transmission. The downstream optical source, carrying the modulated data from the CO, is distributed to OAPs across the entire room using

optical fibers. The downstream signal from an OAP is then radiated optically across the room with the support of an optical lens attached to it. The type of selected optical lens system will determine the radiated beam divergence angle i.e. if it is diffuse or concentrated to a line-of-sight system [6]. This dynamic optical lens is made of a holographic optical element (HOE) property [10], so as to control the emitted radiation for eye safety security. In the context of this thesis, the design and functionality of both the OAP structure and lens properties are not assumed but a direct line-of-sight of a well collimated beam is considered for the simulation of the OWC link.

3.8.1 OWC Transmitter

As discussed earlier, the eye safety feature is not only applied in the HOE lens property but also in the type of laser source used. LEDs that operate in the near infra-red (IR) band are the preferred laser source for indoor applications as it's transmit operating power is limited due to eye safety regulation and are also low cost. This has a practicality function when using POF as the best transmission window is around 450 to 870 nm. Another widely available laser source that operates in this range is the VCSEL which is a low powered laser source which can modulate high bitrate in the 10 Gbit/s transmission speed. Visible Light Communication (VLC) technology based on white LED (WLED) laser source simultaneously produces ambient lighting as well as LED transceiver for wireless data transmission. Another advantage of WLED is the ability to use present home electrical wiring connected to the power grid to both interconnect and power individual WLED devices based on the power line communication (PLC) technology. The challenge with VLC is that room illumination must be at a threshold level according to the device standard, as a lower

dim light level increase SNR. Maximum light intensity isn't needed but the optimal BER might be out of range based on the receiver device requirement. So far, the maximum transmitted data rate for a VLC system using a single LED has been reported [11]. The specific type of LED used produces a 60 MHz higher bandwidth than WLED over OFDM modulation and achieved a 3 Gbit/s data rate speed. For better performance in OWC system, the Intensity modulation and direct detection (IM/DD) scheme is the preferred optical carrier modulation technique. This is because the data is directly modulated onto the intensity of the optical carrier whilst the receiver reproduces the equivalent current values of the received signal power. This is a less complex processing scheme for the photodetector because only the intensity of the waveform is required, there is no phase or frequency translation needed. The subcarrier intensity modulation scheme

3.8.2 Free-space link

The transmission of optical lightwave through the atmosphere isn't without its limitations. There are several factors that combine in limiting the overall performance of the OWC system. As illustrated in Fig 3.3, the atmospheric free-space medium/link has several parameters that impact the radiated beam. In the context of an in-door environment, the appropriate parameters that have the direct effect of transmission have been considered and observed. These atmospheric link impairments are:

- Beam Spread Loss
- Scintillation
- Ambient light noise

3.9 Atmospheric link Impairments

3.9.1 Beam Spread Loss

The propagation of an optical radiated beam through the atmosphere causes degradation of the optical signal power. This decline is signal power is affected by what is known as atmospheric turbulence and also the propagation distance. The resultant increase in the propagation distance and the atmospheric turbulence concentration are directly proportional to the signal degradation. The effect of atmospheric turbulence mainly causes beam spread loss but for insufficient simulation parameters, the geometry model between transmitter and receiver in this thesis considers only a direct LOS link. This means that the receiver is always facing vertical to the OAP transmitter in the room ceiling. The radiated beam no longer assumes a beam spread but rather a direct path loss impairment which can be evaluated as follows, [12]:

$$L = 10 \log_{10} \frac{A_r}{\pi(\beta^2 d^2)} \tag{3.1}$$

where A_r is the receiver area, d is the distance between the OAP transmitter and receiver and β is the beam divergence angle which is considered negligible (i.e. one).

3.9.2 Scintillation

The effect of scintillation arises from the scattering of light from the refraction change in the atmospheric mediums. As a result of the beam scattering a portion of light energy is cast outside of the receiver aperture hence attenuating the optical signal. This effect pertains to both extremely long (km) atmospheric links and indoor

environment where there is presence of gaseous molecules to alter the atmospheric medium such as over a thermal radiator.

3.9.3 Ambient Light Noise

The interference from ambient light noise spans from various noise sources such as thermal noise, fluorescent light interference and ambient light noise. The effective noise power spectral density (N) or ambient light noise [6], can be deduced as:

$$N = 2qRP_n \cong 10^{-23}\ (A^2/Hz) \tag{3.2}$$

where q is the electronic charge, R is responsivity of the receiving p-i-n photodiode and P_n is the average optical power of the ambient light. The signal-to-noise ratio (SNR) can be evaluated based on the transmitted bitrate R_b, at any geometrical location in the room [6];

$$SNR = \frac{R^2 P_r^2}{R_b N} \tag{3.3}$$

where P_r is the received average power and R_b is the bitrate.

3.10 OWC Receiver

Upon reception of the radiated beam, the optical beam is initially filtered using an optical band pass filter (OBPF) to remove unwanted ambient light noise before being focused on the detection surface region of a concentrator lens. The concentrator is an optical passive device that increases the resultant detection of the radiated beam by the photodiode. It can to some extent mitigate the effects of attenuation in free-space by collimating the dispersed beam on its entrance surface area onto a focal

point [12], of the photodetectors receiver aperture. The choice of photodetectors can vary, although an avalanche photodiode (APD) can be used, the p-i-n photodiode is preferred as a result of lower cost and better tolerance to temperature fluctuations. After photodetection, the frequency response and electrical signal characteristics are analysed.

In this thesis, the received radiated beam signal is simulated to assume a complete collimated beam through the concentrator device.

3.11 OWC Indoor Setup

As discussed in the introduction chapter, the aim of this thesis is also to simulate OWC transmission link for indoor applications based on RoF technology. A similar approach has been demonstrated and reported [13], [14] and [15]. In these experiments, a 10 Gbit/s and 12.5 Gbit/s data-rates were transmitted in a room sized replication for personal area networking. Error-free receptions were achieved for a 5.6 km SMF transmission and at an indoor free-space link of below 0.9 m, [13] and [14]. The experiment is also reported to be scalable (for more data speed) and allows mobility due to an intrinsic mirror steering mechanism. In another reported experiment which demonstrates a coupled SMF and 4.4 km GI-MMF transmission from CO, a 30 Gbit/s bidirectional transmission speed is successively achieved over 1.5 m free-space indoor link using DMT modulation technique [15]. These proofs of concept demonstrate the necessity for OWC technology for next generation broadband systems.

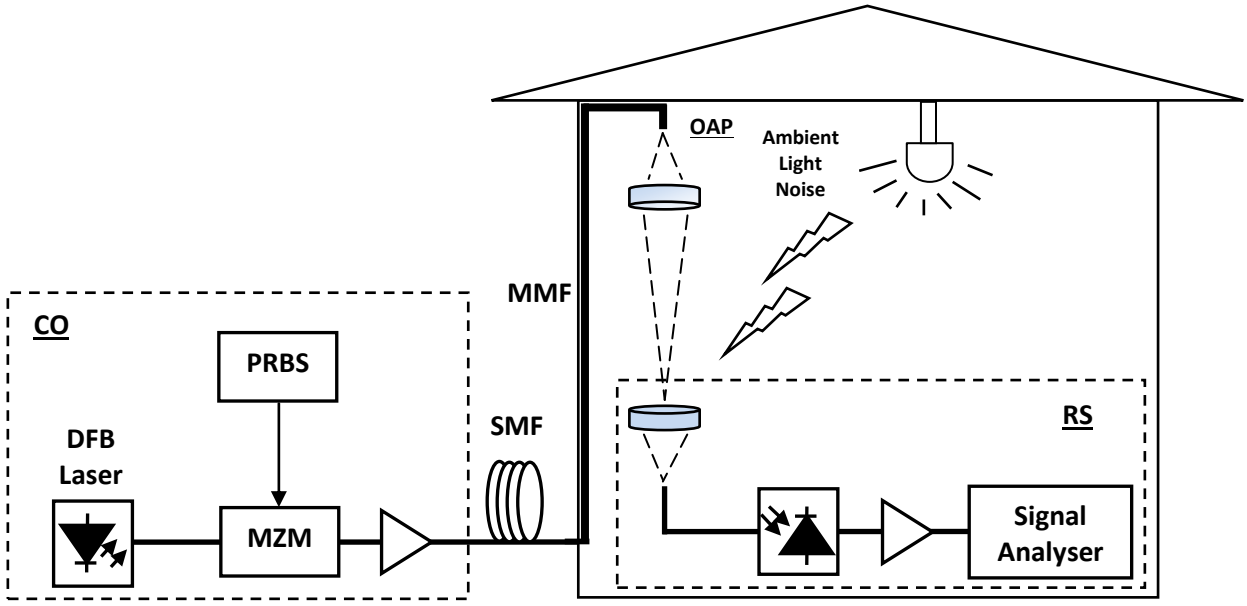

Figure 3.4: OWC system Architecture

As discussed previously, with the advancement of 60 GHz transceivers for compact user terminals, the adoption of OWC for indoor RoF can be conceivable. The proposed architecture of such a system (*without mm-wave transmission*) is demonstrated in Fig 3.4. The signal is generated at CO and transported to the subscriber's home over long-haul SMF coupled with indoor MMF before being transmitted optically for indoor personal area networking. Application of mm-wave signal over OWC system can be viewed as readily option to select either RF or optical signal over-the-air transmission at the subscriber's home. The choice becomes either directly terminating the MMF fiber into a ONT device which then emits RF signal over antenna or the possibility to directly emit optical beam through an OAP.

3.12 Summary

This chapter discussed the fundamental process of optical wireless communication, the devices required to establish free-space optics and the parameters that directly or indirectly (ambient light noise) impair the signal quality at the photodetection receiver. The advantages of OWC and the required modulation techniques were also investigated. Optical radiation is advantageous when the data signal is intensity modulated as signal detection produces better gain. SNR is also improved through optical wireless communication compared to over-the-air antenna receiver sensitivity noise. The architecture also illustrates the coupling of feeder SMF cable with indoor MMF and BI-SMF cable along with the use of optical filters and concentrators inside the OAP to detect the terminating optical beam. Atmospheric anomalies that directly affect the signal are also explained and discussed.

References:

[1] EIA/TIA 455-54A, "Mode scrambler require for overfilled launching conditions to multimode fibers."

[2] L. Raddatz, I. H. White, D. G. Cunningham, and M. C. Nowell, "Increasing the bandwidth-distance product of multimode fiber using offset launch," *Electron. Lett.,* vol. 33, pp. 232-233, 1997.

[3] Z. Haas and M. A. Santoro, "A mode-filtering scheme for improvement of the bandwidth-distance product in multimode fiber systems," *J. Lightwave Technol.,* vol. 11, pp. 1125-1131, 1993.

[4] Z. Haas and M. A. Santoro, "Lightwave transmission system using selected optical modes," US Patent no. 44318, 1993.

[5] L. Raddatz, I. H. White, D. G. Cunningham, and M. C. Nowell, "An experimental and theoretical study of the offset launch technique for the enhancement of the bandwidth of multimode fiber links," *J. Lightwave Technol.,* vol. 16, no. 3, pp. 324-331, March. 1998.

[6] J. M. Kahn and J. R. Barry, "Wireless Infrared Communications," *Proc. IEEE*, vol. 85, no. 2, pp. 265-298, Feb. 1997.

[7] D. Killinger, "Free space optics for laser communication through the air," *Optics & Photonics News,* vol. 13, pp. 36-42, Oct. 2002.

[8] H. Elgala, R. Mesleh, and, H. Haas, "Indoor optical wireless communication: Potential and state-of-the-art," *IEEE Commun. Mag.,* vol. 49, no. 9, pp. 56-62, Sep. 2011.

[9] F. R. Gfeller and U. Bapst, "Wireless In-House Data Communication via Diffuse Infrared Radiation, "*Proc. of IEEE,* vol. 67, no. 11, pp. 1474-1486, Nov. 1979.

[10] D. H. Close, "Holographic optical elements," *Opt. Eng.,* no. 14, pp. 408 – 419, 1975.

[11] D. Tsonev, H. Chun, S. Rajbhandari, *et al.,* "A 3-Gb/s single-LED OFDM-based wireless VLC link using a gallium nitride μLED," *IEEE Photon. Technol. Lett.,* vol. 26, no. 7, pp. 637-640, Apr. 1, 2014.

[12] H. Al Hajjar, B. Fracasso and, F. Lamarque, "Mini optical concentrator design for indoor high bit rate optical wireless communications," in *Optical Wireless Communication (IWOW), 2013. 2nd International Workshop on*, 2013, pp. 147 – 151.

[13] K. Wang, A. Nirmalathas, C. Lim, and E. Skafidas, "High-speed optical wireless communication system for indoor applications," *IEEE Photon. Technol. Lett.,* vol. 23, no. 8, pp. 519 – 521, Apr. 2011.

[14] K. Wang, A. Nirmalathas, C. Lim, and E. Skafidas, "4 x 12.5 Gb/s WDM optical wireless communication system for indoor applications," *J. Lightwave Technol.,* vol. 29, no. 13, pp. 1988-1996, July. 2011.

[15] H. Chen, H. P. A. van den Boom, E. Tangdiongga and, T. Koonen, "30-Gb/s bidirectional transparent optical transmission with an MMF access and an indoor optical wireless link," *IEEE Photon. Technol. Lett.,* vol. 24, no. 7, pp. 572-574, Apr. 1, 2012.

Chapter 4

Optical Carrier Suppression

4.1 Introduction to Optical Carrier Suppression (OCS)

One of the preliminary investigated transmission technologies in delivering mm-wave through optical fiber in this thesis is known as optical carrier suppression (OCS) modulation [1]. As discussed in Chapter 2, OCS uses a much lower oscillator frequency at the CO station to generate the mm-wave signals. The mm-wave signals are generated by doubling the RF carrier frequency through heterodyning of the produced optical sidebands by an external modulator.

The OCS technology when employed can be configured to use modulators with lower bandwidth to generate mm-wave signals. The advantage of this is that it makes it cost effective by reducing the expensive electronics at the OLT site. However there are major drawbacks that make OCS technique inapplicable in commercial application deployment. One of which is the issue concerning modulating mm-wave for upstream transmission, OCS would require the generation of mm-wave local oscillators at upstream site. This isn't practical as remote devices at residential property would be required to generate extremely high frequencies. Hence other

proposed upstream techniques use baseband modulation for upstream transmission because OCS would require mobile devices to deploy several electro-optical devices and modulators. This makes the OCS less practical for indoor RoF transmission. Furthermore, in the transmission of more than one RF band by the same laser source, the up-conversion technique generates interband beating interference. Nonetheless, OCS compared to other transmission schemes, has the highest receiver sensitivity, lowest spectral occupancy and lowest bandwidth requirement for electronic components such as amplifiers and optical modulators [2].

Traditional OCS configuration scheme in mm-wave generation includes a MZM for baseband modulation before up-conversion by a dual-arm MZM. An interesting approach that simplifies the complexity and cost in OCS scheme has been reported in [3]. By adopting a similar approach for OCS mm-wave generation for SMF and MMF cable link transport, the advantages of OCS scheme over SMF and MMF is investigated in this thesis.

4.2 Related Work

4.2.1 OCS optical mm-wave generation and wavelength reuse

There has been several reported work on OCS schemes for RoF mm-wave signal generation and transport over SMF. OCS can be used for increasing capacity for downlink bandwidth in the access network and can be suitable for the next generation access network requirements. One of the reported schemes compares three methods of sideband transmissions DSB, SSB and OCS [5]. The report looks at optical (40 GHz) mm-wave generation for downlink transmission and a full-duplex scheme based on wavelength reuse and not injection of a wavelength source at the uplink site [5] and [6]. The test experiment examines a 2.45 Gbit/s data channel over

25-km SMF optical fiber transmission including the wireless transmission of the data channels over 10.2-m indoor link achieving less than 1.5 dB power penalty.

The result observed showed a receiver sensitivity of the mm-wave signal of -39.7 dBm based on a BER of 10^{-10}. After 40-km transmission the power penalty drops to 2 dB. The eye diagram also displays fluctuating amplitudes of the mm-wave signal as a result of chromatic dispersion. This impediment also is further increased as the SMF is set to 60-km, making the eye diagram practically shut. The test goes on further to examine the simultaneous up-conversion of 32 x 2.5 Gbit/s DWDM data channel transmission over 40-km SMF optical fiber link. The observed result showed a power penalty of all the channels to be approximately 2 dB after 40-km SMF transport. However the report also states that this power penalty was observed to be the same as when one channel was tested. The report demonstrates the suitability of OCS for large area access networks by exhibiting the highest receiver sensitivity, highest spectral efficiency and lowest power penalty over long-haul optical fiber link, all compared with DSB and SSB modulation technology.

4.2.2 OCS modulation scheme of Vector signals

Conventionally OCS scheme uses a homodyne configuration for data modulation [7]. This makes the impracticality of modulating vector signals such as QAM or OFDM which are presently the predominant modulation format for most signal modulation schemes. In this proof-of-concept OCS transport scheme, only one MZM optical modulator is used to modulate the 8PSK vector signal over a subcarrier frequency of 6 GHz [8]. As a result of OCS scheme, the subcarrier frequency is doubled to 12 GHz also transposing the vector signal to a QPSK signal. The observed result showed an error-free transmission at BER 10^{-9} over 50-km SMF transport. The experiment was

repeated using the VPItranmsisionMaker optical transmission software to simulate QPSK vector signal at 60 GHz subcarrier frequency over 25-km SMF optical fiber. The observed result shows a power penalty below 0.8 dB, meaning a less considerable impact of signal degradation by the effects of chromatic dispersion. This system is promising especially when the configuration allows for no utilisation of optical or electrical filters in generating mm-wave signals.

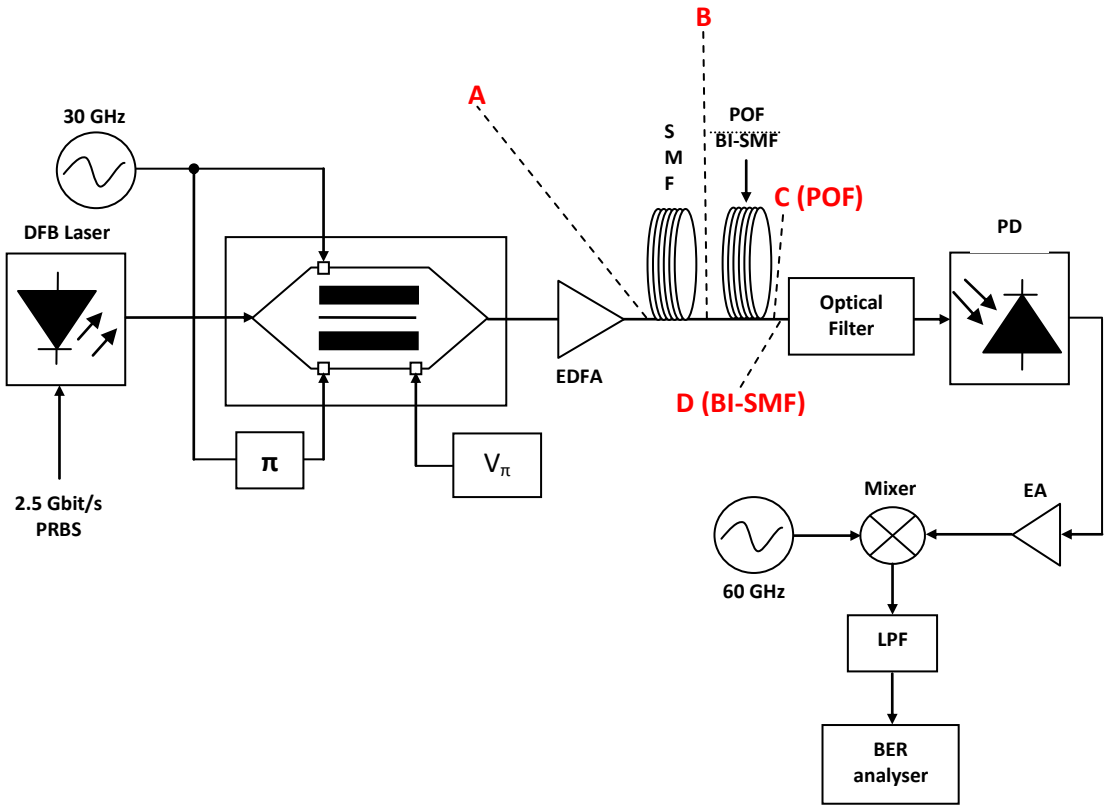

Figure 4.1: The OCS simulation of mm-wave generation based on direct modulation laser and external modulator. EDFA: erbium doped fiber amplifier. PD: PIN photodetector. EA: electrical amplifier. LPF: low pass filter.

4.3 Overview of OCS Modelling

The simulation method involved the direct-modulation along with an external modulator for RF up-conversion. In using a dual-arm MZM modulator driven by two complimentary RF clocks optical sidebands are generated based on optical carrier suppression. The optical mm-wave is amplified and then transmitted through SMF and MMF for downlink stream. Upon reception the mm-wave signal is filtered optically and converted to electrical signal by a photodetector at the receiver site. The mm-wave is then downconverted to baseband signal by using a remote local oscillator of mm-wave frequency.

4.4 OCS Simulation Setup and Results

The configuration of the OCS scheme, [Fig 4.1] involves the direct modulation of an optical continuous wave using a DFB laser source at 193.1 THz frequency (approx. 1550 nm) with a 2.5 Gbit/s PRBS data stream using a 40mW operating power to drive the laser. The optical sideband created is then injected into the dual-arm MZM, driven by two 30 GHz RF sinusoidal signal for optical carrier suppression. This creates a dual band mm-wave optical signal with a generated optical signal at 60 GHz. The optical mm-wave is then transported through 25-km SMF and up to 30-m MMF-POF. The OCS simulation parameters are displayed in Table 4.1. The optical spectrum of the generated mm-wave signal after OCS was observed and can be seen in Fig 4.2. After 25-km SMF transmission, the eye diagram of the optical signal was also observed and can be seen in Fig 4.3. After 25-km SMF transmission of the mm-wave signal, the optical signal is further coupled with either a 30-m MMF-POF optical fiber or the 150-m BI-SMF optical fiber for alternating measurements before optical-to-electrical conversion by the PIN photodetector (pin-PD). The converted electrical

signal was amplified at the centred 60 GHz with 30 dB gain. The simulation of an electrical LO signal at 60 GHz was generated by using a frequency multiplier from 10 to 60 GHz or 20 to 60 GHz or direct 60 GHz, all of which gave the same effect of signal conversion. The electrical LO signal along with a mixer was used to down-convert the electrical mm-wave signal. After which the next action was to filter the electrical signal with a low pass electrical filter then connected to a BER Analyser to measure the received 2.5 Gbit/s signal.

The down-converted 2.5 Gbit/s signal was observed with the BER analyser to obtain both the eye diagrams of the electrical amplified down-converted 2.5 Gbit/s signal after 25-km SMF transmission with either coupled 30-m MMF-POF or 150-m BI-SMF optical cables for observation and can be seen in Fig 4.4 and Fig 4.5 respectively. The downlink BER curve versus the received power was also observed after both the 30-m POF and the 150-m BI-SMF optical cable transmissions which the results can be seen in Fig 4.6 and Fig 4.7 respectively. For a BER of 10^{-10} the power penalty after 25-km SMF and 30-m MMF-POF is 1.7 dB whilst for 25-km SMF plus 150-m BI-SMF transmission, the power penalty is 1.6 dB.

Parameters	Value
DFB laser wavelength	193.1 THz (approx. 1550 nm)
PRBS data rate	2.5 Gbit/s
RF sinusoidal signal	30 GHz
Laser power	40 mW
Laser linewidth	10 MHz
Single mode fiber	25 km
Multimode fiber (POF)	30 m
BI-SMF	150 m
Local Oscillator	60 GHz

Table 4.1: OCS simulation parameters

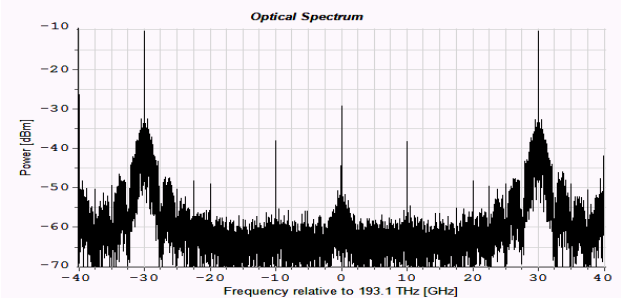

(a)

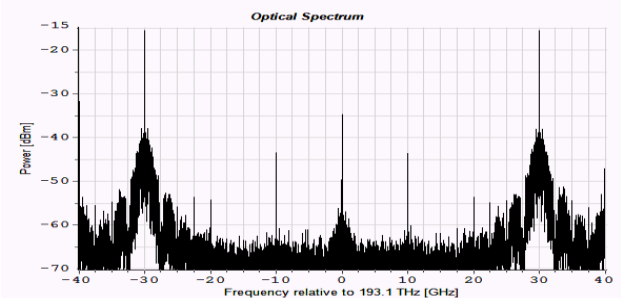

(b)

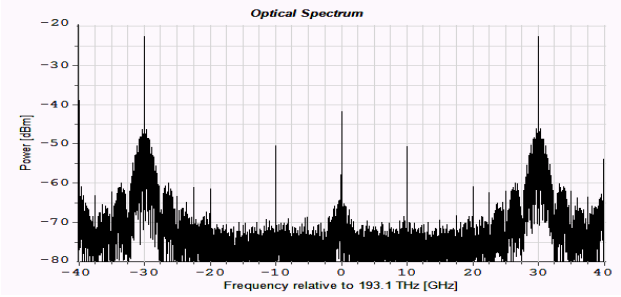

(c)

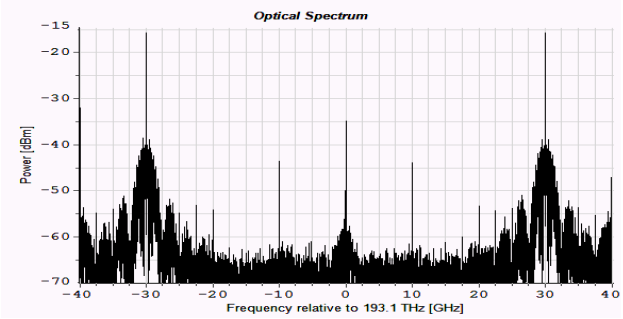

(d)

Figure 4.2: The spectrum of the OCS signal generated at point A,B,C and D in Fig 4.1

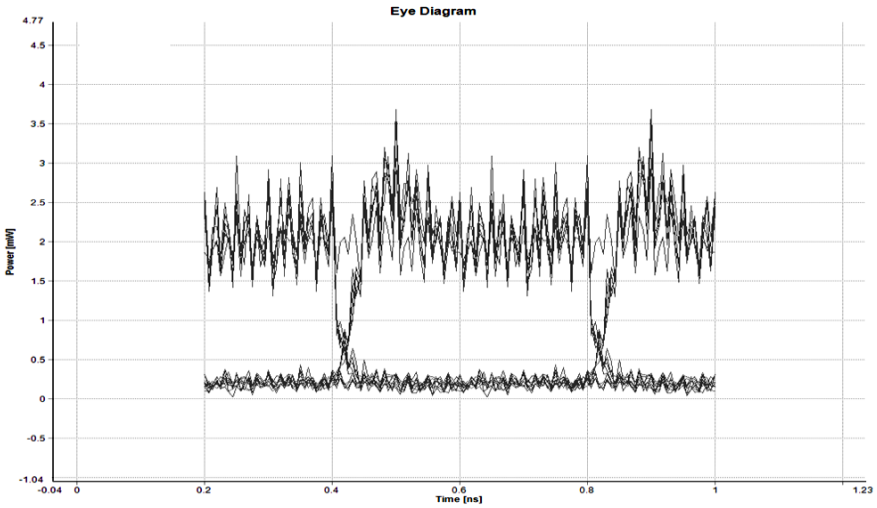

Figure 4.3: The optical eye diagram after 25-km of SMF transmission of the mm-wave signal

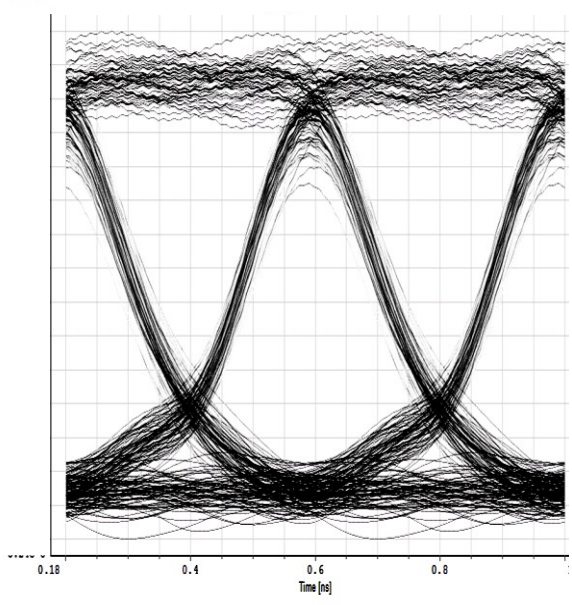

Figure 4.4: Eye diagram of the down-converted 2.5 Gbit/s signal after 25-km (SMF) and 30-m (POF) transmission

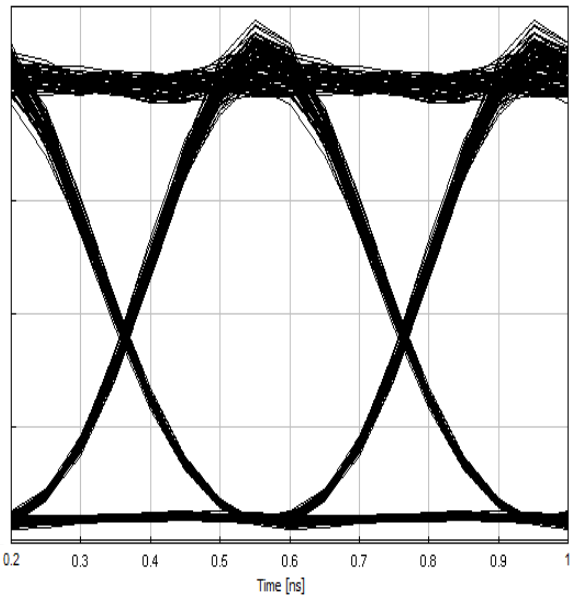

Figure 4.5: Eye diagram of the down-converted 2.5 Gbit/s signal after 25-km (SMF) and 150-m (BI-SMF) transmission

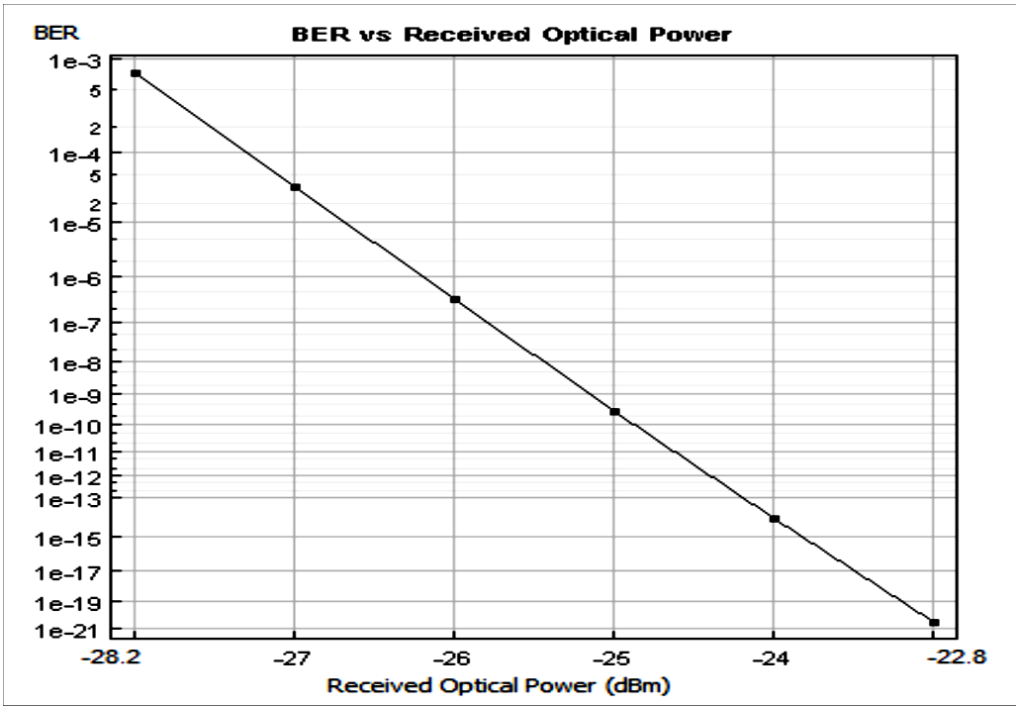

Figure 4.6: The downlink signal BER curve after 30-m POF

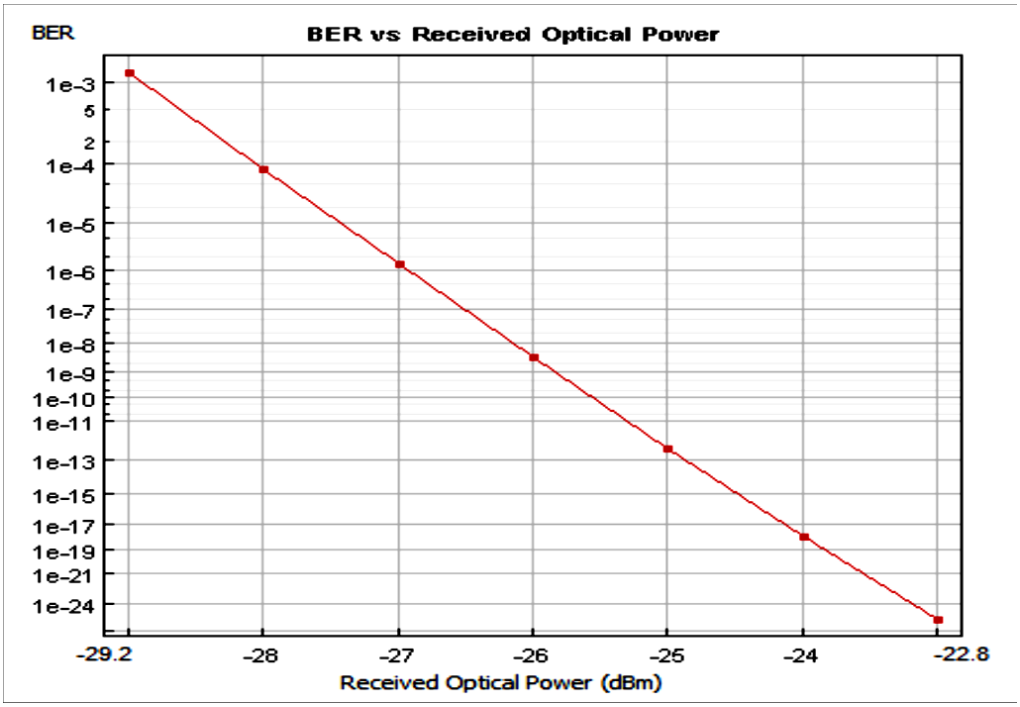

Figure 4.7: The downlink signal BER curve after 150-m BI-SMF

Further MMF-POF lengths were also observed to obtain the received electrical power (pre-electrical amplification) at lengths beyond 30-m (up to 100-m) [Fig 4.8]. Additional simulation of the effects of free space links between the OAP and the PD were observed. The results can be seen in Table 4.2 for free space distances of 5-m which was preselected as the conventional maximum height between an OAP and PD of an electronic device in a given subscriber room geometry.

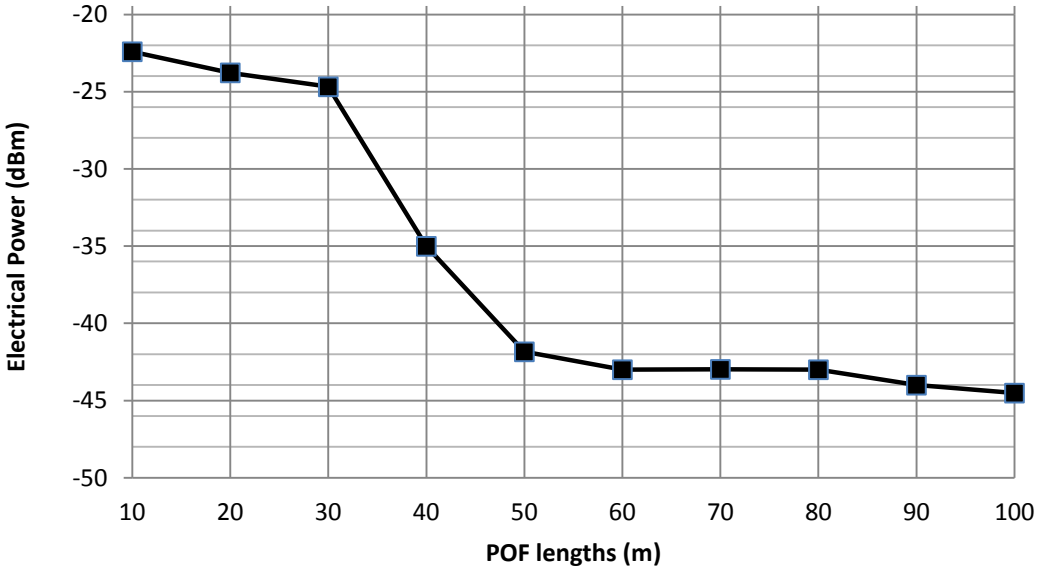

Figure 4.8: Received power of 60 GHz signal versus POF lengths (pre-EA)

Free space link (m)	Received power (dBm)	
	30-m MMF	150-m BI-SMF
1	-25.698	-21.740
2	-25.698	-21.739
3	-25.697	-21.739
4	-25.696	-21.738
5	-25.695	-21.737

Table 4.2: OWC links versus observed received electrical power for POF and BI-SMF cables

4.5 Discussion of Results

It is made clear from Fig 4.3 that the eye diagram witnesses a fluctuation of the optical eye diagram after 25-km SMF transmission. These fluctuations are a result of chromatic dispersion effect [3] and [4]. With further SMF optical fiber lengths at 60-km, it has been reported in [5], that the eye diagram is almost closed after optical mm-wave is transmitted. This report also explains that the OCS scheme can be adaptive for 32 x 2.5 Gbit/s dense-WDM (DWDM) signals over 40-km SMF for WDM PON networks. The report concludes are also validates that the up-conversion of signals based on OCS modulation scheme displays the best performance in receiver sensitivity, the highest spectral efficiency and the smallest power penalty over long distance delivery compare to various types of side-band modulation schemes such as DSB and SSB [5]. The observation of the eye diagram or ISI can be evaluated from Fig 4.4 and Fig 4.5 for POF and BI-SMF respectively. POF exhibits highly dispersive bits compared to BI-SMF cables, this run-off bits is based on the modal dispersive properties of POF including its attenuation of high frequency bands especially in the 60 GHz band range. The results in Fig 4.6 and Fig 4.7 also show that a similar BER performance is achieved at a longer BI-SMF length (150-m) compared to POF. This adds to the advantages of using BI-SMF cable in the access network compared to POF, especially after a long-haul SMF is already deployed in the metro-network between the OLT and the ONU sites.

The received electrical power at various lengths was also observed for POF lengths at 30-m and more [Fig 4.8]. The deliberate 30-m POF length was chosen for this simulation as it allows ease and comparison for other mm-wave techniques described in this thesis where further lengths yielded unobservable simulation result. Based on OCS mm-wave signal transmission over MMF-POF, the graph shows significant attenuation as the POF length is increased beyond 34-m.

4.6 Summary

Transporting mm-wave generated signals over access network fiber links such as POF and BI-SMF in the access network based on OCS scheme showed a reliable signal performance at the receiver station, the spectral efficiency was at its highest, there was constant observed open eye diagram, that is, less to almost no inter-symbol interference witnessed in the delivery of Gbit/s data over long-haul SMF optical fiber plus access network fiber links. These observed results are similar in both simulations conducted in this thesis and the related reported works [6], [7] and [8]. Based on the results achieved in the conducted OCS simulation, the performance of POF have shown reliable power penalty performance and receiver sensitivity. In Fig 4.8, the pre-amplification of the received signal at the photodetector showed that POF lengths can be extended to meters of lengths and carry Gbit/s data with post-amplification gain. The BI-SMF fiber cable had similar attenuation and dispersion properties as the standard SMF fiber used for long-haul links. The BI-SMF fiber link was extended to 150-m [Fig 4.5]. BI-SMF was evaluated to produce comparable performance at 150-m. This proves the adoption of BI-SMF as a better access network optical fiber cable for indoor application compared to POF due to its long reach application beyond the hundred meter length.

In observing the free space links of delivering the OCS RoF signal to a PD. The observed result [Table 4.2] showed attenuated signal as the free space link was increased. The attenuation on the received signal power for both POF and BI-SMF isn't significant but it is expected, as one of the reasons is due to the simulation assuming complete and total collimation of the light beams onto the aperture of the photodetector. Nonetheless Table 4.2 showed distinctive decrease in received signal power as the free space link increased in length. After reception of the signal further

(EA) amplification was used to achieve acceptable power penalty for signal performance.

The considerable aspect of the OCS scheme mentioned in this thesis was also based on the cost effectiveness of using one external modulator compared to other generation schemes that utilised two external modulators.

References:

[1] Sai Naing Min Htet., "Generation of Optical Suppressed Signal for Radio-over-Fiber (RoF) System Using Dual-Drive Mach-Zehnder Modulator," *International Journal of Scientific and Research Publications.,* vol. 4, no. 9, pp. 1-7, Sep. 2014.

[2] J. Yu, *et al*., "Optical millimetre-wave generation or up-conversion using external modulators," *IEEE Photon Lett*., vol. 18, no. 1, pp. 265-267, Jan. 2006.

[3] D. Wake, C. R. Lima, and P. A. Davies, "Transmission of 60-GHz signals over 100 km of optical fiber using a dual-mode semiconductor laser," *IEEE Photon. Technol. Lett.,* vol. 8, no. 4, pp. 578-580, Apr. 1996.

[4] U. Gliese, S. Norskov, and T. N. Nielsen, "Chromatic dispersion in fiber-optic microwave and millimetre-wave links," *IEEE Trans. Microw. Theory Tech*., vol. 44, no. 10, pp. 1716-1724, Oct. 1996.

[5] Z. Jia, J. Yu, G. Ellinas, and G-K. Chang, "Key enabling technologies for optical-wireless networks: optical millimetre-wave generation, wavelength reuse, and architecture," *IEEE Journal of Lightwave Technology*, vol. 25, no. 11, Nov. 2007.

[6] Z. Jia, J. Yu, and G-K. Chang, "A full-duplex radio-over-fiber system based on optical carrier suppression and reuse," *IEEE Photon. Technol. Lett.,* vol. 18, no. 16, pp. 1726-1728, Aug. 2006.

[7] S-H. Fan, C. Liu, and G-K. Chang, "Heterodyne optical carrier suppression for millimetre-wave-over-fiber systems," *IEEE Journal of Lightwave Technology*, vol. 31, no. 19, Oct. 2013.

[8] K. Wang, X. Zheng, H. Zhang, and Y. Guo, "A radio-over-fiber downstream link employing carrier-suppressed modulation scheme to regenerate and transmit vector signals," *IEEE Photon. Technol. Lett.,* vol. 19, no. 18, pp. 1365-1367, Sep. 2007.

Chapter 5

Optical Frequency Multiplication

5.1 Introduction to Optical Frequency Multiplication (OFM)

Another method that involves the transport of mm-wave frequencies past the modal bandwidth of MMF cables is the Optical Frequency Multiplication (OFM) technique.

OFM is a transmission scheme that uses optical signal processing to create radio frequency harmonics by frequency modulation to intensity modulation conversion with the use of an external Mach-Zehnder Interferometer (MZI) or a Fabry-Perot Interferometer (FPI). OFM generates higher microwave frequency by up-conversion of a much lower frequency at the central station (CS). This processing is done by constantly sweeping the lower frequency signal onto the optical continuous wave (CW). This creates the RF harmonics with mm-wave RF frequency, which upon reception are filtered by a photo-detector (PD) and the desired mm-wave signal is filtered using a bandpass filter [1].

Traditional OFM scheme over MMF links [2], [3] uses an interferometer such as the MZI to employ periodic filtering. Its network design is based on phase-modulation

(PM) to intensity modulation (IM) for frequency up-conversion. This OFM scheme can be analysed by focusing on the simpler transmission and receiver components to realise OFM [Fig 5.1].

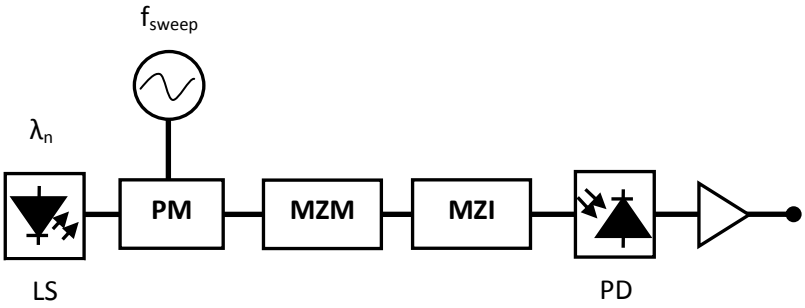

Figure 5.1: OFM architecture with optical filtering

5.2 Theory of OFM based on MZI filtering

The description of the frequency modulation of an optical signal with an optical carrier frequency ω_0, phase $\theta(t)$ and a radian sweep frequency ω_s is expressed as [4]:

$$E(t) = e^{j\theta(t)} \tag{5.1}$$

where $E(t)$ is the electric field's amplitude of the optical light source and the optical phase $\theta(t)$ is expressed as, [4]:

$$\theta(t) = \omega_0 t + \beta \sin(\omega_s t) \tag{5.2}$$

where β is the frequency modulation index. Thus the electrical field of the phase modulated optical signal is expressed as, [4]:

$$E_{in}(t) = E_0 e^{j\theta(t)} \tag{5.3}$$

Substituting Equation 5.2 with 5.3 gives the expression as:

$$E_{in}(t) = E_0 e^{j[\omega_0 t + \beta \sin(\omega_s t)]} \tag{5.4}$$

As suggested in Fig 5.1, a Mach-Zehnder Interferometer (MZI) is used as an optical filter rather than a Fabry-Perot Interferometer. The MZI is a mechanism that inputs a delay onto one path of an optical signal that has been split into two paths. This delay is created physically by making one of the coupled paths longer than the other. This differential path delay of one of the branches of the MZI is expressed as τ and the impulse response of the MZI is expressed as, [4]:

$$h_{MZI}(t) = \frac{1}{2}\{\delta(t) + \delta(t-\tau)\} \tag{5.5}$$

The electrical field of the optical signal after the MZI is given by the convolution of the input field with the impulse response of MZI, i.e. $h_{MZI}(t)$ as:

$$E_{MZI}(t) = E_{in}(t) * h_{MZI}(t) \tag{5.6}$$

Substituting Equation 5.4 and 5.5 into equation 5.6 gives the output electrical field from the MZI as:

$$E_{MZI}(t) = \frac{1}{2}E_0 e^{j[\omega_0 t + \beta \sin(\omega_s t)]} + \frac{1}{2}E_0 e^{[j\omega_0(t-\tau) + j\beta \sin[\omega_s(t-\tau)]]} \tag{5.7}$$

The intensity of the optical signal detected at the PD can be expressed as, [14]:

$$I_o(t) = [E_{MZI}(t) \times E^*_{MZI}(t)] \tag{5.8}$$

$$I_o(t) = \frac{1}{2}\langle R[E_{MZI}(t) \cdot E^*_{MZI}(t)]\rangle = \frac{1}{2}|E_0|^2 \tag{5.9}$$

$$I_o(t) = \frac{1}{2}|E_0|^2 \times [1 + \cos[\omega_0\tau + \beta \sin(\omega_s t) - \beta \sin[\omega_s(t-\tau)]]] \tag{5.10}$$

$$I_o(t) = \frac{1}{2}|E_0|^2 \times \left\{1 + \cos(\omega_0\tau)\cos\left[2\beta \sin\left(\frac{\omega_s\tau}{2}\right)\cos\left(\omega_s t - \frac{\omega_s\tau}{2}\right)\right] - \sin(\omega_0\tau)\sin\left[2\beta \sin\left(\frac{\omega_s\tau}{2}\right)\cos\left(\omega_s t - \frac{\omega_s\tau}{2}\right)\right]\right\}$$

(5.11)

Using the two sets of Jacobi's identities [5], expressed in (5.12) and (5.13) which denotes the Bessel function of the first kind with respect to the q^{th} order, equation (5.11) is transformed into equation (5.14).

$$\cos\left[\left(2\beta\sin\left(\frac{\omega_s\tau}{2}\right)\cos\theta\right)\right] = J_0\left[2\beta\sin\left(\frac{\omega_s\tau}{2}\right)\right] + 2\cdot\sum_{q=1}^{\infty}(-1)^q J_{2q}\left[\left(2\beta\sin\left(\frac{\omega_s\tau}{2}\right)\cos\theta\right)\right]\cos(2q\theta)$$

(5.12)

$$\sin\left[\left(2\beta\sin\left(\frac{\omega_s\tau}{2}\right)\cos\theta\right)\right] = 2\cdot\sum_{q=1}^{\infty}(-1)^q J_{2q-1}\left[\left(2\beta\sin\left(\frac{\omega_s\tau}{2}\right)\cos\theta\right)\right]\cos[(2q+1)\theta]$$

(5.13)

$$I_{PD}(t) = \frac{1}{2}|E_0|^2\cdot\left[1+\cos(\omega_0\tau)\left[J_0\left(2\beta\sin\left(\frac{\omega_s\tau}{2}\right)\right) + 2\sum_{q=1}^{\infty}(-1)^q J_{2q}\left(2\beta\sin\left(\frac{\omega_s\tau}{2}\right)\cos\theta\right)\cdot\cos\left[2q\left(\omega_s t-\frac{\omega_s\tau}{2}\right)\right]\right]\right.$$
$$\left. - 2\sin(\omega_0\tau)\cdot\sum_{q=1}^{\infty}(-1)^q J_{2q-1}\left(2\beta\sin\left(\frac{\omega_s\tau}{2}\right)\cos\theta\right)\cdot\cos\left[(2q-1)\cdot\left(\omega_s t-\frac{\omega_s\tau}{2}\right)\right]\right]$$

(5.14)

The evaluated input OFM signal at the PD $[I_{PD}(t)]$ is given by equation (5.14). To achieve only the even harmonic components on the optical free spectral range and removing the odd harmonic components, the value of q has to be ≥ 0 in the equation:

$$\omega_s\tau = \pi(2q+1) \tag{5.15}$$

In this case where β, the Frequency Modulation index is the variable that depicts the amplitude of the generated harmonic components hence the average harmonic's power. The increase in the frequency modulation index variable also

determines the optical frequency deviation of each peak. This results in a complex up-conversion factor because as more β is applied, the spectral efficiency of the OFM systems reduces. This becomes unfeasible when trying to generate mm-wave as it implies that when the frequency deviation increases to obtain the mm-wave harmonic (e.g. 60 GHz), a compromise in bandwidth is associated. This also means that a slight chirp at the operating wavelength causes the harmonic components to disappear, meaning that a tunable laser source is required at transmission site along with a temperature stabilizer to reduce the temperature dependence of τ.

This process of mm-wave generation becomes ever more complex and an expensive procedure that makes it less attractive for both site and indoor applications. However, OFM in its standard composition is the lesser expensive and complex scheme alternative in mm-wave generation due to its lack of mm-wave local oscillator requirement for heterodyning. This lead to a reported novel scheme of mm-wave generation based on OFM system but including a Dual-Drive Mach-Zehnder Modulator (DD-MZM) [6].

5.3 OFM technique based on DD-MZM adoption

The fundamental configuration for OFM scheme involve the phase modulation of the sweep signals to generate the high order frequency harmonics and then the heterodyning of the signal using the Mach-Zehnder Modulator (MZM). The MZI causes the delay between its two branches for optical interference required for phase modulation to intensity modulation. This proposed approach in this thesis requires the implementation of a DD-MZM device which by principle is a coupled two-part optical phase modulator and removes the requirement of periodic filtering by the

MZI. This configuration has already been reported for mm-wave RoF transmission system [6] and is the basis of this chapter in generating 60 GHz RoF transmission link.

5.3.1 Theory analysis of OFM DD-MZM system

The electrical field of the optical signal after the DD-MZM is given as, [15]:

$$E_{DD} = E_1 e^{j[\omega_\lambda(t+\tau) + \beta_1 \cos((\omega_{sw}t+\omega_{sw}\tau)+\theta)+\Delta\theta+\theta_{N1}]} + E_2 e^{j[\omega_\lambda t+\beta_2 \cos\omega_{sw}t+\theta_{N2}]} \quad (5.16)$$

Where E_1 and E_2, are the electric field's amplitude of both arms of the DD-MZM respectively; ω_λ and ω_{sw}, are the radian frequency of the lightwave and sweep signal respectively; τ, is the differential path delay of both branches of the DD-MZM; β_1 and β_2, are the phase modulation indexes of the two sweep signals respectively; θ, optical phase difference between the two sweep frequencies; $\Delta\theta$, the phase created by the bias voltages of the two arms of the DD-MZM; θ_{N1} and θ_{N2}, the phase noise at the two arms of the DD-MZM respectively.

The intensity of the optical signal detected at the PD can be expressed as, [15]:

$$i_{PD}(t) = [E_{DD}(t) \times E_{DD}^*(t)] \quad (5.17)$$

$$i_{PD}(t) = \frac{1}{2}\langle R[E_{DD}(t) \cdot E_{DD}^*(t)]\rangle = \frac{1}{2}|E_o|^2 \quad (5.18)$$

$$i_{PD}(t) = \frac{1}{2}|E_o|^2 \times \{E_1^2 + E_2^2 + 2E_1E_2\cos[\beta_1\cos(\omega_{sw}t + \omega_{sw}\tau + \theta) - \beta_2\cos\omega_s t + \omega_\lambda\tau + \Delta\theta + \theta_{N1} - \theta_{N2}]\} \quad (5.19)$$

The evaluated Bessel function series of the intensity photo-current OFM DD-MZM signal [15], received at the PD [$i_{PD}(t)$] is given by equation (5.20) [see Appendix B]:

$$i_{PD}(t) = \frac{1}{2}|E_o|^2 \times \left\{ E_1^2 + E_2^2 + 2E_1E_2 \left[J_0\,(\beta_1 + \beta_2) + 2\sum_{q=1}^{\infty} (-1)^q J_{2q}(\beta_1 + \beta_2) \cos(2q\omega_{sw}t) \right] \right\} \tag{5.20}$$

5.4 OFM Simulation Introduction

In recent papers, other reported system design make provision for LTE, Wi-Fi or Ethernet channels transmitted through OFM application, with only SMF cables [6] or where both SMF and POF cables are used, a different modulation technique known as Optical Carrier Suppression (OCS) is implemented [10]. The aim of this section is to demonstrate a feasible transmission network to deliver LTE and Wi-Fi wireless channels over both SMF and POF cables using Optical Frequency Multiplication (OFM) and the Offset Launch (OL) theory to improve the signal bandwidth and characteristics. Orthogonal Frequency Division Multiplexing (OFDM) is used as a modulation technique due to its high spectrum efficiency and high resistance to different types of dispersions such as chromatic dispersion [11]. The combination of SMF and MMF application for data transmission is advantageous but can be challenging due to the high bandwidth impairments caused by the MMF fibers during propagation. To mitigate these bandwidth impairments, an additional scheme for observing the impact of the offset launch (OL) between the SMF and MMF cables are investigated for bandwidth improvement [12].

Chapter 3 demonstrates that conducted theoretical and experimental observations show a four-fold bandwidth improvement compared to standard overfilled launch techniques. Regardless of the type of MMF fiber, their core diameters or core refractive index profiles, improved bandwidth capacity is achieved. This technique

isn't susceptible to environmental conditions and can withstand bending of the MMF links at angles up to 6^{o} from a fixed position [13].

5.4.1 OFM Simulation design

As shown in [Fig 5.2], the simulation design of the OFM downstream segment; a DFB laser emitting an optical polarized signal at 1552 nm was used as the CW laser and inserted into a Dual Drive Mach-Zehnder Modulator (DD-MZM) at the central station (CS). Combinations of two 10 GHz sweep signals with a phase difference of π, are used to drive the DD-MZM to generate optical phase modulation. From equation **B.8** and **B.9**, by selecting the phase modulation index ($\beta_1 + \beta_2$) on each arm of the DD-MZM and 10 GHz frequency sweep signal (ω_{sw}), the corresponding average power of the free spectral range harmonic components was produced along with the 60 GHz modulated signal. The effect of phase modulation-intensity modulation by the DD-MZM creates several optical modes which are then re-modulated in an Intensity Modulator (IM-MZM) by a combined LTE OFDM modulated signals at 1805 MHz and 2.4 GHz Wi-Fi. The IF (LTE) signal contains 16-QAM 100Mbit/s data rate which is modulated onto an OFDM 20 MHz bandwidth signal and then combined with the Wi-Fi signal centred at 2.4 GHz bearing a bandwidth of 16.6 MHz and also carrying a 100 Mbit/s data with at 7 dBm output power. The output signal of the IM-MZM is amplified by an EDFA and transmitted through a downlink coupled 25-km SMF fiber and 10-m MMF-POF fiber before which the signal is received at the base station by a PIN photodetector (PD). With this OFM system any harmonics can be selected by a bandpass filter depending on the required application, thus making way for the advantages of in-door cell re-use.

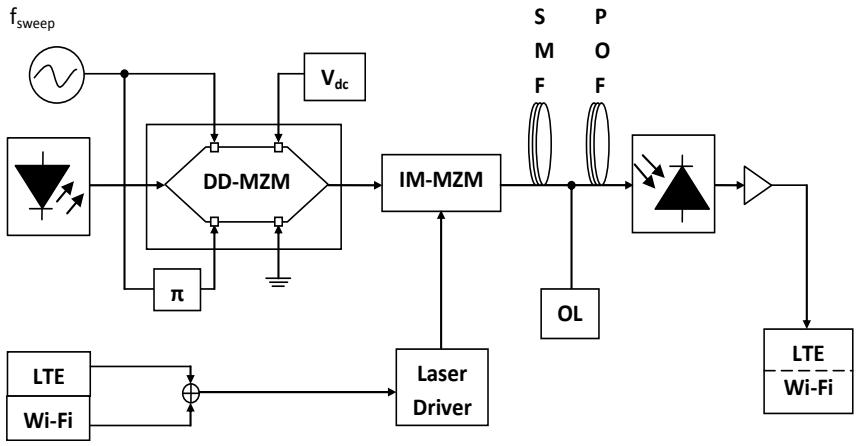

Figure 5.2: The network topology for the OFM technique to deliver LTE and Wi-Fi channels over SMF and MMF-POF cables. DD-MZM: Dual-Drive Mach-Zehnder modulator, IM-MZM: Intensity Modulating Mach-Zehnder modulator, OL: Offset Launch

5.4.2 OFM Simulation Result and Discussion

Fig 5.3 shows the harmonics of the two wireless signal spectrums after detection at the photodetector after POF transmission. In this diagram, several high order harmonics, especially the IF of both Wi-Fi and LTE signals at 62.4 GHz and 61.805 GHz respectively, are present. Also there is the availability of a 60 GHz carrier signal which can be filtered out and used as a local oscillator for the uplink data transmission at the residential property, back to the central station. Fig 5.4 shows the spectrum of the 1805 MHz (or 1.805 GHz) and 2.4 GHz signals after detection by the photodetector and amplified. Fig 5.5 and Fig 5.6 shows the clearly sperated constellation diagrams of both the received LTE and Wi-Fi channels. The optical spectrum of both the 60 GHz carrier and 62.4 GHz signals after 150-m BI-SMF fiber propagation can be seen in Fig 5.7 and after photodetection can be observed in Fig 5.8. The major impact of phase noise in the system can be observed in Fig 5.9. This

change in the angle of the constellation points is the representatrion of phase noise in the OFDM signal and can be mitgated with simple techniques.

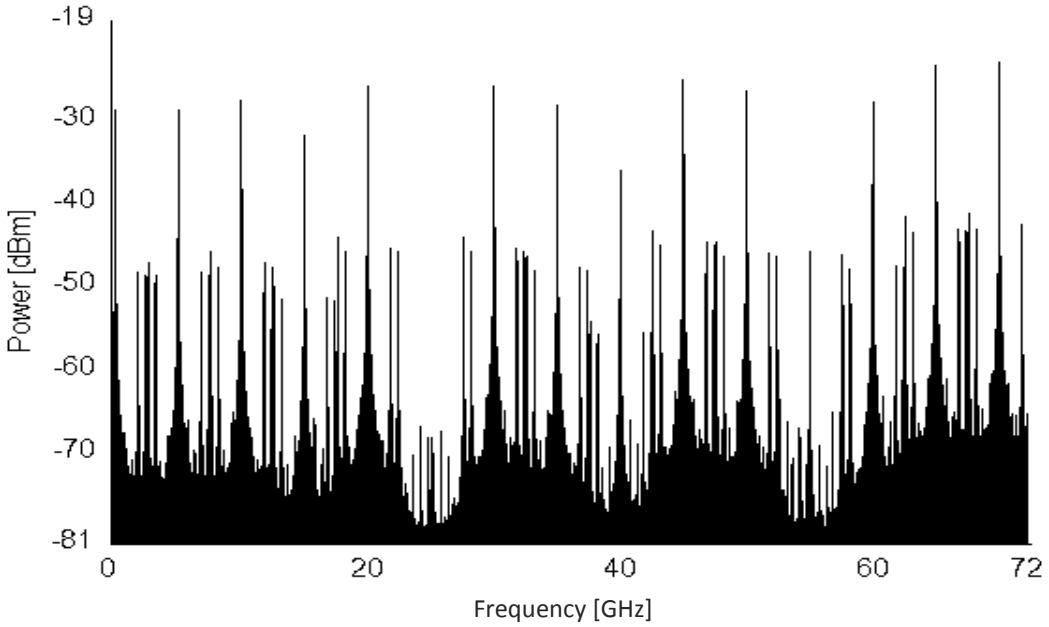

Figure 5.3: The signal spectrum output at the photodetector of POF transmission

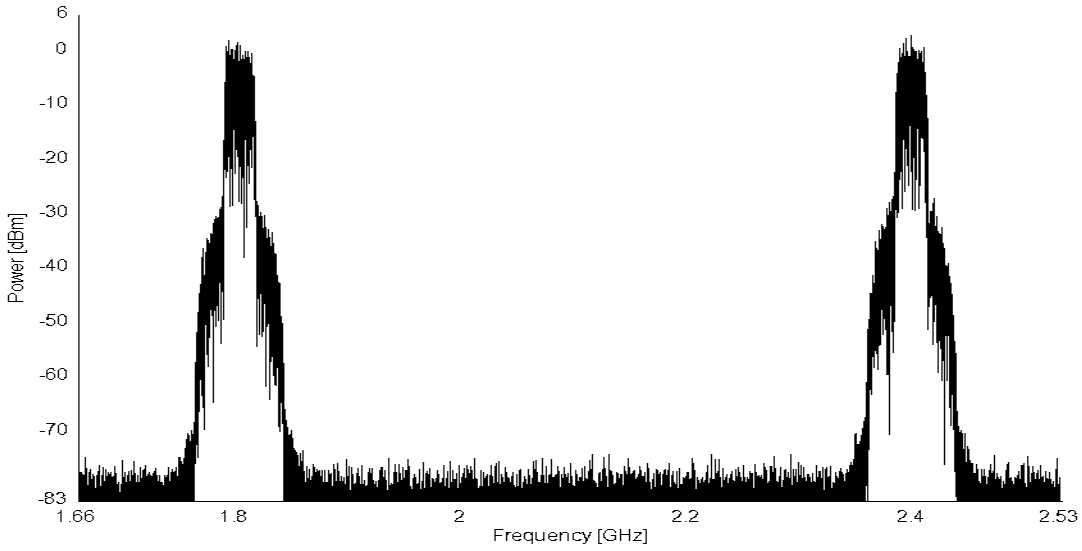

Figure 5.4: The amplified received 1805 MHz and 2.4 GHz OFDM spectrums at the photodetector

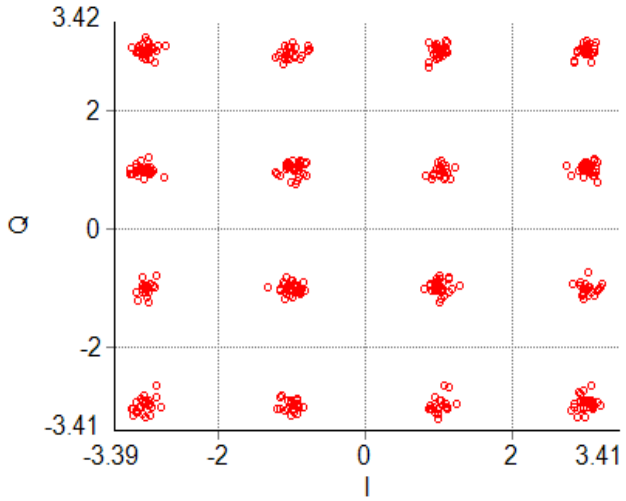

Figure 5.5: The received 1805 MHz OFDM 16-QAM constellation of the LTE signal

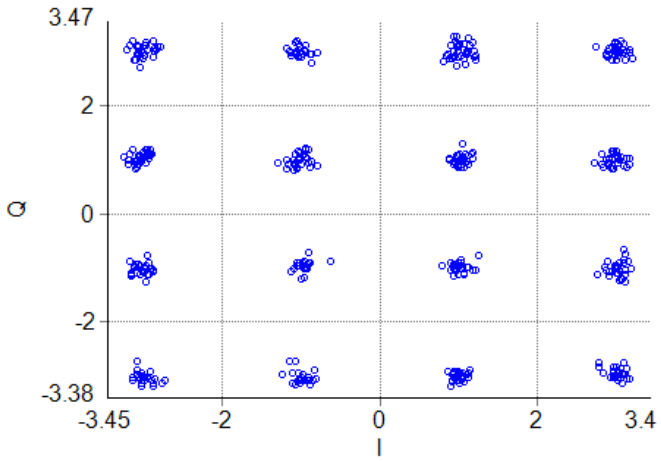

Figure 5.6: The received 2.4 GHz OFDM 16-QAM constellation of the Wi-Fi signal

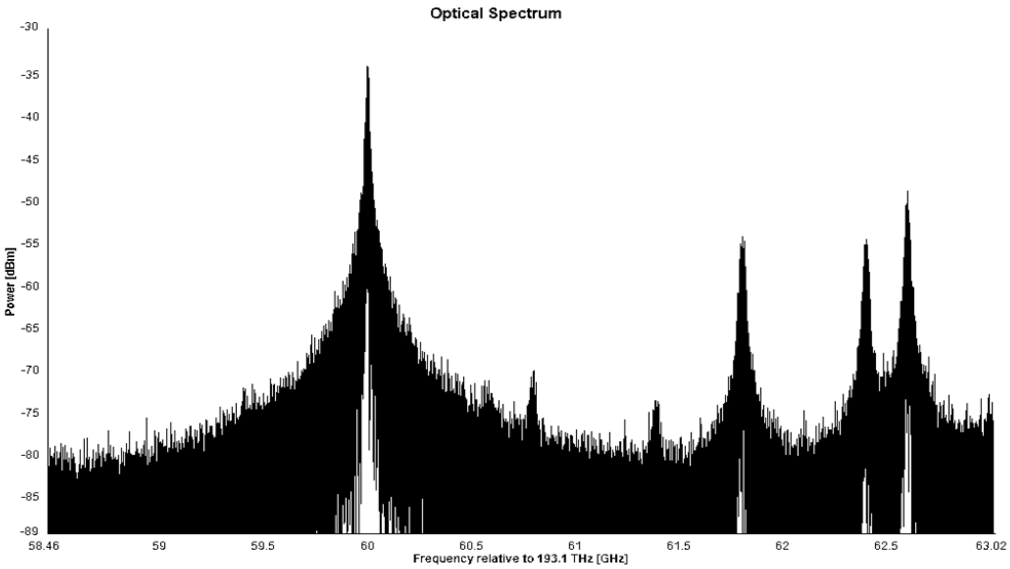

Figure 5.7: The amplified mm-wave band signal spectrum after 150-m BI-SMF optical fiber

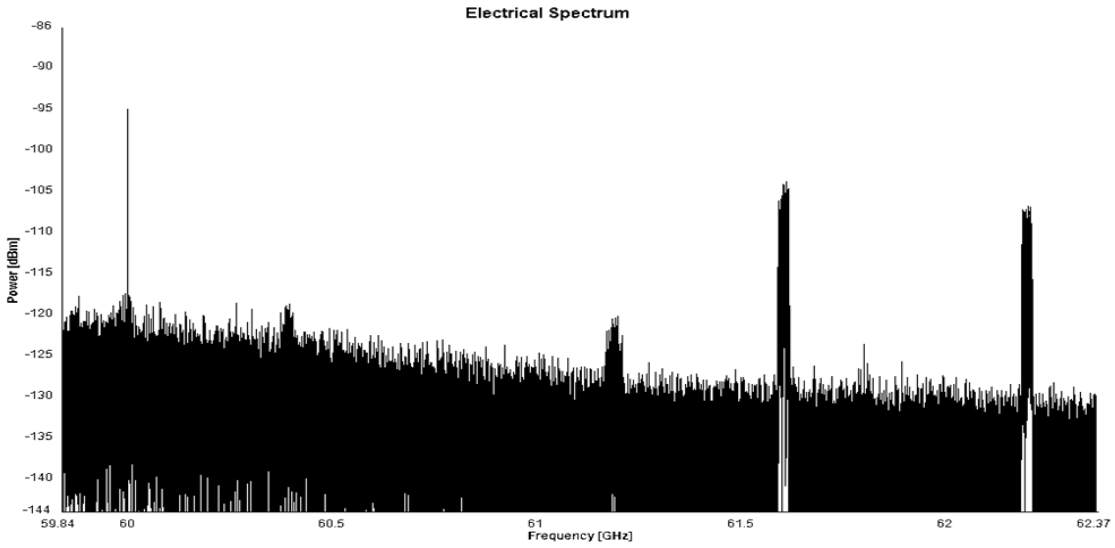

Figure 5.8: The (pre-EA) received electrical signal of both 61.8 GHz and 62.4 GHz signals after 150-m BI-SMF propagation

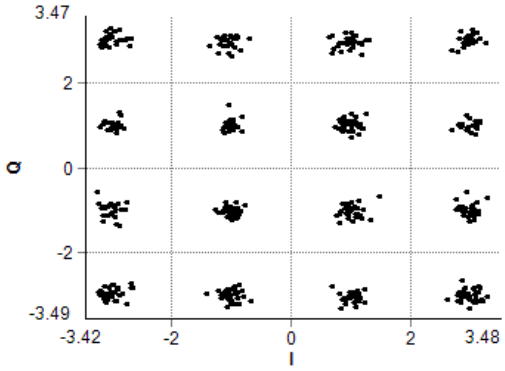

Figure 5.9: The received 62.4 GHz constellation points after 150-m BI-SMF transmission

Free space distance (m)	Received power (dBm)		
	LTE	Wi-Fi	62.4 GHz
1	-68.844	-78.032	-96.398
2	-68.843	-78.031	-96.397
3	-68.842	-78.030	-96.396
4	-68.842	-78.030	-96.396
5	-68.841	-78.029	-96.395

Table 5.1: Received power (pre-EA) of wireless channels over 150-m BI-SMF at various free space distances

5.5 Summary

Based on this simulation, the design of LTE and Wi-Fi signals can be transmitted through both SMF and MMF-POF cables successfully and received at adequate signal level thresholds for indoor home applications. An increase in the length of the MMF-POF optic cable increased the attenuation witnessed on both the LTE and Wi-Fi signals so as a result, the MMF-POF length was observed until 10-m after which signal loss became severe. The offset launch technique applied at the junction of the

SMF and MMF-POF showed very negligible improvement on the signal bandwidth at 22 μm offset launch condition from the centre launch position on the core of the 10-m MMF-POF fiber. In Fig 5.3 and Fig 5.8 the spectrum shows a 60 GHz carrier and Wi-Fi signal at 62.4 GHz. This is beneficial for transmitting the forthcoming IEEE 802.11 b/g/ad WLAN signals for in-door applications. This OFM transmission technique also allows for various wireless signals to be distributed around the home (or building) as a heterogeneous network over an array of antennas. This can be achieved by frequency down-conversion to IF harmonic components in the spectral range to the desired frequency band before antenna radiation. Table 5.1 shows the received electrical power of LTE, Wi-FI and 62.4 GHz signal after free space transmission over a 5-m link. The table results demonstrate negligible change to the received power of the radiated signals. This reinforces the attribute of deploying OWC system in an in-door environment for effective over-the-air transmission.

References:

[1] T. Koonen, A. Ng'oma, P. F. M. Smulders, H. P. A. vd. Boom, I. Tafur Monroy, and G. D. Khoe, "In-House networks using Multimode Polymer Optical Fiber for broadband wireless services", Photonic Network communications, Vol. 5, No. 2, 1777-187, (Kluwer, 2003).

[2] M. Garcia Larrode, A. M. J. Koonen, and J. J. Vegas Olmos, "Over-coming modal bandwidth limitation in radio-over-multimode fiber links," *IEEE Photon. Technol. Lett.*, vol. 18, no. 22, pp. 2428-2430, 2006.

[3] T. Koonen, A. Ng'oma, P. F. M. Smulders, H. P. A. vd. Boom, I. Tafur Monroy, and G. D. Khoe, "In-house networks using Polymer Optical Fibre for broadband wireless applications", in Proceedings of the ISSLS 2002, 2002, pp 285-294.

[4] M. G. Larrode and A. M. J. Koonen, "Theoretical and experimental demonstration of OFM robustness against modal dispersion impairments in radio over multimode fiber links", J. Lightw. Technol., vol. 26, no. 12, pp. 1722-1728, 2008.

[5] G. N. Watson, "A treatise on the theory of Bessel Functions", (Cambridge University Press, London, 1966).

[6] Yi Li, Rujian Lin, Yingchun Li, Jiajun Ye, "Bi-directional mm-Wave R-o-F system based on OFM and modulated by OFDM" in *CCWMC Dec 2009, IET Int. Comm Conf in Shanghai, China*.

[7] H. S. Mackenzie, "Evanescent field devices for non-linear optical applications," Ph.D. dissertation, Cambridge University, U.K., 1987.

[8] J. Gowar, "*Optical Communications Systems*." Englewood Cliffs, NJ: Prentice-Hall, 1984.

[9] M. J. Yadlowsky and A. R. Mickelson, "Distributed loss and mode coupling and their effect on time dependent propagation in multimode fibers," *Appl. Opt.,* vol. 32, pp. 6664-6677, 1993.

[10] Yan Shi, Maria Morant, et al., "Multistandard Wireless Transmission over SSMF and Large-Core POF for Access and In-Home Networks" *IEEE Photonics Technology Letters*, vol. 24, pp. 736-738, May 2012.

[11] Xiaodong Wang. "OFDM and its application to 4G", IntConf Wir Opt Commun WOCC, pp. 69-. (2005).

[12] L. Raddatz, I. H. White, D. G. Cunningham, and M. C. Nowell, "An Experiment and Theoretical Study of the Offset Launch Technique for the Enhancement of the Bandwidth of Multimode Fiber Links," *Journal of Lightwave Technology*, vol. 16, NO. 3, March 1998.

[13] L. Raddatz, I. H. White, D. G. Cunningham, and M. C. Nowell, "Increasing the bandwidth-distance product of multimode fiber using offset launch," *Electron. Lett.,* vol. 33, pp. 232-233, 1997.

[14] A. M. J. Koonen and A. Ngoma, "Integrated broadband optical fibre/wireless LAN access networks," in *Broadband Optical Access Networks and Fiber-to-the-Home: System Technologies and Development Strategies*. New York: Wiley, 2006.

[15] Rujian Lin, Meiwei Zhu, Zheyun Zhou and Jiajun Ye, "Theoretic and experimental study on mm-wave radio over fiber system based on OFM", *Proc. SPIE* 7137, Network Architectures, Management, and Applications VI, 71371M, Novemeber 2008.

Chapter 6

Remote Heterodyne Detection (RHD) - based on optical carrier suppression (OCS) modulation

6.1 Remote Heterodyne Detection (RHD)

6.1.1 Outline of Simulation

This chapter investigates the design of a low power consumption mm-wave radio-over-fiber transmission over 25-km SMF and 30-m MMF for in-door applications using a dual drive Mach-Zehnder modulator (DD-MZM) and WDM multiplexers. This architecture includes the generation of both a 60 GHz mm-wave signal and a remote local oscillator (LO) for uplink transmission at the residential gateway by utilizing the coexistence of two lasers and a DD-MZM at the central office to create optical carrier suppression modulation. At the receiver gateway, Offset Launch conditions between the SMF and MMF-POF fiber optic cables is used to mitigate the impact of multimodal dispersion found in the multimode optical fiber.

6.1.2 Introduction to RHD

As discussed in *Chapter 1*, one of the improvements in access technology included the use of WDM systems which gave rise to coherent optical communication. Remote Heterodyne Detection (RHD) is based on coherent optical communication and generates mm-wave frequency by combining two laser transmitters with a frequency offset. The optical output realizes OCS modulation to generate subcarriers and modulating data with mm-wave (60 GHz) frequency spacing [Fig 6.1] before SMF and MMF transport.

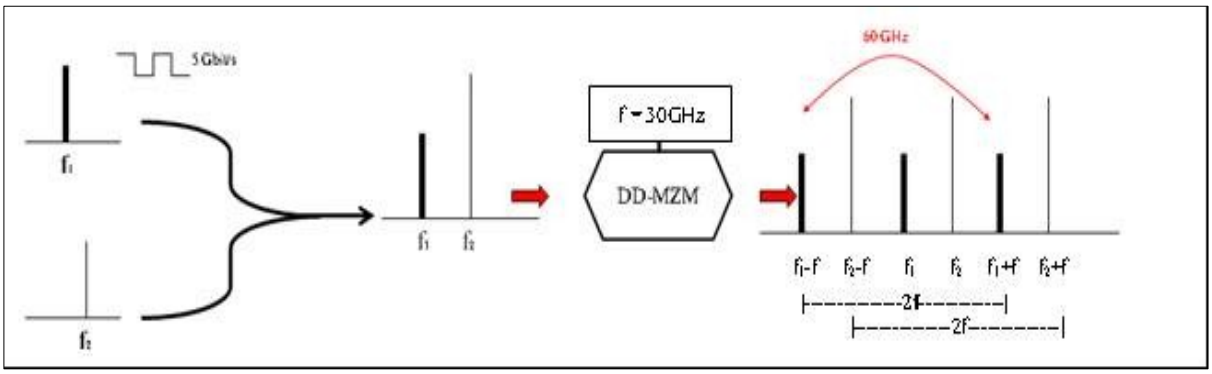

Figure 6.1: RHD mm-wave system based on OCS modulation

This chapter demonstrates the application of remote heterodyning detection technique (RHD) [4], to deliver 2.5, 5 and 10 Gbit/s data over a combination of SMF and MMF-POF cables. The combination of SMF and MMF utilization for mm-wave transmission is highly favourable but yet challenging due to the high bandwidth impairments induced by the MMF-POF material. To mitigate this impairment, offset launch conditions between the SMF and MMF cables are investigated [5]. The DFB laser source operating at 850-nm wavelength was used because of its low attenuation window in the MMF (POF) spectrum, [Fig 2.3]. DFB laser source modules operating approximately at 850-nm although uncommon have been reported in [8]

and [9]. It has been reported that both theoretical and experimental observations show a four-fold bandwidth improvement compared to standard overfilled launch techniques. Regardless of the type of MMF fiber, their core diameters or core refractive index profiles, improved bandwidth capacity is achieved. This technique isn't susceptible to environmental conditions and can withstand bending of the MMF links at angles up to 6^{o} from an ordinary stationary position [6]. The central station (CS) design involves the uplink transmission of a 5 Gbit/s data rate over a 60 GHz carrier signal using a combination of an external modulator and two laser sources with a frequency difference of 20 GHz apart. Only one of the two laser sources is modulated with data which are both coupled into the DD-MZM. A combination of two 30 GHz sweep signals with a phase difference of π, are used to drive the DD-MZM biased at minimum transmission point to generate optical phase modulation subcarriers and modulating data with a 60 GHz spacing. The output signal of the DD-MZM is amplified by an Erbium Doped Fiber Amplifier (EDFA) and propagated downlink through a coupled 25-km SMF and a 30-m MMF-POF before reception at the BS. After the fiber propagation, a selection of two WDM demultiplexers (DMUX) and Multiplexers (MUX) were used at the BS to separate the subcarriers and the modulating sidebands. This allows for then successful detection of the 60 GHz mm-wave signal with modulating data and without modulating data at the BS meaning a 60 GHz mm-wave signal transmission is received with an additional 60 GHz mm-wave LO at the BS for further uplink transmission.

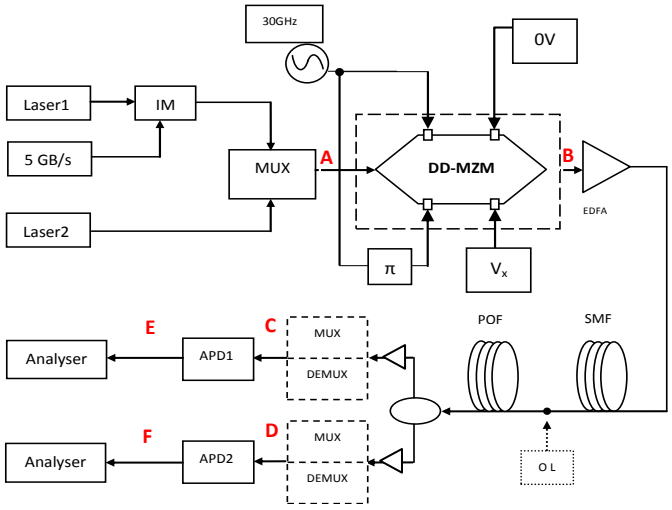

Figure 6.2: The design of the proposed mm-wave delivery over SMF and POF. IM: intensity modulator, DD-MZM: Dual-Drive Mach-Zehnder Modulator, EDFA: erbium-doped fiber amplifier, OL: offset launch, MUX/DEMUX: optical multiplexers, APD: Avalanche photodiode, EA: electrical amplifier.

6.2 RHD Simulation design

The simulation design of the 60 GHz mm-wave generation over optical fibers is illustrated in Fig 6.2. Two tunable lasers, Laser1 and Laser2, are emitting an optical polarized signal at 850nm (352.70 THz) and 849.95nm (352.72 THz) respectively at the CS. The frequency difference between the two laser sources is set to 20 GHz. The linewidths of Laser1 and Laser2 are set to 200 MHz whilst both powers of the Lasers are set at 1-mW. 5 Gbit/s pseudo-random binary sequence (PRBS) is used to modulate the continuous carrier light-wave from Laser1 by the intensity modulator (IM). Both carrier waves (CW) are coupled together by a multiplexer. The parameters of the DD-MZM are as follows; the frequency sweep signal, f_{sweep} = 30 GHz, V_{π} = 4V, $V_{Rf\text{-}up}$ = 1V, $V_{Rf\text{-}down}$ = 1V, $V_{bias\text{-}up}$ = 0V, $V_{bias\text{-}down}$ = 4V. The DD-MZM biased at the minimum transmission point realizes optical carrier suppression (OCS) modulation of

the received signals before amplification by an EDFA and transmitted through a coupled 25-km SMF (with a fiber dispersion setting as 16 ps/nm.km) and 30-m POF optical fibers. Both SMF and MMF cable have attenuation parameters set at 0.2 dB/km and 2.18 dB/km respectively. After transmission over the optical fibers cable links, the signal is split into two paths using multiplexers (DE/MUX) to separate the modulated data and subcarriers causing a frequency spacing of 60 GHz. The separated modulated signals are amplified and received at the avalanche photodetector APD1 whilst the two subcarriers of 60 GHz spacing are received at APD2 which can be utilized as a local oscillator after heterodyning. As the linewidth of the laser source at CS cannot be set at 0, any increase in linewidth is found to have an adverse effect in power improvement of the mm-wave signal due to phase noise [7].

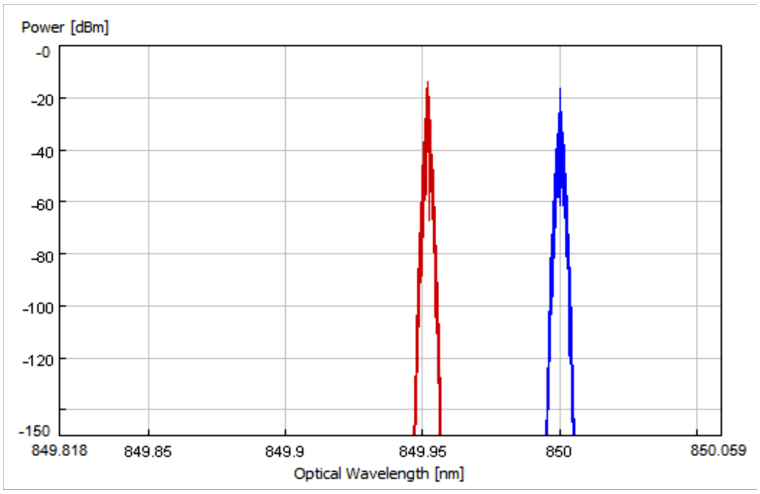

(a)

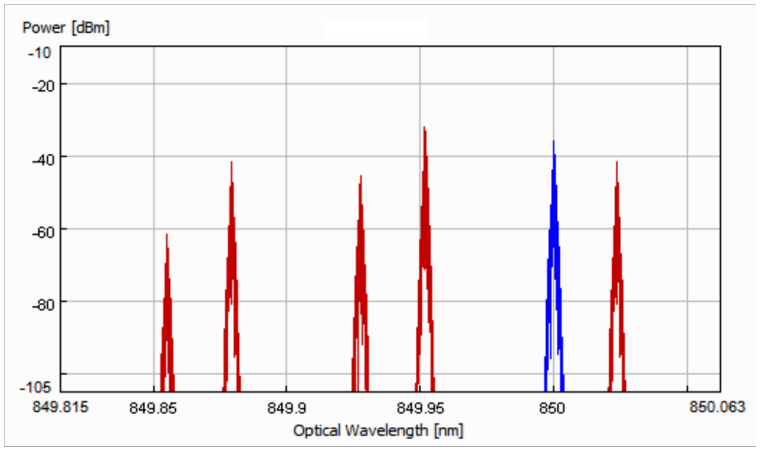

(b)

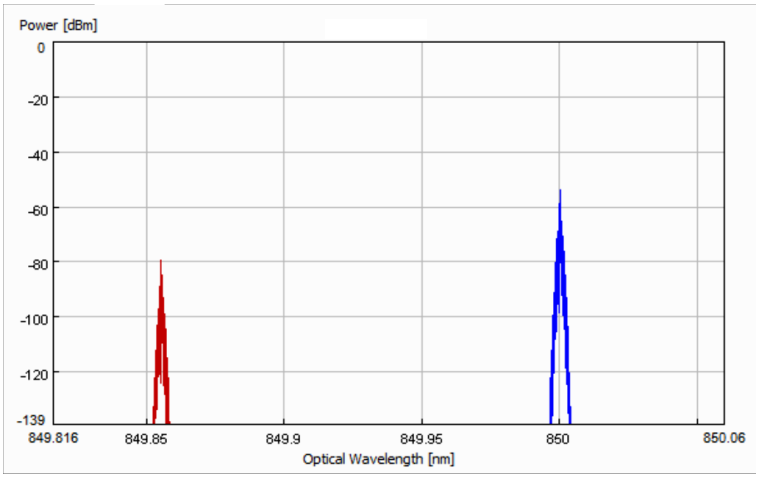

(c)

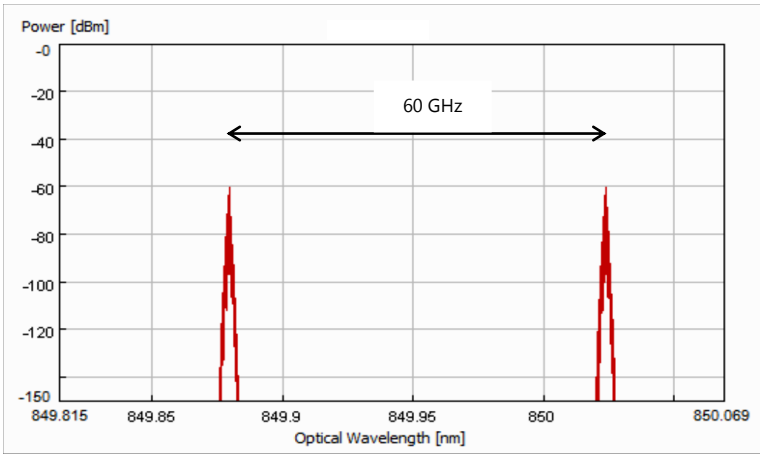

(d)

Figure 6.3: Simulation result: optical spectrum at A(a),B(b),C(c),D(d) in Figure 6.2

6.2.1 Simulation Results and Discussion for 25-km SMF and 30-m POF

The optical spectrum of the generated subcarriers and modulated data can be seen in Fig 6.3(b). At the receiver gateway, the spectrum can be separated using multiplexers to obtain mm-wave signal at 60 GHz apart, Fig 6.3(c) and also two subcarriers that are 60 GHz apart, see Fig 6.3(d). The power decline compared to selected laser linewidth variations over SMF and MMF POF cables at 30-m and 15-m lengths can be seen in Fig 6.4. From this result, it can be concluded that the minimum linewidth can be selected in order to improve the received power performance of the modulated signal at the photodetectors. This can also be observed for preselecting the data rate at 2.5 and 5 Gbit/s at CS transmission for different lengths of MMF-POF cables.

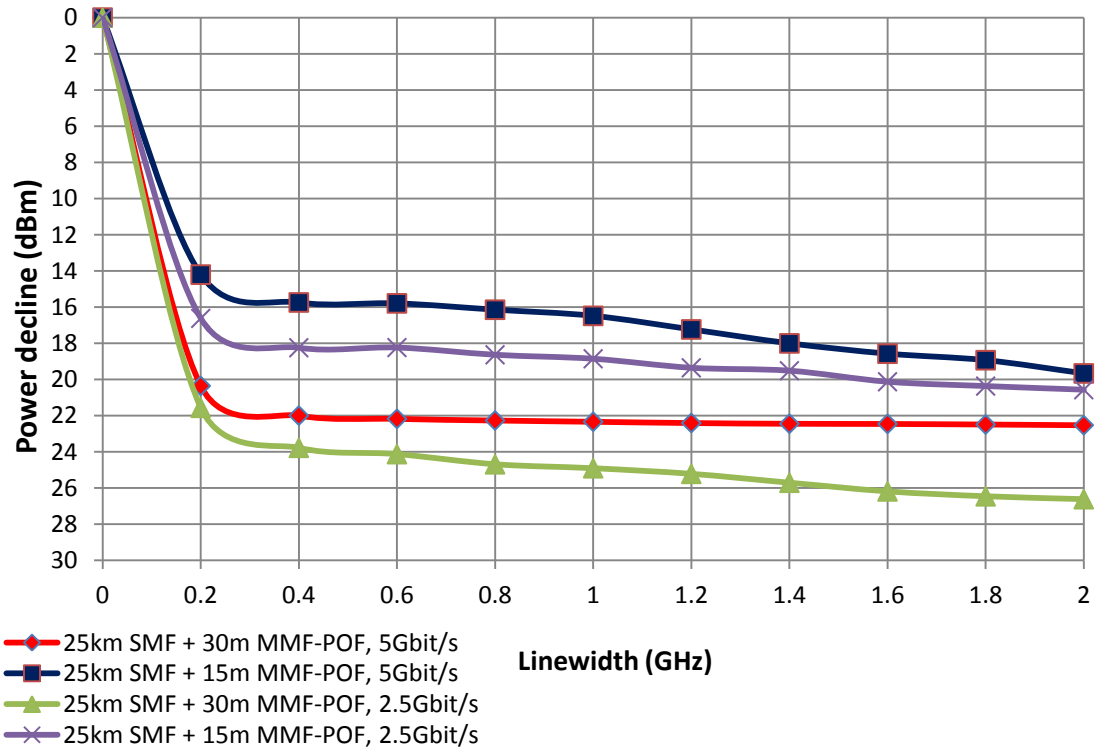

Figure 6.4: The decline in power of the mm-wave signal at various laser linewidths

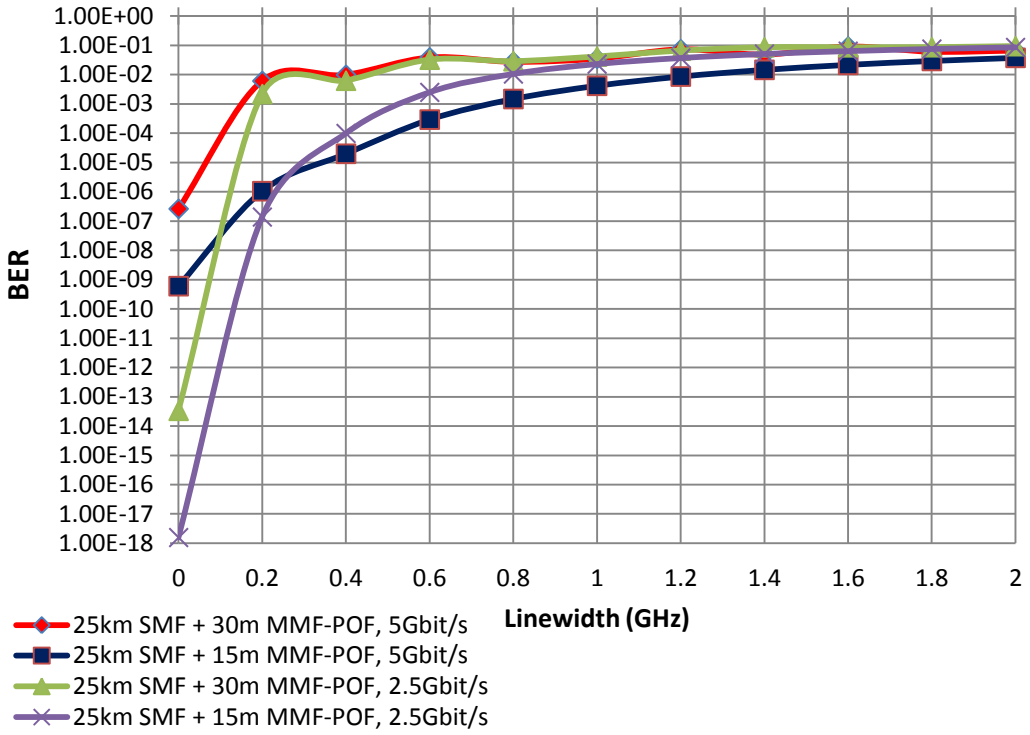

Figure 6.5: The bit-error-rate performance at various laser linewidths

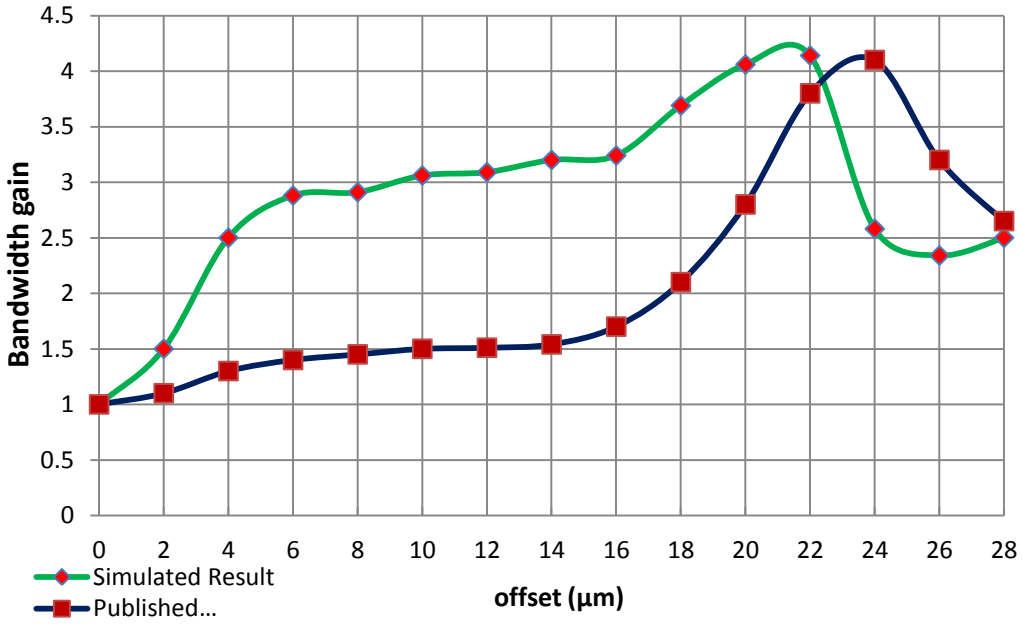

Figure 6.6: The bandwidth improvement against various offset launch conditions for SMF fiber. Published Result** [6]

The received BER peformance was also observed against various laser linewidths, Fig 6.5. Based on the result in Fig 6.4 and Fig 6.5 it is therfore observed necessary to keep the laser's linewidth at a minimum, in order to maximize the received power of the mm-wave signal. As discussed earlier, the effect of various offset launch (OL) conditions has proven to increase the bandwidth of the modulated signal at photodetection, [Fig 6.6]. The observed result is simlar to previous published work in [6].

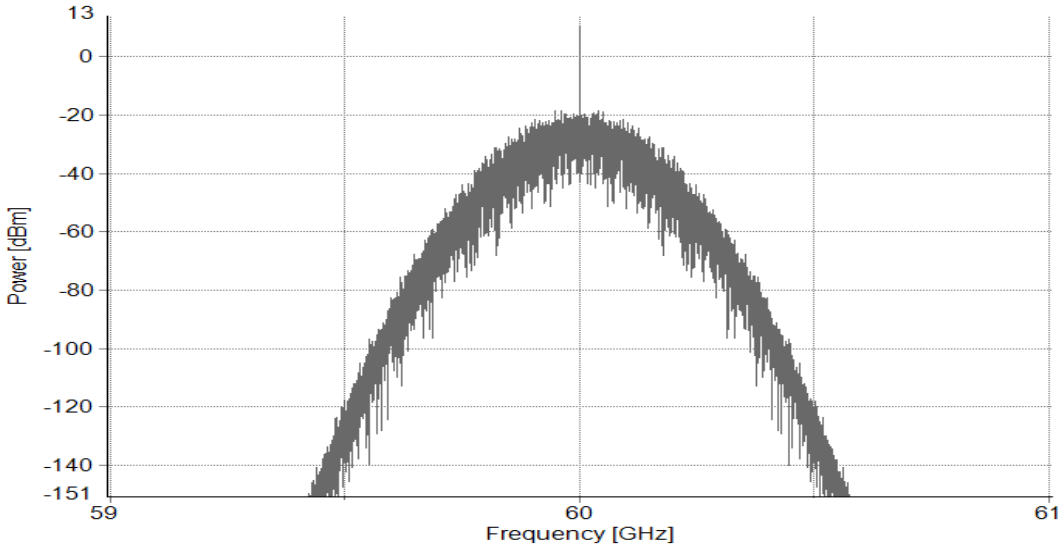

Figure 6.7: RF spectrum of received 60 GHz signal at point E in Figure 6.2

6.3 Mm-wave and Wi-Fi simulation design

The architecture of this design includes the addition of a 2.4 GHz Wi-Fi signal carrying a 100 MBit/s (OFDM) data multiplexed at the CO for downlink transmission through coupled 25-km SMF and 30-m MMF-POF [Fig 6.8]. At the receiver station (RS), the two wireless channels were separated using bandpass filter and multiplexer.

The received Wi-Fi data signal at 2.4 GHz is demodulated and processed with an OFDM receiver while the 10 Gbit/s mm-wave baseband data is filtered and analysed.

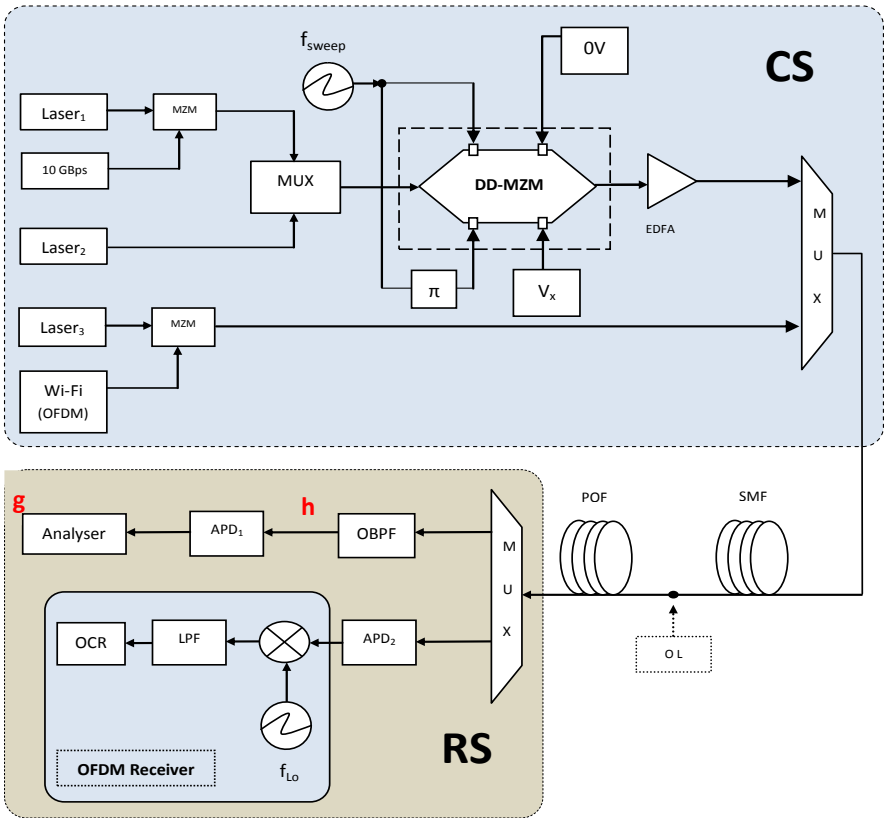

Figure 6.8: The mm-wave and Wi-Fi delivery over SMF and POF

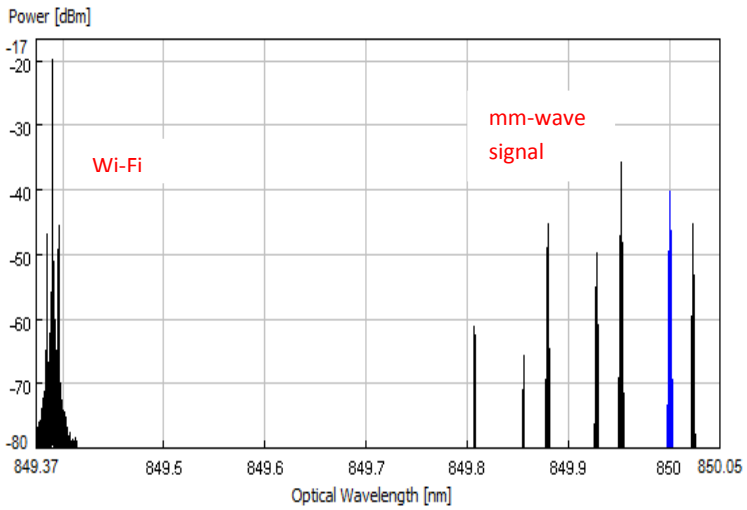

Figure 6.9: The WDM of mm-wave and Wi-Fi delivery over SMF and POF

The best offset launch condition set at 22 µm was observed to improve the Inter-Symbol-Interference (ISI) charcateristics of the mm-wave signal data received at point “g” in Fig 6.8 which displayed a closing eye-diagram with significant interference as observed in Fig 6.10. The received 16-QAM constellation of the Wi-Fi signal can also be observed in Fig 6.12.

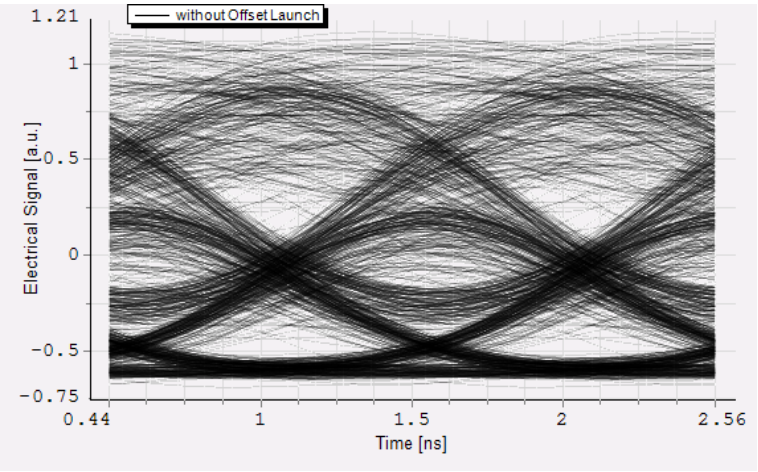

Figure 6.10: Eye-diagram for 10 Gbit/s data without Offset Launch

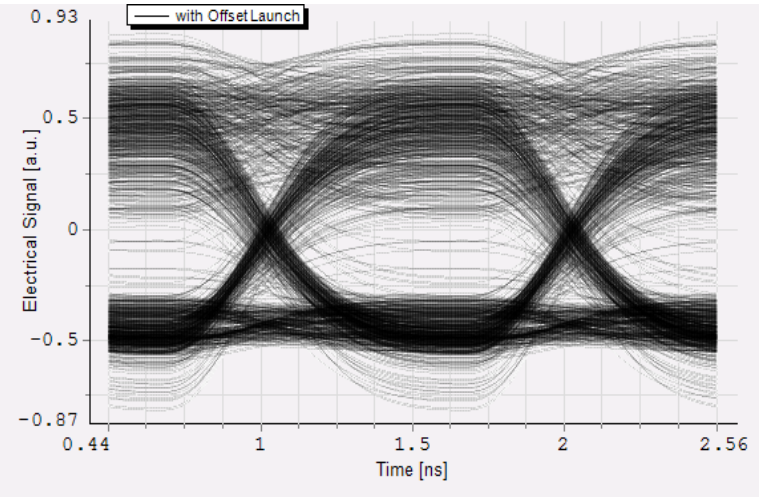

Figure 6.11: Eye-diagram for 10 Gbit/s data with Offset Launch

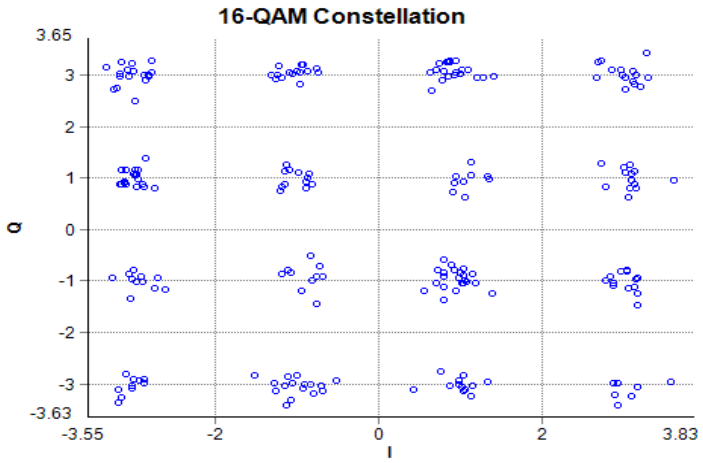

Figure 6.12: The 16-QAM constellation of the received Wi-Fi OFDM signal

The BI-SMF optical cable was replaced with the MMF-POF cable for futher result anlaysis. The observed result showed a much more improved ISI performance [Fig 6.13] compared to the MMF. In Fig 6.14, the received mm-wave signal power at the receiver station (RS) showed a higher received power in comparsion to the POF cable application.

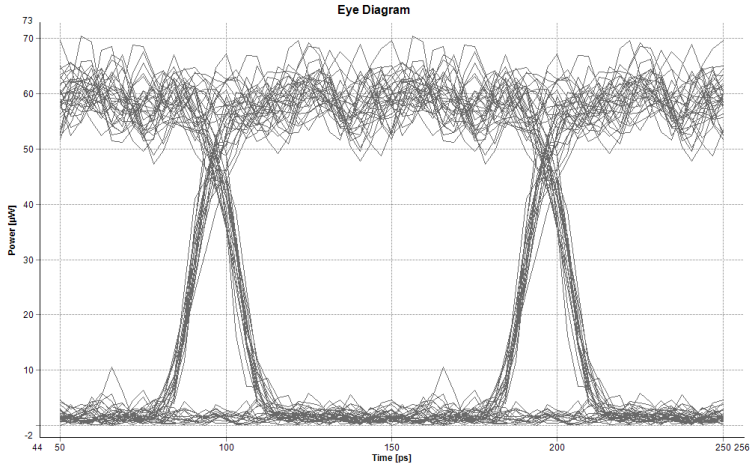

Figure 6.13: Eye-diagram of 10 Gbit/s data over 150-m BI-SMF

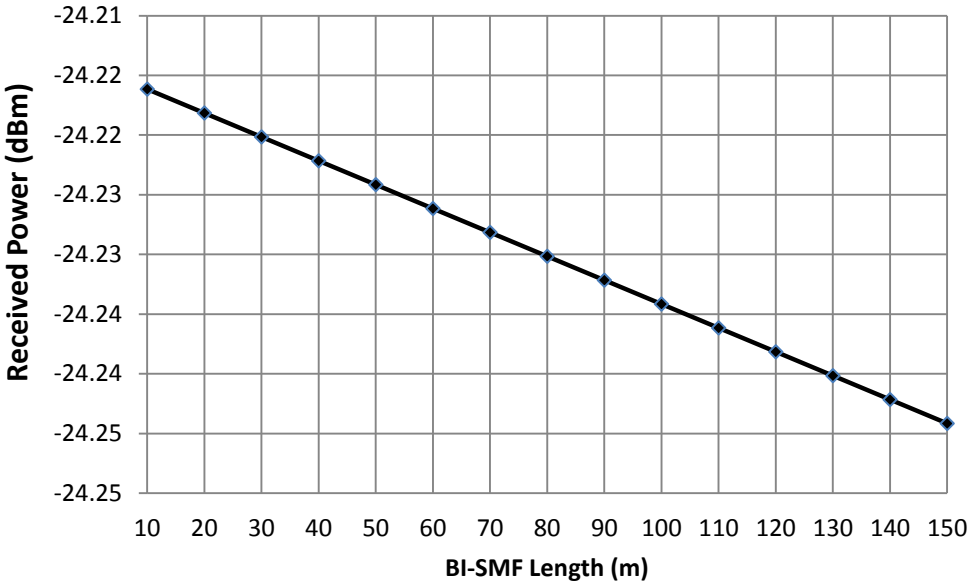

Figure 6.14: Received 60 GHz signal power versus BI-SMF fiber lengths

6.4 Mm-wave RHD over OWC link with MMF and BI-SMF

In the subcsribers home where mm-wave services application will be adopted. The use of optical wireless communication link over mm-wave RHD transmission scheme was also observed in this thesis. Both the receiver power decline and BER performance (for non-LOS) were examined of the received mm-wave signal as can be seen in Fig 6.15 and Table 6.1 respectively. The mm-wave 10 Gbit/s datarate was considered for a direct LOS beam transmission onto a photodetector after both 30-m POF and 150-m BI-SMF over a free space link of 100-cm. The observed result is presented in Fig 6.15. The graph illustrates approximate equal power decline is experienced for radiated beam through both the POF and BI-SMF cable at different free space distances.

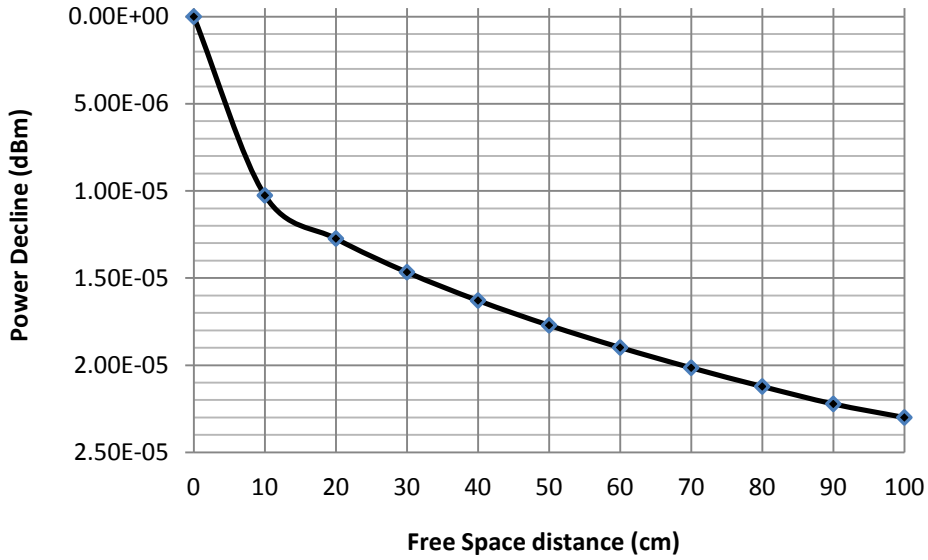

Figure 6.15: Power Decline versus free-space distance after 150-m BI-SMF transmission

5-m Free Space distance	**(30m) POF**	**(150m) BI-SMF**
Launch Waist Beam (metre)	**-Log(BER)**	
0.02	33.00852	44.4221
0.05	33.00599	44.4199
0.1	33.00561	44.4196
0.2	33.00554	44.4195
0.5	33.00552	44.4195
1	33.00551	44.4195
2	33.00551	44.4195
3	33.00551	44.4195
4	33.00551	44.4195
5	33.00551	44.4195

Table 6.1: Launch waist beam versus 60 GHz signal BER over 30-m POF and 150-m BI-SMF

6.5 SNR evaluation for OWC using BI-SMF optical fiber

Based on the SNR equation (*Chapter 3*) that desribes the OWC link in a given geometrical room:

$$SNR = \frac{R^2 P_r^2}{R_b N}$$

Where R, is the responsivity of the receiving photodiode. P_r is the received average power and R_b is the bitrate and N represents the ambient light noise:

R = [responsivity of the receiving photodiode] = 1 A/W

R_b = [bitrate] = 10 Gbit/s

N = [selected ambient light noise threshold] =$10^{-23}\ A^2/Hz$

P_r = received power (dBm to Watt) between OAP and PD [Fig 6.14]:

The SNR over 150-m BI-SMF fiber optic cable is evaluated as:

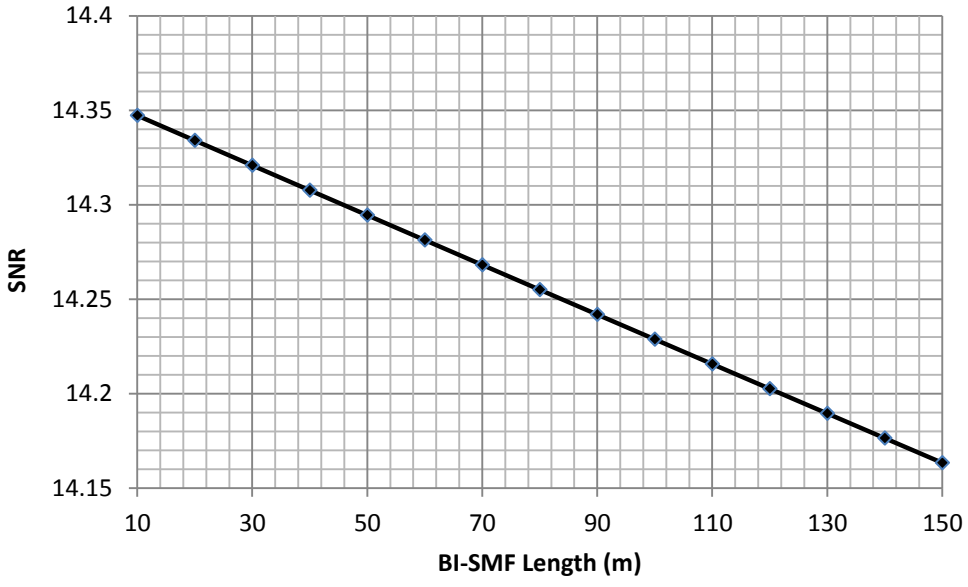

Figure 6.16: SNR versus BI-SMF optical fiber lengths

6.5.1 Mm-wave with Wi-Fi Results and Discussion

As expected, observed in Fig 6.4, results show that reducing the linewidth of the modulated data reduces the attenuation on the 60 GHz data signal and also improves the BER performance [Fig 6.5]. By altering the offset launch conditions between the SMF and MMF (POF) a consistent steady increase in bandwidth gain was recorded. Where the offset launch condition was centred, the closing of the eye-diagram can be observed in Fig 6.10 and at launch condition of 22 μm, the eye-diagram gains a broader opening [Fig 6.11] as expected based on other reported results [6]. In the simulated WDM system [Fig 6.8], where 2.4 GHz Wi-Fi signal carrying 100 Mbit/s data was added with the 60 GHz signal produced clearly separated constellation points Fig 6.12.

POF maintained a limited signal performance over short optical fiber lengths (30-m) whilst BI-SMF results showed better ISI performance [Fig 6.13] and received power [Fig 6.14] at the receiver station (or ONU). Additional observed unrecorded results also showed BI-SMF cable maintained a 2% reduction of received power for 300-m fiber cable from 150-m. The effects of increasing the launch beam waist/diameter from the OAP over a 5-m free space link showed minor changes on the received optical signal power regardless of POF or BI-SMF transmissions. This result, although accurately recorded, highlights the necessity of a field based assessment for verification. Further evaluation was observed for the received SNR of the radiated beam as it propagates through free space with different lengths of BI-SMF in Fig 6.16. The graph clearly demonstrates the effect of ambient noise can attenuate the mm-wave signal power as it propagates through 5-m free space distance.

6.6 Summary

The simulated delivery of mm-wave modulated 2.5, 5 and 10 Gbit/s data signal over 25-km SMF, 30-m and 15-m POF cables for FTTH and inside the home architecture using the MMF-POF and BI-SMF fibers has been effectively demonstrated. This approach to mm-wave delivery is very cost effective as it uses low operating power at the central station to deploy mm-wave signals. It also provides an alternative to the latest WiGig delivery of 60 GHz signal [1] to subscriber's home with MMF inclusion for ultrafast data delivery for both uplink and downlink capabilities. However there are complexities with the use of optical multiplexers at the receiver station. In future system modelling, an optical interleaver can be used to separate the mm-wave carriers and signals rather than the cumbersome optical WDM employed in this case.

References:

[1] Wireless Gigabit Alliance, http://www.wigig.org

[2] Pham T.T, Lebedev A, Beltran M, Yu X, er al., "SMF/MMF Based In-Building Gigabit Wireless Access Systems Using Simplified 60-GHz Transceivers," in *ECOC*, Geneva, September 2011.

[3] Yan Shi, Maria Morant, et al., "Multistandard Wireless Transmission over SSMF and Large-Core POF for Access and In-Home Networks," *IEEE Photonics Technology Letters*, vol. 24, pp. 736-738, May 2012.

[4] U. Gliese, T. N. Nielsen, S. Nrskov and K. E. Stubkjaer, "Multifunction fiber-optic microwave links based on remote heterodyne detection," *IEEE Trans. Microwave Theory Tech.,* vol. 46, pp. 458-468, 1998.

[5] L. Raddatz, I. H. White, D. G. Cunningham, and M. C. Nowell, "An Experiment and Theoretical Study of the Offset Launch Technique for the Enhancement of the Bandwidth of Multimode Fiber Links," *Journal of Lightwave Technology*, vol. 16, no. 3, March 1998.

[6] L. Raddatz, I. H. White, D. G. Cunningham, and M. C. Nowell, "Increasing the bandwidth-distance product of multimode fiber using offset launch," *Electron. Lett.,* vol. 33, pp. 232-233, 1997.

[7] Jing Li, TiGang Ning, Li Pei, and ChunHui Qi, "Scheme for a High-Capacity 60 GHz Radio-over-fiber Transmission System," *IEEE Journal of Optical Communication Network,* vol. 1, no. 4, September 2009.

[8] J. W. Zimmerman, R. K. Price, U. Reddy, N. L. Dias, and J.J. Coleman, "Narrow linewidth surface-etched DBR lasers: Fundamental design aspects and applications," *IEEE Journal of Selected Topics in Quantum Electronics*, vol. 19, no. 4, July/August 2013.

[9] R. K. Price, J. J. Borchardt, V. C. Elarde, R. B. Swint, and J.J. Coleman, "Narrow-linewidth asymmetric cladding Distributed Bragg Reflector semiconductor lasers at 850 nm," *IEEE Photon. Technol. Lett.,* vol. 18, no. 1, pp. 97-99, Jan. 2006.

Chapter 7

Conclusion and Future work

7.1 Conclusion

The delivery of Gbit/s broadband speed to MDU or SFU buildings isn't feasible over existing infrastructure and as a result this thesis sets out to investigate various transport mechanisms that can deliver the future broadband data streaming over optical fiber in a residential property.

7.2 Design of mm-wave transmission schemes

7.2.1 OCS technology design

The transmission method of mm-wave signal over optical fiber was first approached in Chapter 2 of this thesis. Optical Carrier Suppression (OCS) transmission scheme used a much lower oscillator frequency at the CO station to generate the mm-wave signals. The mm-wave signals were generated by doubling the RF carrier frequency through heterodyning of the produced optical sidebands by an external modulator. One of the significant features of OCS technology scheme is its low-cost capability at

the OLT site by using modulators with low bandwidth to generate the desired mm-wave signals. Rather than directly modulating the data onto a 60 GHz carrier-wave signal, OCS used a process of doubling the RF sidebands through the processes of heterodyning creating a much larger frequency passband in the mm-wave region. This optical transmission scheme fundamentally has the highest receiver sensitivity, lowest spectral occupancy and bandwidth requirement for optical modulators. Also including in the advantages of OCS technology is that the effects of fading are significantly reduced through OCS scheme making it dispersion tolerant over long-haul optical fiber transmission as OCS doesn't directly modulate a larger RF carrier frequency than in conventional DSB scheme. However, the OCS transport scheme when applicable for upstream transmission requires the subscriber site to have expensive electrical components such as an RF local oscillator for up converting the baseband signals at mm-wave frequency which isn't cost effective.

In this thesis, the simulation of OCS transport scheme was configured to deliver Gbit/s data rate over mm-wave signal (i.e. 60 GHz) to a receiver station over long-haul SMF and coupled access network optical fibers, 30-m POF and 150-m BI-SMF. POF being a highly dispersive optical fiber and attenuates mm-wave signal consistently irrespective of what transport scheme is adopted. As a result, the best performance length achieved for POF (MMF) was approximately 30-m without observing remarkable signal loss before photodetection. In the observed BER result, POF produced an evaluated power penalty of 1.7 dB at 30-m length whilst its counterpart BI-SMF had a power penalty of 1.6 dB. This showed the considerable difference in how BI-SMF optical fiber cable produced a much better performance BER over a longer length fiber cable than POF in transporting microwave/mm-wave signals. The observation of the eye diagram also displayed inter-symbol interference i.e. eye-closure as the POF length was varied beyond 34-m.

As discussed earlier, since OCS reduces fading by having a considerably high dispersion tolerance over long-haul fibers which are generally SMF optical fibers. This makes BI-SMF more suitable for propagating mm-wave signals for in-door applications compared to the much more highly dispersive (POF) MMF fiber cable which attenuates the microwave signals. This can be observed from the received power spectrum results which showed less signal attenuation over longer fiber lengths. Further to this simulation was the observation of optical wireless communication of the radiated beam between POF, BI-SMF optical access points and the PD. The OWC performance had less notable signal degradation at distances up to 5-m with both optical access fibers which implies the feasibility of deploying mm-wave OWC systems onto a stationary in-door receiver device for an all optical communication right from the OLT site as the application may warrant.

7.2.2 OFM mm-wave transport scheme over harmonic components

The transmission scheme of producing RF harmonic components over a free spectral range was observed. The fundamental theory of optical frequency multiplication (OFM) in the frequency domain product was analysed and evaluated in Chapter 5. The process of harmonics generation based on heterodyning of the RF harmonics components was analysed. In the conventional OFM which used a phase modulation and direct detection system, the configuration requires an optical filter to cause RF beating at the photodetector (PD) output in order to generate the harmonic components. Removal of the optical filter placed between the MZM and the PD produced only a DC power. A more promising OFM scheme of generating the desired RF harmonics without the need of periodic filtering is to use the DD-MZM. The generation of the mm-wave was achieved using a low RF sweep signal at

transmission. The simulation configured a standard LTE signal and traditional Wi-Fi both carrying a 100 Mbit/s 16-QAM data over long-haul SMF optical fiber coupled with POF or BI-SMF cables. The Wi-Fi signal can be filtered at a higher RF harmonics to obtain the desired mm-wave signal (60 GHz + $f_{wi\text{-}fi}$) with a throughput data rate of 100 Mbit/s. The theoretical evaluation of OFM scheme already proved that as the RF generated harmonic components approaches mm-wave bands or more, the bandwidth of the RF component becomes significantly reduced. Further increase in the POF lengths experienced a considerably high dispersion and attenuation on the mm-wave signal even as the offset launch technique was varied but was incapable of bandwidth optimisation. The effects of free space transmission to achieve optical wireless communication in an in-door environment showed little to no signal degradation based on the recorded results. The adoption of the BI-SMF produced a better system performance at a much longer fiber length.

One of the key benefits of researching OFM technique was that a local mm-wave signal is also obtainable from the OFM spectral range which can be used for upstream transmission of the subscriber's data back to the OLT site.

7.2.3 RHD coherent transmission technique of 60 GHz signal

Remote heterodyne detection (RHD) is based on coherent optical communication and generates mm-wave frequency by combining two laser transmitters with a frequency offset the generated two optical peaks are biased at minimum transmission point to realize OCS modulation. In effect, RHD technology based on OCS modulation implements the features of OCS technology which has considerably high dispersion tolerance over SMF optical fibers, better receiver sensitivity

performance and utilization of considerably low bandwidth utilisation for mm-wave generation.

In the simulation of the RHD scheme discussed in Chapter 6 for Gbit/s data rates over both POF and BI-SMF cables has been presented. By using both laser sources transmitting continuous wave wavelengths of "near infra-red" (NIR) region, an investigation into the performance of POF was examined. Seeing as the NIR region on the electromagnetic spectrum produced the least amount of attenuation on optical wavelengths, the transport of mm-wave signals over NIR region proved to be successful over long haul optical fiber and MMF (POF). The simulation result, as expected, showed that reducing the linewidth of the modulated data reduced the attenuation on the 60 GHz data signal and also improved the BER performance. Further to this simulation analysis, investigation of altering the offset launch conditions between the SMF and MMF (POF) was considered. The observed result showed a consistent steady increase in bandwidth gain as offset launch condition was altered. A peak bandwidth gain at 22 μm offset launch condition was observed to improve the eye diagram and resulting mm-wave signal. In a configured WDM system, 2.4 GHz WI-Fi signal carrying 100 Mbit/s data was also multiplexed along with the 60 GHz signal for the simulation of proposed IEEE 802.11 b/g/ad multistandard channel delivery to a subscriber's home. POF maintained a limited signal performance over short optical fiber lengths (30-m) whilst BI-SMF results showed better ISI and received power at the receiver station (or ONU). Additional observed unrecorded results also showed BI-SMF cable maintained a 2% reduction of received power for 450-m fiber cable from 150-m.

Based on the application of POF for in-door access fiber connectivity, this thesis has presented three mm-wave transport technologies that demonstrated the feasibility in propagating Gbit/s over the MMF for access network communication.

Although the performance of the MMF length was significantly shorter in length by a factor of 5 compared to its counterpart, the BI-SMF, the POF cable can be used for more stringent handling applications for in-door connectivity due to its larger core diameter. However, based on the analysis conducted in this thesis, BI-SMF cable displayed an improved performance in propagating 60 GHz signals over longer fiber links for indoor connectivity.

7.3 Future Work

Although the transport of the mm-wave is possible as demonstrated in this thesis, there are however several drawbacks in their RoF transmission schemes. Based on reported and widely researched experiments, coherent optical communication has proven to be the most feasible and reliable approach to delivering mm-wave signal over optical fiber cables for Gbit/s data rate transmission. The downside factor is the cost aspect of using two laser sources at the transmission site. This cost factor also correlates with the number of DWDM channels required. The type of transport technology also adversely reflects the entire cost of the ISP architecture, from OLT to ONU design. This is a major factor in adopting the chosen mm-wave transport scheme. The all-optical communication architecture which includes FTTC, FTTH and F*i*TH are extensively practical and already being deployed globally to meet SFBB. The type of access point (AP) can be distinguished to two designs, remote antenna unit (RAU) or optical access point (OAP) with each component having differentiating benefits for optical upstream and downstream transmissions in an in-door environment. The low-cost optical fiber cable POF when used as an access network cabling link has been demonstrated elsewhere in its capability of supporting 40 Gbit/s transmission over 100-m cable length (Chapter 2). Its SMF variant counterpart,

BI-SMF is currently being investigated on and only very few reported experiments based on BI-SMF are available but yet its support for triple-play multimedia services as well as terabit/s data transport has been documented. Where POF, to the best of our knowledge, has the best fabricated fiber cable with attenuation properties at 8 dB/km and BI-SMF based on the latest ITU-Recommendation is 0.4 dB/km giving the practical confidence in implementing BI-SMF cable as best practice for in-door networking over POF fiber cable option.

Although ideally the offset launch conditions specified in this thesis between the long-haul SMF fiber and MMF (POF) seems impractical and cumbersome for field site deployment as a long term residential solution, especially in the case of maintenance and repair. Nonetheless its application can be applicable in improving the signal bandwidth of POF signals. In this thesis RHD simulation, the received mm-wave signal at the PD produces a 60 GHz passband signal which in a future proposed scheme can be directly injected into a low-cost eye-safe vertical cavity surface emitting laser (VCSEL) at the residential gateway before connecting the MMF (POF) and using an APD photodetector for optical-to-electrical signal conversion.

There are cumulative factors that lead to signal degradation due to the connected electronics and optical devices such as the laser sources, couplers and photodetectors (PD). These devices create impairments such as shot noise and timing jitter which have an adverse effect on the received bit. As transmitted bit increases the power penalty required to compensate for the noise increases. Using OAP rather than RAU at the in-door transmission point limits one aspect of the attributed noise found in the PD and electronic antenna components when transmitting Gbit/s data to a mobile receiver device. Hence the benefits of free-space optics for OWC transmission as mm-wave signal delivery option as opposed to direct antenna radiation. Further investigation on the signal degradation in the bi-

directional transmission over OAP and RAU comparison needs to be made with extensive consideration of which optical access fiber gives better performance for in-door mm-wave optical fiber communication system. Finally, the transport of all triple play services such as DVBTv-IPTv, VoIP and Wi-Fi (incl. IEEE 802.11 b/g/n/ac/ad) should be investigated to demonstrate a comprehensive RoF delivery technology.

In an environment where all future electronic devices are geared towards internet connectivity and preparing for the internet of things evolution, the complexity of the network design should primarily consider the energy consumption, optical technology can deliver the energy efficiency that is sustainable.

Appendix A:

Theoretical calculation that models the effect of offset launch conditions on MMF bandwidth:

The outline of this modelling considers the electrical field distribution of the propagating modes in which they have similar propagation constants [Ch. 3 Ref. 7]. By evaluating the scalar wave equation of the waveguides [Ch. 3 Ref. 8], and taking into account the linearly polarized modes with both cylindrical and radial order as parameters. The thoroughly characterised group velocity (v_g) of the polarized modes without spreading effect can be expressed as:

$$v_g = \frac{\delta\omega}{\delta k} \approx \frac{\Delta\omega}{\Delta k} \quad \textbf{(A.1)}$$

The power coefficient of each radiated mode is assumed as well as the power of the ingress mode from the SMF. A summation of modal power (n_M) in both SMF and MMF fibers can be considered as a function of their electric field of both independent fiber modes (E_M) and injected beam (E_I) and expressed as:

$$n_M = \frac{|\iint E_I E_M^* \, r \, dr \, d\emptyset \,|^2}{\iint |E_I|^2 r \, dr \, d\emptyset \iint |E_M|^2 r \, dr \, d\emptyset'} \quad \textbf{(A.2)}$$

The model further expresses the assumption of symmetrical radiation of all modes and computes a 4 for all cases when modes have group velocity not zero and computes a 2 for modes with zero group velocity. The definitive number of radiated modes (m) in the fiber is evaluated through:

$$m = \frac{(\sum a_i)^2}{\sum a_i^2} \quad \textbf{(A.3)}$$

The simulation also considers the effect of modal loss for each individual mode, deduces the expression into the propagation constant ($R_{v\mu}^2$) of the respective modes [Ch. 3 Ref. 9], to further yield the equation as:

$$R_{v\mu}^2 = \frac{1}{2} \frac{n_{core}}{n_{core} - n_{cladd}} \left(1 - \frac{\beta_{v\mu}^2}{K_0^2 \, n_{core}^2}\right) \quad \textbf{(A.4)}$$

- K_0 = free space wave number
- $\beta_{v\mu}$ = propagation constant
- n_{core} = core refractive index
- n_{cladd} = cladding refractive index

Appendix B:

Evaluation of Optical Frequency Multiplication using Dual-Drive Mach-Zehnder Modulator:

The OFM transmission system based on OFM using DD-MZM has the electrical field of the optical signal after the DD-MZM given as:

$$E_{DD} = E_1 e^{j[\omega_\lambda(t+\tau) + \beta_1 \cos((\omega_{sw}t+\omega_{sw}\tau)+\theta)+\Delta\theta+\theta_{N1}]} + E_2 e^{j[\omega_\lambda t+\beta_2 \cos \omega_{sw}t+\theta_{N2}]} \quad \textbf{(B.1)}$$

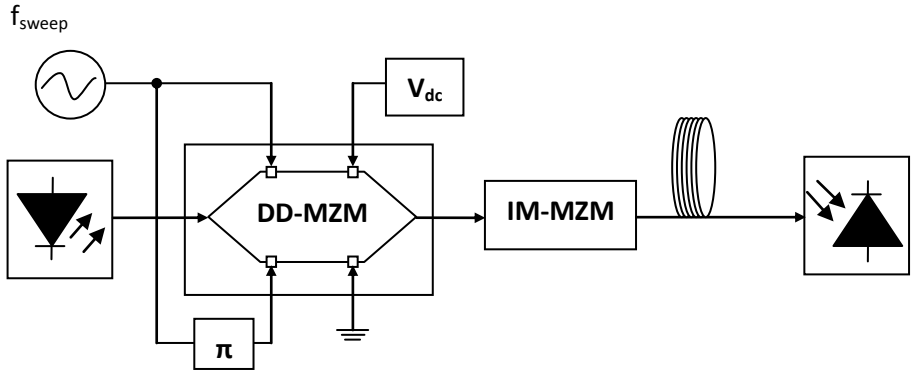

Fig B.1: OFM architecture with DD-MZM

The intensity of the optical signal detected at the PD can be expressed as:

$$i_{PD}(t) = [E_{DD}(t) \times E_{DD}^*(t)] \quad \textbf{(B.2)}$$

$$i_{PD}(t) = \frac{1}{2}\langle R[E_{DD}(t) \cdot E_{DD}^*(t)]\rangle = \frac{1}{2}|E_o|^2 \quad \textbf{(B.3)}$$

In the equation **(B.4)** E_1 and E_2, are the electric field's amplitude of both arms of the DD-MZM respectively; ω_λ and ω_{sw}, are the radian frequency of the lightwave and sweep signal respectively; τ, is the differential path delay of both branches of the DD-MZM; β_1 and β_2, are the phase modulation indexes of the two sweep signals respectively; θ, optical phase difference between the two sweep frequencies; $\Delta\theta$, the phase created by the bias voltages of the two arms of the DD-MZM; θ_{N1} and θ_{N2}, the phase noise at the two arms of the DD-MZM respectively.

$$i_{PD}(t) = \frac{1}{2}|E_o|^2 \times \{E_1^2 + E_2^2 + 2E_1E_2\cos[\beta_1\cos(\omega_{sw}t + \omega_{sw}\tau + \theta) - \beta_2\cos\omega_{sw}t + \omega_\lambda\tau + \Delta\theta + \theta_{N1} - \theta_{N2}]\} \quad \textbf{(B.4)}$$

For trigonometry simplification, make $A = \omega_{sw}\tau + \theta$ and $B = \omega_\lambda\tau + \Delta\theta$ to express equation **(B.4)** as:

$$i_{PD}(t) = \tfrac{1}{2}|E_o|^2 \times \{E_1^2 + E_2^2 + 2E_1E_2\cos[\beta_1\cos(\omega_{sw}t + A) - \beta_2\cos\omega_{sw}t + B + \theta_{N1} - \theta_{N2}]\} \quad \textbf{(B.5)}$$

$$i_{PD}(t) = \tfrac{1}{2}|E_o|^2 \times \{E_1^2 + E_2^2 + 2E_1E_2\cos[\beta_1\cos\omega_{sw}t\cos A - \beta_1\sin\omega_{sw}t\sin A - \beta_2\cos\omega_{sw}t + B + \theta_{N1} - \theta_{N2}]\} \quad \textbf{(B.6)}$$

As the two arms of DD-MZM is of the same length, therefore the delay $\tau = 0$, this makes $A = 180°$ (i.e. set at π, see Fig B.1)...hence $[\sin A = 0]$ and $[\cos A = -1]$. The phase noise at the two arms of the DD-MZM is assumed identical θ_{N1} and θ_{N2} cancel each other out making $\theta_{N1} - \theta_{N2} = 0$. If the phase created by the bias voltage $\Delta\theta$, is set at 0 initially, with $\tau = 0$, this makes $B = 0$ meaning that the odd harmonics are eliminated, leaving only the even harmonic components. Equation **(B.6)** is now expressed as:

$$i_{PD}(t) = \tfrac{1}{2}|E_o|^2 \times \{E_1^2 + E_2^2 + 2E_1E_2\cos[-\beta_1\cos\omega_{sw}t - \beta_2\cos\omega_{sw}t]\} \quad \textbf{(B.7)}$$

$$i_{PD}(t) = \tfrac{1}{2}|E_o|^2 \times \{E_1^2 + E_2^2 + 2E_1E_2\cos[-2\,(\beta_1 + \beta_2)\cos\omega_{sw}t]\} \quad \textbf{(B.8)}$$

The evaluated Bessel function series of the intensity photo-current OFM DD-MZM signal received at the PD $[i_{PD}(t)]$ is now expressed as:

$$i_{PD}(t) = \frac{1}{2}|E_o|^2 \times \left\{E_1^2 + E_2^2 + 2E_1E_2 \left[J_0\,(\beta_1 + \beta_2) + 2\sum_{q=1}^{\infty}(-1)^q J_{2q}(\beta_1 + \beta_2)\cos(2q\omega_{sw}t)\right]\right\} \quad \textbf{(B.9)}$$

List of published papers

- Uchenna. O. Igweani, Hamed. Al-Raweshidy, "mm-wave and Wi-Fi transmission over single and multi-mode optical fibers", IEEE Optical Wireless Communications (IWOW), 2013 2nd International Workshop on, pp. 54 – 57, 2013.
- Uchenna. O. Igweani, Hamed. Al-Raweshidy, "60 GHz delivery over SMF and MMF for in-door applications", IEEE Africon, pp. 1 – 3, 2013.
- Uchenna. O. Igweani, Hamed. Al-Raweshidy, "OFM transmission of wireless channels over SMF and POF optical fibers", IEEE Computer Science and Electronic Engineering Conference (CEEC), 2013 5th, pp. 125 – 127, 2013.

Paper under review

- Uchenna. O. Igweani, Hamed. Al-Raweshidy, "Radio-over-Fiber Downstream Technologies for Direct and Optical Wireless Communication Detection System for In-door Application", IEEE Journal of Lightwave Technology, 2014.